

AD \_\_\_\_\_

Award Number: DAMD17-97-1-7249

TITLE: Effects of FOS, JUN, TGF-B, and Glucocorticoids on Polarized  
Membrane Traffic

PRINCIPAL INVESTIGATOR: Keith E. Mostov, M.D., Ph.D.

CONTRACTING ORGANIZATION: University of California, San Francisco  
San Francisco, California 94143-0962

REPORT DATE: October 2000

TYPE OF REPORT: **Final**

PREPARED FOR: U.S. Army Medical Research and Materiel Command  
Fort Detrick, Maryland 21702-5012

DISTRIBUTION STATEMENT: Approved for Public Release;  
Distribution Unlimited

The views, opinions and/or findings contained in this report are those of the author(s) and should not be construed as an official Department of the Army position, policy or decision unless so designated by other documentation.

20011005 299

**REPORT DOCUMENTATION PAGE**Form Approved  
OMB No. 074-0188

Public reporting burden for this collection of information is estimated to average 1 hour per response, including the time for reviewing instructions, searching existing data sources, gathering and maintaining the data needed, and completing and reviewing this collection of information. Send comments regarding this burden estimate or any other aspect of this collection of information, including suggestions for reducing this burden to Washington Headquarters Services, Directorate for Information Operations and Reports, 1215 Jefferson Davis Highway, Suite 1204, Arlington, VA 22202-4302, and to the Office of Management and Budget, Paperwork Reduction Project (0704-0188), Washington, DC 20503

<b>1. AGENCY USE ONLY (Leave blank)</b>		<b>2. REPORT DATE</b> October 2000	<b>3. REPORT TYPE AND DATES COVERED</b> Final ( 30 Sep 97 - 29 Sep 00)	
<b>4. TITLE AND SUBTITLE</b> Effects of FOS, JUN, TGF-B, and Glucocorticoids on Polarized Membrane Traffic			<b>5. FUNDING NUMBERS</b> DAMD17-97-1-7249	
<b>6. AUTHOR(S)</b>  Mostov, Keith E., M.D., Ph.D.				
<b>7. PERFORMING ORGANIZATION NAME(S) AND ADDRESS(ES)</b>  University of California, San Francisco San Francisco, California 94143-0962  E-Mail: mostov@itsa.ucsf.edu			<b>8. PERFORMING ORGANIZATION REPORT NUMBER</b>	
<b>9. SPONSORING / MONITORING AGENCY NAME(S) AND ADDRESS(ES)</b>  U.S. Army Medical Research and Materiel Command Fort Detrick, Maryland 21702-5012			<b>10. SPONSORING / MONITORING AGENCY REPORT NUMBER</b>	
<b>11. SUPPLEMENTARY NOTES</b>  This report contains colored photos				
<b>12a. DISTRIBUTION / AVAILABILITY STATEMENT</b> Approved for Public Release; Distribution Unlimited				<b>12b. DISTRIBUTION CODE</b>
<b>13. ABSTRACT (Maximum 200 Words)</b>  In polarized MDCK kidney epithelial cells, components of the plasma membrane fusion machinery, the t-SNAREs syntaxin 2, 3, 4 and SNAP-23 are differentially localized at the apical and/or basolateral plasma membrane domains. Here we identify syntaxin-11 as a novel apical and basolateral plasma membrane t-SNARE. Surprisingly, all of these t-SNAREs redistribute to intracellular locations when MDCK cells lose their cellular polarity. Apical SNAREs re-localize to the previously characterized vacuolar apical compartment (VAC) while basolateral SNAREs redistribute to a novel organelle that appears to be the basolateral equivalent of the VAC. Both 'intracellular plasma membrane compartments' have an associated prominent actin cytoskeleton and receive membrane traffic from cognate apical or basolateral pathways, respectively. These findings demonstrate a fundamental shift in plasma membrane traffic towards intracellular compartments while protein sorting is preserved when epithelial cells lose their cell polarity.				
<b>14. SUBJECT TERMS</b> Breast Cancer, IDEA Award				<b>15. NUMBER OF PAGES</b> 51
				<b>16. PRICE CODE</b>
<b>17. SECURITY CLASSIFICATION OF REPORT</b> Unclassified	<b>18. SECURITY CLASSIFICATION OF THIS PAGE</b> Unclassified	<b>19. SECURITY CLASSIFICATION OF ABSTRACT</b> Unclassified	<b>20. LIMITATION OF ABSTRACT</b> Unlimited	

## Table of Contents

	PAGE
Cover.....	1
SF 298.....	2
Table of Contents.....	3
Introduction.....	4
Body.....	4-17
Key Research Accomplishments.....	17
Reportable Outcomes.....	17
Conclusions.....	17
References.....	17-19
Appendices.....	20, 36

#### 4. Introduction

In polarized MDCK kidney epithelial cells, components of the plasma membrane fusion machinery, the t-SNAREs syntaxin 2, 3, 4 and SNAP-23 are differentially localized at the apical and/or basolateral plasma membrane domains. Here we identify syntaxin-11 as a novel apical and basolateral plasma membrane t-SNARE. Surprisingly, all of these t-SNAREs redistribute to intracellular locations when MDCK cells lose their cellular polarity. Apical SNAREs re-localize to the previously characterized vacuolar apical compartment (VAC) while basolateral SNAREs redistribute to a novel organelle that appears to be the basolateral equivalent of the VAC. Both 'intracellular plasma membrane compartments' have an associated prominent actin cytoskeleton and receive membrane traffic from cognate apical or basolateral pathways, respectively. These findings demonstrate a fundamental shift in plasma membrane traffic towards intracellular compartments while protein sorting is preserved when epithelial cells lose their cell polarity.

#### 5. Body

Traffic between membranous compartments is mediated by the SNARE machinery in virtually all membrane traffic pathways investigated so far (1, 2, 3, 4). During vesicle docking, membrane proteins on the vesicle (v-SNAREs) and the target membrane (t-SNAREs) bind to each other to form a complex which ultimately leads to fusion of the lipid bilayers. One aspect of the SNARE hypothesis is that successful membrane fusion requires the binding of matching combinations of v- and t-SNAREs thereby ensuring the necessary specificity of vesicle fusion. Accordingly, each membrane organelle and each class of transport vesicles should be defined by a certain set of t- and v-SNARE isoforms. Many SNAREs have been identified to date, and protein sequence analysis has shown that v- and t-SNAREs of the currently known SNARE sub-families are evolutionarily related to each other and belong to a common superfamily (5, 6). It is conceivable that the specificity of vesicle fusion is not directly determined by t-SNARE/v-SNARE interactions *per se* but rather by interactions involving larger complexes including SNAREs and their regulatory proteins such as those of the rab and sec1 protein families (7, 8, 9).

Epithelial cells display an additional layer of complexity as they are typically polarized and possess two distinct plasma membrane domains (10, 11, 12, 13, 14). The apical and basolateral plasma membrane domains have different protein and lipid compositions which reflect the different function of these domains. This plasma membrane polarity is established and maintained by protein sorting and specific vesicle trafficking routes in the biosynthetic and endocytic pathways. In agreement with the SNARE hypothesis, the apical and basolateral plasma membrane domains of epithelial cells contain distinct t-SNAREs (15). Two protein families have been identified as t-SNAREs, the syntaxin and SNAP-25 families. In the polarized renal epithelial cell line MDCK, syntaxins 3 and 4 are localized at the apical or basolateral plasma membrane, respectively (16). Syntaxin 3 functions in transport from the trans-Golgi network as well as the endosomal recycling pathway, both leading to the apical plasma membrane (17). Syntaxin 2 is localized to both domains of MDCK cells (16), as is SNAP-23 (18), a ubiquitously expressed member of the SNAP-25 family (19). SNAP-23 binds to syntaxins 3 and 4 *in vivo* (20, 21) and is involved in biosynthetic and endocytic recycling and transcytotic pathways to both plasma membrane domains in MDCK cells (17, 22). The subcellular localization of these SNAREs is

generally very similar in other epithelial cell lines and tissues although variations have been reported (15, 20, 23, 24, 25, 26).

Temporary or permanent loss of cell polarity is a common phenomenon during the development of epithelial tissues (27, 28) as well as in a number of pathological conditions (10, 28, 29). It is largely unknown how apical and basolateral membrane traffic pathways behave in epithelial cells that have lost or not yet acquired their cellular polarity under any of the above circumstances. This is a fundamental question in cell biology. For example, changes in these pathways may play an important role in the acquisition of the invasive phenotype of tumor cells, e.g. by mistargeting of cell adhesion molecules, or erroneous secretion of proteases that attack basement membrane and extracellular matrix proteins. It is well established that the malignancy of epithelial-derived tumors (carcinomas) correlates directly with the degree of de-differentiation. A hallmark of de-differentiation or anaplasia is the loss of cellular polarity. A better knowledge of the changes in membrane traffic pathways that occur when epithelial cells lose or gain cell polarity will help us understand normal epithelial function as well as pathologic conditions.

In the present paper we have investigated the subcellular localization of plasma membrane t-SNAREs, as part of the machinery accomplishing membrane traffic, in polarized vs. non-polarized MDCK cells. We identified syntaxin 11 as a novel plasma membrane t-SNARE in addition to syntaxins 2, 3, 4 and SNAP-23. All plasma membrane t-SNAREs undergo dramatic changes in subcellular localization in MDCK cells depending on the state of cell polarity. Apical t-SNAREs relocate to an intracellular vacuolar apical compartment (VAC) while basolateral t-SNAREs relocate to a novel compartment. The presence of t-SNAREs in these intracellular compartments suggests that they function in the fusion of incoming transport vesicles and that these compartments are actively connected to cellular membrane traffic. Indeed, we find that the apical and basolateral intracellular compartments are functionally equivalent to the apical or basolateral plasma membrane of fully polarized cells, respectively, as they receive membrane traffic from cognate apical or basolateral transport pathways.

These results suggest that fundamental rearrangements occur with respect to membrane traffic in epithelial cells that have lost their cellular polarity. Nevertheless, the localization of plasma membrane t-SNAREs does not become randomized but the cells re-direct plasma membrane transport pathways into intracellular compartments and preserve protein sorting.

## **MATERIALS AND METHODS**

### ***Materials***

Cell culture media were from Cell Gro, Mediatech (Washington, DC). Fetal bovine serum was from Hyclone, (Logan, UT). G418 was obtained from GIBCO-BRL (Gaithersburg, MD). Transwell polycarbonate cell culture filters were purchased from Corning Costar Corporation (Massachusetts, MA). Canine apo-transferrin was purchased from Sigma (St. Louis, MO), loaded with iron and dialyzed against PBS. The cDNA of human syntaxin 11 in the expression vector pcDNA3 has been described earlier (30). cDNAs for the expression of syntaxin-GST fusion proteins were gifts from Dr. Mark Bennett, University of California at Berkeley, CA.

### ***Antibodies***

Polyclonal antibodies against rat syntaxins 2, 3 and 4 were raised in rabbits against GST fusion proteins of the cytoplasmic domains. The antibodies were affinity-purified using the respective

syntaxin cytoplasmic domains that were separated from GST by thrombin cleavage and coupled to Affigel (Biorad). The rabbit polyclonal antibody against an N-terminal peptide of human SNAP-23 was affinity-purified as described before (18). The affinity-purified rabbit polyclonal antibody against a peptide of the N-terminal 15 amino acids of human syntaxin 11 has been described (30). The rat monoclonal antibody against ZO-1, the mouse monoclonal antibodies against ubiquitin and alpha-fodrin (non-erythroid spectrin) were obtained from Chemicon International (Temecula, CA). The mouse monoclonal antibodies against  $\gamma$ -tubulin and pan-cytokeratin were obtained from Sigma (St. Louis, MO). AC17, a mouse monoclonal antibody against the lysosomal/late endosomal membrane glycoprotein LAMP-2 (31) was a gift from E. Rodriguez-Boulan (Cornell University Medical College, New York, NY). The mouse monoclonal antibody against gp135, an endogenous apical plasma membrane protein in MDCK cells (32), was a gift from G. Ojakian (SUNY Health Science Center, Brooklyn, NY). The mouse monoclonal antibody against E-cadherin, rr1 (33), was donated by B. Gumbiner (Sloan-Kettering, NY). The mouse monoclonal antibody, 6.23.3, against an endogenous MDCK basolateral plasma membrane protein of 58 kDa (34) was a gift from K. Matlin (Harvard Medical School, Boston). The rabbit polyclonal antibody against canine gp80/clusterin (35) was a gift from C. Koch-Brandt (Universität Mainz, Germany). Purified human polymeric IgA was kindly provided by J.-P. Vaerman (Catholic University of Louvain, Brussels, Belgium). Anti-Na<sup>+</sup>/K<sup>+</sup>-ATPase (alpha subunit, MA3-928) was from Affinity Bioreagents (Golden, CO). Fluorescein dichlorotriazine (DTAF)-labeled anti-human IgA antibody was from Organon Teknika Corp. (Durham, NC). The antibody against canine apo-transferrin has been described earlier (36). The mouse monoclonal antibody against Golgin-97 was from Molecular Probes (Eugene, OR). Secondary antibodies cross-absorbed against multiple species and conjugated to FITC, Texas Red or Cy5 were from Jackson ImmunoResearch (West Grove, PA).

### ***SDS-PAGE and immunoblotting***

Total membrane fractions of MDCK, HepG2, HeLa and HT29 cells were prepared by scraping the cells from confluent dishes in PBS containing protease inhibitors and homogenization by repeated passage through a 22 gauge needle. Nuclei and unbroken cells were removed by centrifugation at 500 g for 2 minutes. The membranes were recovered by centrifugation at 16,000 g for 10 min and dissolved in SDS-PAGE sample buffer. Equal amounts of protein were separated on a 12% SDS-polyacrylamide gel followed by transfer to nitrocellulose and incubation with the affinity-purified syntaxin 11 antibody. Bands were visualized by enhanced chemiluminescence.

### ***Cell Culture***

MDCK strain II cells were maintained in Minimal Essential Medium, supplemented with 10% FBS, 100 U/ml penicillin and 100  $\mu$ g/ml streptomycin in 5% CO<sub>2</sub>/95% air. For experiments with polarized MDCK cells, the cells were cultured on 12 mm, 0.4  $\mu$ m pore size Transwell polycarbonate filters for the indicated period of time. For experiments with non-polarized MDCK cells, the cells were sparsely seeded onto glass cover slips in Minimal Essential Medium without FBS and allowed to attach for 2 hours. Afterwards, the medium was changed to s-MEM (GIBCO-BRL; Gaithersburg, MD) using three washes of 10 minutes each, and the cells were incubated overnight (i.e. 16-18 hours). In some experiments the cells were allowed to endocytose IgA or

transferrin during this over night incubation by adding 50 microgram/ml polymeric IgA or 1 microgram/ml iron-loaded canine transferrin, respectively.

### ***Transfection***

For expression of human syntaxin 11, MDCK cells were transfected with the syntaxin 11 cDNA in the expression vector pCDNA3 by the calcium phosphate method, followed by selection in media containing 350 µg/ml G418 (as described in (37)). For all experiments, a mixture of the G418-resistant cells, displaying a wide range of expression levels, was used. MDCK cells stably expressing rat syntaxins 2, 3 and 4 are described in (16). MDCK cells expressing human SNAP-23 were described in (18). MDCK cells expressing the wild-type rabbit pIgR (38), signal-less pIgR (39) or GPI-pIgR (40) have been described previously.

### ***Confocal Immunofluorescence Microscopy***

Cells were either fixed in methanol at -20 °C or with 4% paraformaldehyde and permeabilized with 0.025% (wt/vol) saponin Sigma (St. Louis, MO) in phosphate buffered saline, and blocked with 10% FBS or 5% BSA followed by sequential incubations with primary antibodies and FITC- and/or Texas red-conjugated secondary antibodies. In some cases, nuclei were stained with 5 µg/ml propidium iodide (Vector; Burlingame, CA) after treatment with 100 µg/ml RNase A. The samples were analyzed using a LEICA TCS-NT confocal microscope.

## **RESULTS**

### ***Syntaxin 11 is expressed at the plasma membrane in polarized but not non-polarized MDCK cells.***

The following t-SNAREs are localized to the plasma membrane in mammalian cells: the neuron-specific syntaxins 1A, 1B and SNAP-25 function in the fusion of synaptic vesicles with the presynaptic plasma membrane. The more widely expressed syntaxins 2, 3, and 4 and SNAP-23 have been studied in various cell types where they are generally localized at the plasma membrane (16, 18, 20, 41, 42). All other syntaxin homologues studied so far are localized to various intracellular organelles where they are believed to be functionally involved in membrane trafficking pathways directed to these organelles.

The recently discovered syntaxin 11, has an unusual primary structure as it lacks a C-terminal transmembrane domain (30, 43, 44). Nevertheless, syntaxin 11 is membrane-bound. In transiently transfected, non-polarized, NRK or HeLa cells, syntaxin 11 was found in intracellular vesicles that partially co-localized with endosomal and trans-Golgi network markers (30, 43). Syntaxin 11 is widely expressed in several tissues including tissues rich in epithelia such as lung, placenta, liver and kidney while it is absent in brain (30, 43, 44). This tissue distribution prompted us to investigate whether syntaxin 11 is expressed in several pure epithelial cell lines. By western blot syntaxin 11 can be detected in total membrane fractions of MDCK cells and Caco-2 colon carcinoma cells as well as in HeLa cells while it is undetectable in the intestinal epithelial cell line HT-29 and hepatocyte-derived HepG2 cells. The gel mobility of endogenous syntaxin 11 in HeLa cells is slightly higher than in MDCK and Caco-2 cells. The reason for this difference is unknown and may be caused by differences in posttranslational modification.

Next, we studied the subcellular localization of syntaxin 11 in MDCK cells since this epithelial cell line has been most extensively studied with respect to the localization and function of t-SNAREs. Since our syntaxin 11 antibody did not react well for immunocytochemistry with the endogenous canine protein, MDCK cells were stably transfected with the cDNA of the human protein. Confocal immunofluorescence microscopy revealed that syntaxin 11 is localized predominantly at the plasma membrane in polarized MDCK cells, rather than in intracellular compartments as previously reported for non-polarized cells. The majority of syntaxin 11 localizes to both the apical and basolateral plasma membrane with some additional intracellular punctate staining mostly in the apical cytoplasm. This localization was independent of the level of syntaxin 11 expression as found by comparing individual cells with a wide range of expression levels in a mixed population of stably transfected cells. Also, the level of exogenous human syntaxin 11 expression was similar to the endogenous level in MDCK cells.

Surprisingly, in non-polarized MDCK cells, e.g. shortly after plating and not allowing the cells enough time to form cell-cell interactions, syntaxin 11 was found to be intracellular with very little, if any, plasma membrane staining.

Under these conditions, syntaxin 11 localizes to bright punctate vesicles similarly as previously reported in non-polarized fibroblastic cells (30, 43). Co-staining of syntaxin 11 with an antibody against the lysosomal/late endosomal protein LAMP-2 shows no significant overlap indicating that syntaxin 11 is not simply being degraded in non-polarized MDCK cells. The observed dramatic change in localization of syntaxin 11 depending on the state of cellular polarity of MDCK cells suggests that it normally functions at the plasma membrane in polarized epithelial cells while it may have a different function in non-polarized cells.

*The subcellular localization of all plasma membrane t-SNAREs changes during the development of epithelial polarity.*

As with syntaxin 11, we observed that the previously characterized plasma membrane t-SNAREs in MDCK cells also undergo similar dramatic changes in subcellular localization depending on the degree of cellular polarity. In a time course of MDCK cells at various stages during the establishment of a fully polarized monolayer. The cells were plated at high density onto polycarbonate filters and the localization of syntaxins 2, 3, 4, 11 and SNAP-23, as well as the tight junction protein ZO-1, were monitored at different times after plating. After 2 hours, the cells are irregularly shaped and start to form cell-cell contacts. At this stage, all plasma membrane t-SNAREs are found predominantly in intracellular vesicles in addition to a variable amount of plasma membrane staining. In approximately 10% of the cells, large intracellular vacuolar structures can be observed (arrows). After one day, the monolayer is confluent and uninterrupted circumferential tight junctions are established. A substantial portion of all SNAREs has re-localized to the plasma membrane in a polarized manner. Syntaxins 2 and 11 as well as SNAP-23 are found at both the basolateral and apical plasma membrane in addition to some remaining intracellular labeling. Syntaxin 3 is absent from the basolateral domain but localizes to the apical domain in addition to intracellular lysosomes as established previously (16, 24). Syntaxin 4, in turn, is absent from the apical domain but has partially re-localized to the basolateral domain. During the course of the experiment, until day 7, the cells grow somewhat in height and form a straight apical surface. All of the SNAREs continue to move to their final destination at their

specific plasma membrane domains, however, even after 7 days some intracellular staining remains in each case as observed previously (16, 18).

This change in subcellular localization of the machinery that normally mediates vesicle fusion at the plasma membrane suggests that these membrane traffic pathways are fundamentally altered in epithelial cells during the course of the establishment of cellular polarity.

*Sustained inhibition of epithelial polarity causes intracellular accumulation of apical and basolateral t-SNAREs into distinct compartments.*

To study the nature of the intracellular location of plasma membrane t-SNAREs in detail we sought to arrest MDCK cells in a non-polarized state. The formation of a polarized epithelial layer can be prevented experimentally by the inhibition of E-cadherin-mediated interactions between neighboring cells (28, 45, 46). Inhibition of calcium-dependent homotypic E-cadherin binding by withdrawal of high calcium concentrations in the medium keeps MDCK cells in a non-polarized state. It has been observed previously that, when grown in low-calcium medium, MDCK cells form large intracellular vacuoles that bear ultrastructural resemblance to the apical plasma membrane including the presence of microvilli and an associated actin cytoskeleton. This compartment was termed 'vacuolar apical compartment' or VAC (47). Similar vacuoles are found in a variety of carcinomas (48, 49, 50).

We studied the subcellular localization of plasma membrane SNAREs in MDCK cells grown under these conditions. A high percentage (>50%) of the cells display one or more large vacuolar compartments that are positive for the endogenous apical marker protein gp135 and are indistinguishable in appearance from previously published . Plasma membrane t-SNAREs that normally localize to the apical domain (syntaxins 2, 3, 11, SNAP-23), co-localize with gp135 in these VACs. In contrast, the normally exclusively basolateral syntaxin 4 is excluded from gp135-positive VACs. Instead, in addition to small vesicles, syntaxin 4 is found in larger structures that resemble VACs but exclude gp135. The SNAREs that are normally localized to both apical and basolateral plasma membrane domains (syntaxins 2, 11, SNAP-23), can be found in large gp135-negative structures (arrows) in addition to gp135-positive VACs. These results suggest that at least two distinct intracellular organelles exist in non-polarized MDCK cells to which plasma membrane t-SNAREs are targeted.

To verify the results obtained with exogenously expressed syntaxin 3 in MDCK cells we investigated whether endogenous syntaxin 3 would also localize to VACs in a different cell line. The human colon carcinoma cell line Caco-2 was grown in low-calcium medium as above and stained for endogenously expressed syntaxin 3 and the microvillar protein villin. While syntaxin 3 and villin are localized at the apical plasma membrane in fully polarized Caco-2 cells (20, 24, 26) (and data not shown), they are strongly enriched in VACs in non-polarized cells . This result indicates that the localization of syntaxin 3 in VACs is a general phenomenon of non-polarized epithelial cells and not an artifact of syntaxin overexpression.

We and others found previously that syntaxin 3 partially localizes to lysosomes in addition to the apical plasma membrane in fully polarized MDCK and Caco-2 cells (16, 24). To investigate whether VACs containing syntaxin 3 may represent an enlarged type of lysosomes in cells grown under low-calcium conditions, MDCK cells were co-labeled for syntaxin 3 and the late endosomal/lysosomal protein LAMP-2. VACs and lysosomes are clearly distinct. This demonstrates that VACs are not simply enlarged lysosomes and suggests that they are not

connected to the late endosomal/lysosomal system and therefore not degradative compartments. Moreover, none of the other plasma membrane SNAREs co-localized with LAMP-2 in MDCK cells grown in low calcium medium (data not shown).

*Syntaxin 4 is a marker for a novel intracellular organelle in non-polarized MDCK cells.*

VACs have been described previously in non-polarized MDCK cells, and our finding that they contain apical-specific t-SNAREs suggest that they receive apical-specific membrane traffic. Our finding of syntaxin 4-positive intracellular organelles suggests that another class of intracellular plasma membrane-like organelles exists that may be the basolateral equivalent to the VAC. Since such an organelle has not been described before we sought to investigate its composition and relationship to other organelles in more detail by the following co-labeling studies. Basolateral, syntaxin 4-positive compartment also contains two proteins that are normally specifically localized at the basolateral plasma membrane domain in polarized MDCK cells: an endogenous 58 kDa basolateral plasma membrane protein (6.23.3) and the Na/K-ATPase. Both proteins appear to be even more concentrated in the intracellular compartments than syntaxin 4 which is also present at the plasma membrane. These data indicate that the syntaxin 4-positive compartment has a protein composition similar to the basolateral plasma membrane of polarized cells.

It is important to note that the degree of intracellular localization of SNAREs or any of the plasma membrane marker proteins studied here in non-polarized MDCK cells is very heterogeneous. We typically observed a range of individual cells displaying varying degrees of retention ranging from complete absence of plasma membrane markers from the plasma membrane to almost complete absence of these markers in intracellular organelles.

Next, we investigated whether E-cadherin might be accumulated in the syntaxin 4-positive compartment. In control cultures E-cadherin co-localizes with syntaxin 4 at the cell-cell contacts. In contrast, E-cadherin expression is strongly down-regulated in cells grown in low-calcium medium. The remaining minor amounts of E-cadherin partially co-localize with syntaxin 4 in intracellular organelles in addition to a diffuse staining pattern, but are not detectable at sites of cell-cell contact. Therefore, in contrast to the antigen 6.23.3. and the Na/K-ATPase, the normally lateral plasma membrane protein E-cadherin is not only being retrieved from the surface but its expression is also down-regulated.

Both apical and basolateral plasma membrane domains of polarized epithelial cells are generally associated with an actin cytoskeleton. Phalloidin-staining shows that in non-polarized MDCK cells in addition to the plasma membrane, both syntaxin 3 (data not shown) and syntaxin 4 positive vacuoles display an associated actin cytoskeleton. This result distinguishes VACs and the intracellular syntaxin 4-positive compartment from endosomes or other intracellular organelles which do not typically contain a prominent actin cytoskeleton.

Alpha-fodrin (non-erythroid spectrin) is a component of the actin-associated cytoskeleton that normally underlies the lateral plasma membrane in polarized epithelial cells and has been implicated in the sorting of basolateral membrane proteins, such as the Na/K-ATPase, by selective retention at the basolateral surface (51, 52, 53). We found that in MDCK cells grown in LC medium fodrin significantly co-localizes with syntaxin 4 in intracellular organelles in addition to plasma membrane-staining and diffuse cytoplasmic staining. This suggests that intracellular syntaxin 4-positive organelles not only possess the machinery for fusion of incoming transport

vesicles (syntaxin 4) but also the cytoskeletal components required for selective retention of basolateral membrane proteins and explains the accumulation of Na/K-ATPase in these organelles.

Cytokeratin intermediate filaments are normally closely attached to the basolateral plasma membrane domain of polarized epithelial cells by anchoring to desmosomes and hemidesmosomes. Using a pan-keratin antibody we found that intermediate filaments are largely retracted from the plasma membrane in MDCK cells grown in LC medium. They are concentrated in the center of the cell where they often appear to be closely associated with syntaxin 4-positive intracellular organelles.

The syntaxin 4-positive organelles often localize in a perinuclear position in MDCK cells grown in LC medium. Since this is typically also the localization of the Golgi apparatus within non-polarized we double-labeled cells for syntaxin 4 and the Golgi protein Golgin-97. Both proteins localize quite distinctly with no significant overlap, excluding the possibility that the syntaxin 4-positive organelles represent a distended Golgi apparatus in MDCK cells grown in LC medium.

Many cellular organelles tend to cluster around the microtubule organizing center (MTOC) which is typically found in a perinuclear position in non-polarized cells and indicates that these organelles are clustered there by microtubule-mediated transport. Co-staining of MDCK cells grown in LC medium for syntaxin 4 and  $\gamma$ -tubulin shows that although the syntaxin 4-positive organelles can be located very close to the MTOC, they show a more dispersed distribution suggesting that they are not necessarily being actively recruited towards the MTOC.

Recently, a novel organelle, termed 'aggresome' has been discovered in cells that either express excessive amounts of misfolded proteins or whose proteasome degradation machinery is inhibited (54, 55). They are pericentriolar cytoplasmic inclusions containing misfolded, ubiquitinated protein ensheathed in a cage of intermediate filament and closely associated with the centrosome. Since aggresomes share common features with our syntaxin 4-organelles morphologically, we investigated whether these two organelles could be related to or identical to each other. When MDCK cells grown in LC medium were stained for syntaxin 4 and ubiquitin only a diffuse cytoplasmic signal could be detected for ubiquitin that was clearly different from the large syntaxin 4-positive organelles (data not shown). Next, we treated the cells with the proteasome-inhibitor ALLN to induce the formation of aggresomes. Under these conditions, ubiquitin-positive aggresomes can clearly be identified which do not significantly overlap with syntaxin 4-positive organelles, demonstrating that they are distinct.

Together, the data suggests that although 'apical' and 'basolateral' t-SNAREs are localized intracellularly in non-polarized epithelial cells, they are nevertheless sorted to distinct compartments. These intracellular compartments resemble the respective plasma membrane domains due to the presence of 'apical' or 'basolateral' t-SNAREs as well as other plasma membrane marker proteins and an actin-based cytoskeleton.

### *'Intracellular plasma membrane organelles' can be observed under normal calcium conditions*

To exclude the possibility that the observed generation of apical and basolateral intracellular organelles in MDCK cells grown in LC medium may be caused by a decrease in the intracellular calcium concentration or any other non-relevant effect, we seeded MDCK cells sparsely in medium containing serum and a normal concentration of calcium. After 16 hours, the cells were

stained for syntaxin 4 and gp135. Under these conditions, a mixture of patches of confluent cells and smaller aggregates down to single cells is observed. Consistently, cells that are located at the edge of a cell patch tend to display intracellular syntaxin 4-positive organelles, while syntaxin 4 is restricted to the basolateral plasma membrane in cells that are completely surrounded by other cells. Single cells very frequently show intracellular syntaxin 4-positive organelles under these conditions while gp135-positive VACs are relatively sparse. Omission of serum increases the frequency of VACs in agreement with a previous report (50) but has no further apparent effect on syntaxin 4-positive organelles. Altogether, these results demonstrate that the occurrence of intracellular apical and basolateral organelles is not a function of the calcium concentration *per se* but rather depends on the degree of cell-cell interactions.

### *Protein sorting is preserved in non-polarized MDCK cells*

The presence of normally apical and basolateral plasma membrane t-SNAREs in cognate intracellular compartments in non-polarized cells suggests that these SNAREs function in the membrane fusion of vesicles from incoming transport pathways that are equivalent to the plasma membrane-directed transport pathways in polarized cells. We investigated how several proteins whose trafficking in polarized MDCK cells is well characterized are targeted in non-polarized cells.

The soluble secretory protein gp80/clusterin is endogenously expressed in MDCK cells and is normally secreted apically and basolaterally (approx. 2:1 ratio) in polarized MDCK cells (35). It shows that at steady-state, 16 hours after plating in low-calcium medium, large amounts of gp80 are retained inside individual cells and localize to both gp135-positive VACs and syntaxin 4-positive basolateral organelles. The protein must have reached these organelles on a direct route after biosynthesis because otherwise it would be secreted and lost from the cells. To estimate what proportion of gp80 is secreted vs. accumulated, we performed pulse-chase experiments and compared polarized cells grown on polycarbonate filters with non-polarized cells grown in low-calcium medium. After 3 hours, the secretion of newly synthesized gp80 from polarized cells is complete with 62% secreted apically and 36% basolaterally. In contrast, 13% of gp80 remain intracellular after three hours on a whole-population-basis. Considering that only approximately half of the cells display clearly identifiable apical and basolateral intracellular compartments under the culture conditions, we estimate that approximately one quarter of the synthesized gp80 is diverted into apical and basolateral intracellular organelles while the remainder is secreted.

Next, we investigated trafficking of the polymeric immunoglobulin receptor (pIgR). In polarized MDCK cells, pIgR is first transported to the basolateral plasma membrane domain and is subsequently transcytosed to the apical plasma membrane and released into the apical medium after proteolytic cleavage (56). We asked whether pIgR would be 'transcytosed' into the VAC in non-polarized MDCK cells. We found that after 16 hour incubation in low-calcium medium, a large amount of pIgR accumulates in the VAC. To support the interpretation that this is equivalent to the situation in polarized cells and follows an indirect route via the plasma membrane, we incubated non-polarized MDCK cells expressing pIgR in the presence of polymeric immunoglobulin A (IgA), the ligand of pIgR. If at least a fraction of the pIgR is targeted first to the plasma membrane before it reaches the VAC we would expect that it has the ability to transport IgA from the medium into the VAC. We found that this is the case. After incubation for 16 hours

the majority of the internalized IgA is found in gp135-positive VACs demonstrating the specificity of this cognate transcytotic pathway in non-polarized MDCK cells.

Two mutant forms of the pIgR have been previously generated that are deficient in direct TGN-to-basolateral plasma membrane transport in polarized MDCK cells and are instead directly targeted to the apical domain. Signal-less-pIgR (SL-pIgR) is a transmembrane protein in which the basolateral targeting signal in the cytoplasmic domain of pIgR has been deleted (39). In the GPI-anchored pIgR (GPI-pIgR) the entire cytoplasmic domain has been deleted (40) resulting in the attachment of a GPI-anchor (S.L., K.M., T.W., manuscript in preparation). We have previously shown that the trafficking to the apical plasma membrane of SL- and GPI-pIgR involves syntaxin 3 and SNAP-23 (17). Both proteins are transported to the gp135-positive VAC in non-polarized MDCK cells. To assess whether the VAC is reached directly after biosynthesis or indirectly after initial delivery to the plasma membrane, we measured the surface delivery of SL-pIgR quantitatively by pulse-chase analysis. We made use of the previous finding that the extracytoplasmic domain of pIgR contains a cleavage site that allows the rapid release of this domain into the medium in the presence of low amounts of *Staphylococcus aureus* V8 endoprotease. Surface delivery of SL-pIgR in filter-grown polarized cells is complete after 3 hours with an apical/basolateral ratio of approximately 4:1. In contrast to the observed diminished secretion of gp80 (see above), the kinetics of SL-pIgR surface delivery were nearly identical between polarized and non-polarized cells. This indicates that almost all of the SL-pIgR that is found in the VAC at steady-state has reached this organelle indirectly via the plasma membrane. This is supported by the finding that SL-pIgR is able to transport IgA from the medium into the VACs (data not shown).

In contrast to IgA, transferrin is normally endocytosed from the basolateral plasma membrane and recycled back to the same domain in polarized MDCK cells. Only a very small percentage, if any, of internalized transferrin is transcytosed to the apical plasma membrane (22, 57). If the VAC is indeed a cognate compartment to the apical plasma membrane, we expect that transferrin added to the medium would have no access to this compartment. After 16 hour incubation, transferrin is internalized in non-polarized MDCK cells but remains excluded from the gp135-positive VAC. Instead, internalized transferrin significantly co-localizes with syntaxin 4 in large intracellular organelles. This result shows that transferrin is endocytosed and - instead of being recycled to the basolateral plasma membrane in polarized cells - at least a fraction of it is transported to the intracellular syntaxin 4 compartment. The majority of the additional small punctate transferrin-staining does not coincide with syntaxin 4 but is typical for endosomes which transferrin normally travels through. These results indicate that the intracellular syntaxin 4-compartment is distinct from typical endosomes but receives endocytic traffic characteristic of the basolateral plasma membrane.

Together, these results strongly suggest that the intracellular apical and basolateral compartments in non-polarized MDCK cells are cognate compartments to the apical and basolateral plasma membrane in polarized cells. They are equipped with a set of t-SNAREs that corresponds to the respective domains of polarized cells and receive membrane traffic from equivalent biosynthetic and endocytic pathways. The over-all conclusion from these findings is that protein sorting is still preserved after MDCK cells have lost their cell polarity and that apical and basolateral proteins are not simply being randomly mixed together.

In the present paper we show that t-SNAREs that are normally localized at the plasma membrane in polarized epithelial cells distribute to intracellular compartments when cell polarity

is lost or not yet established. Syntaxin 11 was identified as a new additional plasma membrane SNARE in polarized MDCK cells. This increases the number of epithelial plasma membrane syntaxins to four and raises the question whether they all serve separate membrane traffic pathways. Only syntaxins 3 and 4 show a polarized distribution at the apical and basolateral plasma membrane domain, respectively, while syntaxins 2 and 11 and SNAP-23 localize to both domains. SNAP-23 may be a common binding partner of all plasma membrane syntaxins as it can bind to syntaxins 1, 2, 3, 4 and 11 (19, 30). To date, the only functional information on the involvement of syntaxin homologues in plasma membrane traffic in polarized cells is available for syntaxin 3 which plays a role in transport from the TGN and from apical endosomes to the apical plasma membrane (17, 58) and syntaxin 4 which was found to be involved in the biosynthetic pathway leading to the basolateral plasma membrane (58). The role of the nonpolarized syntaxins 2 and 11 remains unclear but they may serve non-polarized pathways directed towards both domains. Syntaxin 11 has been reported to localize to endosomal and TGN-related compartments when exogenously expressed in non-polarized NRK or HeLa cells (30, 43). We show that in non-polarized MDCK cells syntaxin 11 is also localized to punctate intracellular vesicles with very little, if any, detectable plasma membrane staining. However, as the cells form a polarized monolayer, the majority of syntaxin 11 re-localizes to both the apical and basolateral plasma membrane domains. This suggests that, at least in polarized epithelial cells, syntaxin 11 functions primarily as a plasma membrane t-SNARE. The tissue distribution of syntaxin 11 (30, 43, 44), suggests that it may be predominantly expressed in epithelial cells which is supported by our finding that it is expressed in several epithelial cell lines. This emphasizes the importance of studying localization and function of SNAREs in fully differentiated cells, such as polarized epithelial cells.

All of the plasma membrane t-SNAREs re-localize to varying degrees to intracellular compartments in MDCK cells when the formation of a polarized cell monolayer is prevented either temporarily during the course of the establishment of a monolayer or after a sustained inhibition of cell contacts in low-calcium medium. t-SNAREs are an integral part of the machinery accomplishing the final step of each membrane trafficking pathway. Therefore, this surprising result strongly suggests that membrane trafficking pathways that are normally directed to the plasma membrane in polarized epithelial cells undergo a fundamental shift towards intracellular compartments upon loss of cell polarity. This may have profound implications for our understanding of the pathogenesis of diseases involving a loss of epithelial polarity, e.g. the mistargeting of basement membrane proteins, proteases, integrins etc. that play a role in the pathogenesis of invasive and metastatic carcinomas (28), or the mistargeting of ion transporters, growth hormone receptors etc. in non-cancerous epithelial diseases such as polycystic kidney disease (59, 60). Also, during tubule formation - e.g. in kidney development - epithelial cells temporarily lose their cellular polarity while cell-rearrangements occur (61).

Is it possible that the observed intracellular localization of SNAREs in non-polarized MDCK cells is an artifact caused by heterologous SNARE-expression or calcium-deficiency? Most experiments presented here made use of canine MDCK cells that stably express rat (syntaxins 2, 3, 4) or human (syntaxin 11, SNAP-23) t-SNAREs. The following considerations argue against the idea that heterologously expressed SNAREs would be targeted different from endogenous SNAREs. First, the expression-levels are generally comparable to the endogenous levels (16, 18)). Second, the comparison of either different clones with varying SNARE-expression levels or individual cells in a mixed clonal population fails to reveal a correlation between

expression-level and subcellular localization, both in polarized and non-polarized cells. Third, the localization of syntaxins (16) and SNAP-23 (18) in transfected MDCK cells could be confirmed with endogenously expressed proteins in other cell lines or tissues (20, 23, 24, 25, 26). Fourth, in this study we have shown that endogenously expressed syntaxin 3 in Caco-2 cells localizes to VACs just as in transfected MDCK cells. Altogether, we therefore consider it unlikely that SNARE-expression levels as used in this study have adverse effects on SNARE-targeting in MDCK cells. The possibility that cellular calcium-depletion per se may cause the generation of intracellular plasma membrane organelles independent of epithelial cell polarity is unlikely for the following reasons. First, VACs have been observed by others in mammary carcinoma cells grown in medium containing a regular calcium concentration (50). Second, VAC-like organelles are frequently found in a variety of carcinomas in situ (49, 50) and in intestinal epithelial cells in the genetic disorder microvillus inclusion disease (62). Third, the intracellular calcium concentration has been measured previously in MDCK cells grown in high- or low-calcium medium and was found to be not significantly different (47). Fourth, we observed VACs and syntaxin 4-positive basolateral organelles in MDCK cells that are grown in regular-calcium medium either for brief periods of time, and in single cells or cells at the edge of cell patches after sparse seeding and growth for 16 hours.

The VAC has been described and characterized previously in non-polarized MDCK cells and other epithelial cell lines as well as in carcinomas (47, 50, 63, 64, 65). In contrast, to our knowledge, the basolateral compartment that we identified here is a novel organelle that has not been described previously, perhaps because of the lack of availability of a marker protein such as syntaxin 4. Our data shows that the syntaxin 4-compartment contains other, normally basolateral, plasma membrane proteins such as the Na/K-ATPase and the antigen 6.23.3. In addition, this compartment possesses a prominent membrane cytoskeleton containing actin and fodrin which is typical for the basolateral plasma membrane in polarized cells. This organelle excludes apical plasma membrane markers including the apical-specific syntaxin 3. We could show that this novel organelle does not overlap with the morphologically similar Golgi apparatus or the aggresome. The absence of the lysosomal protein LAMP-2 as well as ubiquitin makes it highly unlikely that the syntaxin 4-positive organelles, or VACs, are degradative compartments.

The presence of, normally apical or basolateral, plasma membrane t-SNAREs on intracellular organelles in non-polarized cells suggests that plasma membrane proteins and secretory proteins are targeted into these vacuoles. Since apical and basolateral SNAREs are found in two separate organelles, this suggests that protein sorting is still preserved in non-polarized MDCK cells. Our finding that internalized IgA reaches only the VAC while transferrin reaches the syntaxin 4-positive organelle demonstrates that both compartments receive endocytic traffic and that trafficking into these organelles is specific. Both compartments also receive direct biosynthetic traffic since the soluble secretory protein gp80 accumulates in them. By pulse-chase analysis, we found however that only a fraction of gp80 (estimated 25%) is deposited into VACs and syntaxin 4-organelles while the majority is secreted. This fits with the finding that even in non-polarized cells, variable amounts of plasma membrane SNAREs are typically located at the plasma membrane in addition to intracellular organelles. In contrast to the soluble marker gp80, the sorting of integral membrane proteins into apical and basolateral intracellular organelles appears to be more efficient. At steady-state, gp135 is often very strongly enriched in VACs while Na/K-ATPase and the 6.23.3-antigen are strongly enriched in basolateral organelles. Our data indicates that this high efficiency is mostly due to sorting after endocytosis of these proteins. Pulse-chase

analysis of the SL-pIgR shows that nearly all of the newly synthesized protein is initially targeted to the surface. Since SL-pIgR is able to internalize IgA into VACs, and since we find SL-pIgR enriched in VACs at steady-state, the majority of the protein must be internalized and transported to VACs after its initial plasma membrane-delivery. This is the first direct evidence that trafficking into VACs follows mostly an indirect route via the plasma membrane. It had been suggested previously that trafficking of the influenza hemagglutinin into VACs occurs directly from the TGN (66), but the possibility of an indirect pathway could not be experimentally excluded.

Together, our results suggests that apical/basolateral sorting is preserved in non-polarized epithelial cells and leads to specific intracellular organelles. It has been found previously that non-polarized, fibroblastic cells also have the capability to sort apical and basolateral plasma membrane proteins (presumably in the TGN) and transport them on separate routes to the identical plasma membrane (67, 68). A major difference between non-polarized cells of epithelial and non-epithelial origin may therefore be that in the former plasma membrane proteins are eventually retained inside the cell rather than displayed at the surface.

What can be the possible function of "intracellular apical and basolateral plasma membranes"? These compartments are observed in epithelial cells that have lost their cellular polarity temporarily (e.g. sparsely seeded cells that have not yet established cell contacts) or permanently (e.g. when cell contacts are inhibited or in tumor cells). It is likely that many plasma membrane or secreted proteins are still synthesized under these conditions. We speculate that there may be two reasons for the intracellular sequestration of plasma membrane proteins by non-polarized epithelial cells. The phenomenon may be a cellular survival mechanism: to re-localize (normally apical and basolaterally separated) ion channels and transporters to intracellular compartments which would prevent potential ATP-depletion due to futile cycles of ion transport in and out of the cell. Also, excessive intracellular ion accumulation or depletion would be prevented. This view is supported by our finding that the majority of Na/K-ATPase re-localizes to VBCs. The phenomenon may also be an organismal protection mechanism since it would prevent the unwanted surface-display of inappropriate proteins, e.g. proteases, cell-cell- or cell-matrix interacting proteins that may promote tumor invasion and metastasis. Interestingly, a variety of hydrolytic enzymes that are normally expressed at the apical plasma membrane of Caco-2 cells have been found in VACs after microtubule disruption (63). The finding that neither the apical nor basolateral vacuoles appear to be degradative, lysosomal compartments indicates that proteins may be stored in them for later use once cell contacts have been re-established. This is supported by the observation that VACs can be rapidly exocytosed as a whole from MDCK cells after re-establishment of cell-cell contacts (64) or after raising the intracellular cAMP concentration (65).

## FOOTNOTES

### Abbreviations:

IgA, immunoglobulin A

MDCK, Madin-Darby canine kidney

pIgR, polymeric immunoglobulin receptor

SL-pIgR, Signal-less-pIgR

SNARE, soluble N-ethyl maleimide sensitive factor (NSF) attachment protein (SNAP) receptor

t-SNARE, target membrane SNARE

v-SNARE, vesicle membrane SNARE

TGN, trans Golgi network  
VAC, vacuolar apical compartment

## 6. KEY RESEARCH ACCOMPLISHMENTS

- We identified syntaxin-11 as a novel apical and basolateral plasma membrane t-SNARE.
- All plasma membrane t-SNAREs, 2,3,4, 11, redistribute to intracellular locations when MDCK cells lose their cellular polarity.
- Apical SNAREs re-localize to the previously characterized vacuolar apical compartment (VAC).
- Basolateral SNAREs redistribute to a novel organelle that appears to be the basolateral equivalent of the VAC.
- Both 'intracellular plasma membrane compartments' have an associated prominent actin cytoskeleton and receive membrane traffic from cognate apical or basolateral pathways, respectively.

## 7. REPORTABLE OUTCOMES

Pollack, A.L., Runyan, R.B. and Mostov, K.E. Morphogenetic mechanisms of epithelial tubulogenesis: MDCK cell polarity is transiently rearranged without loss of cell-cell contact during scatter factor/hepatocyte growth factor-induced tubulogenesis. *Dev. Biol.*, 204:64-79, 1998.

Low, S.-H., Miura, M., Roche, P.A., Valdez, A.C., Mostov, K.E., and Weimbs, T. Intracellular redirection of plasma membrane trafficking after loss of epithelial cell polarity. *Mol. Biol. Cell*, 11:3045-3060, 2000.

## 8. CONCLUSIONS

In conclusion, we have shown that upon loss of cell polarity epithelial cells re-localize plasma membrane t-SNAREs and re-direct membrane trafficking pathways to intracellular cognate apical and basolateral compartments. This is likely to be a general phenomenon in epithelia and may play a fundamental role in the pathogenesis of epithelial diseases that involve a break-down of cell polarity.

## 9. REFERENCES

1. J. E. Rothman, G. Warren, *Curr Biol* **4**, 220-33 (1994).
2. P. I. Hanson, J. E. Heuser, R. Jahn, *Curr Opin Neurobiol* **7**, 310-5 (1997).
3. J. C. Hay, R. H. Scheller, *Curr Opin Cell Biol* **9**, 505-512 (1997).
4. B. J. Nichols, H. R. Pelham, *Biochim Biophys Acta* **1404**, 9-31 (1998).

5. T. Weimbs, et al., *Proc. Natl. Acad. Sci. USA* **94**, 3046-3051 (1997).
6. T. Weimbs, K. E. Mostov, S. H. Low, K. Hofmann, *Trends in Cell Biology* **8**, 260-262 (1998).
7. S. Christoforidis, H. M. McBride, R. D. Burgoyne, M. Zerial, *Nature* **397**, 621-5 (1999).
8. L. Gonzalez, Jr., R. H. Scheller, *Cell* **96**, 755-8 (1999).
9. S. R. Pfeffer, *Nature Cell Biology* **1**, E17-E22 (1999).
10. D. Louvard, M. Kedinger, H. P. Hauri, *Annu Rev Cell Biol* **8**, 157-95 (1992).
11. K. Simons, et al., *Cold Spring Harb Symp Quant Biol* **57**, 611-9 (1992).
12. A. H. Le Gall, C. Yeaman, A. Muesch, E. Rodriguez-Boulan, *Semin Nephrol* **15**, 272-84 (1995).
13. D. G. Drubin, W. J. Nelson, *Cell* **84**, 335-44 (1996).
14. C. Yeaman, K. K. Grindstaff, W. J. Nelson, *Physiol Rev* **79**, 73-98 (1999).
15. T. Weimbs, S. H. Low, S. J. Chapin, K. E. Mostov, *Trends in Cell Biology* **7**, 393-399 (1997).
16. S. H. Low, et al., *Mol. Biol. Cell* **7**, 2007-2018 (1996).
17. S. H. Low, et al., *J Cell Biol* **141**, 1503-13 (1998).
18. S. H. Low, et al., *J. Biol. Chem.* **273**, 3422-3430 (1998).
19. V. Ravichandran, A. Chawla, P. A. Roche, *J. Biol. Chem.* **271**, 13300-13303 (1996).
20. T. Galli, et al., *Mol Biol Cell* **9**, 1437-48 (1998).
21. J. F. St-Denis, J. P. Cabaniols, S. W. Cushman, P. A. Roche, *Biochem J* **338**, 709-15 (1999).
22. S. M. Leung, D. Chen, B. R. DasGupta, S. W. Whiteheart, G. Apodaca, *J Biol Chem* **273**, 17732-41 (1998).
23. H. Y. Gaisano, et al., *Mol. Biol. Cell* **7**, 2019-2027 (1996).
24. M. H. Delgrossi, L. Breuza, C. Mirre, P. Chavrier, A. Le Bivic, *J Cell Sci* **110**, 2207-14 (1997).
25. H. Fujita, P. L. Tuma, C. M. Finnegan, L. Locco, A. L. Hubbard, *Biochem J* **329**, 527-38 (1998).
26. K. Riento, et al., *J Cell Sci* **111**, 2681-8 (1998).
27. L. Sorokin, P. Ekblom, *Kidney Int* **41**, 657-64 (1992).
28. W. Birchmeier, J. Behrens, K. M. Weidner, J. Hulsken, C. Birchmeier, *Curr Top Microbiol Immunol* **213**, 117-35 (1996).
29. E. M. Fish, B. A. Molitoris, *N Engl J Med* **330**, 1580-8 (1994).
30. A. C. Valdez, J.-P. Cabaniols, M. J. Brown, P. A. Roche, *J. Cell Sci.* **112**, 845-54 (1999).
31. I. R. Nabi, E. Rodriguez-Boulan, *Mol Biol Cell* **4**, 627-35 (1993).
32. G. K. Ojakian, R. Schwimmer, *J Cell Biol* **107**, 2377-87 (1988).
33. B. Gumbiner, K. Simons, *J Cell Biol* **102**, 457-68 (1986).
34. J. Balcarova-Stander, S. E. Pfeiffer, S. D. Fuller, K. Simons, *Embo J* **3**, 2687-94 (1984).
35. J. Urban, K. Parczyk, A. Leutz, M. Kayne, C. Kondor-Koch, *J Cell Biol* **105**, 2735-43 (1987).
36. G. Apodaca, K. A. Katz, K. E. Mostov, *J. Cell Biol.* **125**, 67-86 (1994).
37. P. Breitfeld, Casanova, J.E., Harris, J.M., Simister, N.E., and Mostov, K.E., *Meth. Cell Biol.* **32**, 329-337 (1989).
38. K. E. Mostov, D. L. Deitcher, *Cell* **46**, 613-621 (1986).
39. J. E. Casanova, G. Apodaca, K. E. Mostov, *Cell* **66**, 65-75 (1991).

40. K. E. Mostov, A. de Bruyn Kops, D. L. Deitcher, *Cell* **47**, 359-364 (1986).
41. M. K. Bennett, et al., *Cell* **74**, 863-73 (1993).
42. G. Wang, et al., *J Cell Sci* **110**, 505-13 (1997).
43. R. J. Advani, et al., *J Biol Chem* **273**, 10317-24 (1998).
44. B. L. Tang, D. Y. Low, W. Hong, *Biochem Biophys Res Commun* **245**, 627-32 (1998).
45. M. E. Bracke, F. M. Van Roy, M. M. Mareel, *Curr Top Microbiol Immunol* **213**, 123-61 (1996).
46. B. M. Gumbiner, *Cell* **84**, 345-57 (1996).
47. D. E. Vega-Salas, P. J. Salas, E. Rodriguez-Boulan, *J Cell Biol* **104**, 1249-59 (1987).
48. H. F. Kern, H. D. Roher, M. von Bulow, G. Kloppel, *Pancreas* **2**, 2-13 (1987).
49. L. Remy, *Biol Cell* **56**, 97-105 (1986).
50. D. E. Vega-Salas, J. A. San Martino, P. J. Salas, A. Baldi, *Differentiation* **54**, 131-41 (1993).
51. W. J. Nelson, R. W. Hammerton, *J Cell Biol* **108**, 893-902 (1989).
52. W. J. Nelson, R. W. Hammerton, A. Z. Wang, E. M. Shore, *Semin Cell Biol* **1**, 359-71 (1990).
53. R. W. Hammerton, et al., *Science* **254**, 847-50 (1991).
54. J. A. Johnston, C. L. Ward, R. R. Kopito, *J Cell Biol* **143**, 1883-98 (1998).
55. W. C. Wigley, et al., *J Cell Biol* **145**, 481-90 (1999).
56. K. E. Mostov, et al., *Cold Spring Harb. Symp. Quant. Biol.* **60**, 775-781 (1995).
57. G. Odorizzi, I. S. Trowbridge, *J Cell Biol* **137**, 1255-64 (1997).
58. F. Lafont, et al., *Proc Natl Acad Sci U S A* **96**, 3734-8 (1999).
59. N. S. Murcia, R. P. Woychik, E. D. Avner, *Pediatr Nephrol* **12**, 721-6 (1998).
60. L. P. Sullivan, D. P. Wallace, J. J. Grantham, *Physiol Rev* **78**, 1165-91 (1998).
61. A. L. Pollack, R. B. Runyan, K. E. Mostov, *Dev Biol* **204**, 64-79 (1998).
62. N. A. Ameen, P. J. I. Salas, *Traffic* **1**, 76-83 (2000).
63. T. Gilbert, E. Rodriguez-Boulan, *J Cell Sci* **100**, 451-8 (1991).
64. D. E. Vega-Salas, P. J. Salas, E. Rodriguez-Boulan, *J Cell Biol* **107**, 1717-28 (1988).
65. M. Brignoni, et al., *Exp Cell Res* **205**, 171-8 (1993).
66. M. Brignoni, et al., *J Cell Sci* **108**, 1931-43 (1995).
67. A. Müsch, H. Xu, D. Shields, E. Rodriguez-Boulan, *J Cell Biol* **133**, 543-58 (1996).
68. T. Yoshimori, P. Keller, M. G. Roth, K. Simons, *J Cell Biol* **133**, 247-56 (1996).

# Morphogenetic Mechanisms of Epithelial Tubulogenesis: MDCK Cell Polarity Is Transiently Rearranged without Loss of Cell–Cell Contact during Scatter Factor/Hepatocyte Growth Factor-Induced Tubulogenesis

Anne L. Pollack,<sup>\*,†,1</sup> Raymond B. Runyan,<sup>†</sup> and Keith E. Mostov<sup>\*</sup>

<sup>\*</sup>Department of Anatomy, Department of Biochemistry and Biophysics, and Cardiovascular Research Institute, University of California at San Francisco, Box 0452, San Francisco, California 94143; and <sup>†</sup>Department of Cell Biology and Anatomy, University of Arizona Health Sciences Center, Box 245044, Tucson, Arizona 85724-5044

Many organ systems are composed of networks of epithelial tubes. Recently, molecules that induce development of epithelial tubules and regulate sites of branching have been identified. However, little is known about the mechanisms regulating cell rearrangements that are necessary for tubule formation. In this study we have used a scatter factor/hepatocyte growth factor-induced model system of MDCK epithelial cell tubulogenesis to analyze the mechanisms of cell rearrangement during tubule development. We examined the dynamics of cell polarity and cell–cell junctions during tubule formation and present evidence for a multistep model of tubulogenesis in which cells rearrange without loss of cell–cell contacts and tubule lumens form *de novo*. A three-dimensional analysis of markers for apical and basolateral membrane subdomains shows that epithelial cell polarity is transiently lost and subsequently regained during tubulogenesis. Furthermore, components of cell–cell junctional complexes undergo profound rearrangements: E-cadherin is randomly distributed around the cell surface, desmoplakins I/II accumulate intracellularly, and the tight junction protein ZO-1 remains localized at sites of cell–cell contact. This suggests that differential regulation of cell–cell junctions is important for the formation of tubules. Therefore, during tubulogenesis, cell–cell adhesive contacts are differentially regulated while the polarity and specialization of plasma membrane subdomains reorganize, enabling cells to remain in contact as they rearrange into new structures. © 1998 Academic Press

**Key Words:** tubulogenesis; epithelial polarity; cell–cell adhesion; kidney; morphogenesis.

## INTRODUCTION

Tubulogenesis is a developmental process common to the formation of many organs, including lung, salivary gland, mammary gland, pancreas, and kidney. Recent studies have shown that induction of morphogenesis of epithelial tubules in several different organs requires a complex interplay of many factors and receptors (Kjelsberg *et al.*, 1997;

Sakurai *et al.*, 1997a,b; Sariola and Sainio, 1997; Vainio and Muller, 1997). For instance, during mammalian metanephric kidney development, glial cell-derived neurotrophic factor and its receptors, c-ret and GFR $\alpha$ -1, have been shown to be involved in induction of tubulogenesis from the ureteric bud (Moore *et al.*, 1996; Pichel *et al.*, 1996; Sanchez *et al.*, 1996; Schuchardt *et al.*, 1994). Similarly, genetic analysis has identified several genes that control initiation of branching and direction of outgrowth of epithelial tubules during tracheal development in *Drosophila* (Klambt *et al.*, 1992; Sutherland *et al.*, 1996). In addition, antibody treatment of cultured kidney organ rudiments has demonstrated that scatter factor/hepatocyte growth factor (SF/

<sup>1</sup> To whom correspondence should be addressed at the Department of Cell Biology and Anatomy, Box 245044, University of Arizona Health Sciences Center, Tucson, AZ 85724-5044. Fax: (520) 626-2097. E-mail: luar@ns.arizona.edu.

HGF) can regulate tubule development (Woolf *et al.*, 1995). These growth factors and receptors can be considered the "upstream" regulators of tubulogenesis.

The "downstream" response to induction of epithelial tubulogenesis presumably involves cell movements and changes in cell adhesion, intercellular junctions, and cell polarity. In contrast to the inductive signals, downstream responses during epithelial tubulogenesis have previously received relatively little discussion in the cell biological literature (Gumbiner, 1992), perhaps because of the relative difficulty of examining tubulogenesis in experimental systems that have often involved the culturing of embryonic organ rudiments. In this paper we studied the downstream responses to induction of tubule formation in order to understand the mechanisms of cell rearrangement during tubulogenesis.

A significant advance for studying mechanisms of tubulogenesis was made by the development of an *in vitro* tubulogenesis model system using Madin-Darby canine kidney (MDCK) epithelial cells induced by SF/HGF (Montesano *et al.*, 1991a,b). The bipartite name of SF/HGF reflects that it was independently isolated for two separate functions. SF was first identified as a factor in fibroblast-conditioned medium that, when added to MDCK cells grown as small islands on an impermeable support, causes the cells to scatter. HGF was defined by its ability to induce mitogenesis of cultured hepatocytes. It was later discovered that these two factors are identical and that SF/HGF is a ligand for the c-met protooncogene (c-met), a receptor tyrosine kinase (Birchmeier and Birchmeier, 1993; Comoglio, 1993; Furlong, 1992; Rosen *et al.*, 1994). Previous studies have shown that SF/HGF induces collagen gel cultures of various epithelial cell types to undergo morphogenesis into organ-like structures that have characteristics of the organ from which the cells were derived (Brinkmann *et al.*, 1995). MDCK cells form hollow fluid-filled cysts when cultured in collagen gels. Exposure of these preformed epithelial cysts to SF/HGF causes the cysts to develop branching tubules in a process that resembles tubulogenesis *in vivo*.

When grown as a monolayer on a permeable filter support, MDCK cells form a well-polarized epithelial monolayer, exhibiting apical and basolateral plasma membrane domains with unique compositions and well-defined cell-cell junctional complexes containing tight junctions (TJ), adherens junctions, and desmosomes (DS) (Drubin and Nelson, 1996; Rodriguez-Boulton and Nelson, 1989; Weimbs *et al.*, 1997). Previous studies have shown that MDCK epithelial cells within both initial cysts and end-stage lumen-containing tubules are polarized with microvilli on luminal membranes, distinct apical and basolateral membranes, and cell-cell junctional complexes on lateral membrane borders (Montesano *et al.*, 1991b; Santos *et al.*, 1993; Wang *et al.*, 1990a). However, the dynamic changes in localization of apical/basolateral membrane markers and cell-cell junctional proteins during the transition between cyst and tubule have not been identified.

SF/HGF-induced tubulogenesis of MDCK cells in culture provides an excellent model system to study MDCK cell polarity and cell-cell interactions during tubulogenesis. Studies in which this system has been manipulated by genetic or pharmacological means have already proven to be a rich source of information on the mechanisms of tubulogenesis (Barros *et al.*, 1995; Boccaccio *et al.*, 1998; Cantley *et al.*, 1994; Crepaldi *et al.*, 1997; Derman *et al.*, 1995; Dugina *et al.*, 1995; Sachs *et al.*, 1996; Sakurai *et al.*, 1997a; Sakurai and Nigam, 1997; Santos *et al.*, 1993; Santos and Nigam, 1993; Weidner *et al.*, 1995). For instance, we have previously used this system to express a mutant  $\beta$ -catenin and show that correct interaction of  $\beta$ -catenin with APC protein is essential for a very early step in tubulogenesis (Pollack *et al.*, 1997). Similar studies have shown that  $\alpha 2$  integrins are critical for tubule formation (Berdichevsky *et al.*, 1994; Saelman *et al.*, 1995; Schwimmer and Ojakian, 1995). Moreover, recent work has dissected signaling pathways regulating tubulogenesis that are activated through the c-met receptor (Boccaccio *et al.*, 1998; Ponzetto *et al.*, 1994; Royal *et al.*, 1997; Sachs *et al.*, 1996; Weidner *et al.*, 1996, 1995). Given the pace of past progress and the future potential using this system, it is imperative to define the basic nature of the cell rearrangements and changes in cell adhesion, junctions, and polarity during tubule formation. This analysis will form the basis for the dissection of the mechanisms of cell rearrangements during tubulogenesis.

Several different models have been suggested to explain the morphogenetic mechanisms by which cells rearrange to form tubules. A two-stage dissociation/reassociation model proposed by Thiery and Boyer (1992) attempted to reconcile the apparently contradictory actions of SF/HGF in inducing scattering of MDCK cells grown on plastic versus tubulation of MDCK cells grown in collagen gels. In the first stage of this model, MDCK cells would detach from the cyst, lose their polarity, and migrate as single cells out from the cyst and into the surrounding collagen gel. In the second stage, the migrating single cells would coalesce and reassemble into multicellular structures that form tubules of polarized cells. A contrasting model, implicit in much of the discussions of tubulogenesis, envisions that tubules form as "outpouchings" from the cyst; in this model the lumen of the developing tubule is always continuous and directly connected to the lumen of the cyst (Gilbert, 1994; Sariola and Sainio, 1997). These two models make very different predictions not just about cell rearrangements, but about cell-cell adhesion, cell junctions, and cell polarity. In the two-stage dissociation/reassociation model, cells transiently lose all cell-cell adhesion and probably most, if not all, polarity, before reestablishing these *de novo*. In contrast, the outpouching model predicts that the cells never lose adhesion or polarity and remain in a monolayer organized around a lumen.

To test the mechanisms of cell rearrangement in tubulogenesis we investigated epithelial cell-cell interactions and polarity during transitional stages in the development of lumen-containing tubules by examining the spatiotemporal

**TABLE 1**  
Protein Markers for Epithelial Cell Polarity and Cell-Cell Junctions

Protein	Location in polarized epithelial cells	Proposed function	References
E-cadherin	Basolateral plasma membrane	Adherens junction cell-cell adhesion	Takeichi, 1991
gp135	Apical plasma membrane	?	Ojakian and Schwimmer, 1988
Desmoplakins I and II	Cytoplasmic plaque components of desmosomes on lateral plasma membrane	Desmosome cell-cell adhesion	Pasdar <i>et al.</i> , 1988b Garrod, 1993
ZO-1	Peripheral membrane component of tight junctions at the border between apical and basolateral plasma membrane	Tight junction cell-cell adhesion	Stevenson <i>et al.</i> , 1986

distribution of markers for apical and basolateral membranes and cell-cell junctions at multiple time points throughout tubule formation. We find that during the transition from a cyst to a tubule there is an initial loss of cell polarity, which is reestablished as lumen formation proceeds. We also find that lumen formation occurs *de novo* at sites of cell-cell contact, rather than by extrusion of the cyst lumen. Cell-cell adhesion is maintained throughout tubulogenesis. However, the patterns of relocation of components of adherens junctions, tight junctions, and desmosomes are distinct and suggest that differential regulation, rather than disruption of cell-cell associations, is an important mechanism for tubulogenesis.

## MATERIALS AND METHODS

### Cell Culture

MDCK type II cells (originally isolated at the EMBL in Heidelberg) (Louvard, 1980) were maintained in MEM containing Earle's balanced salt solution (MEM-EBSS; Cellgro, Mediatech, Inc., Washington, DC) supplemented with 5% FCS (Hyclone, Logan, UT), 100 U/ml penicillin, and 100 µg/ml streptomycin in 5% CO<sub>2</sub>/95% air. For growth of cells in three-dimensional collagen gels, MDCK cells were trypsinized and then triturated at room temperature into a single-cell suspension of  $5 \times 10^4$  cells/ml in a type I collagen solution containing 66% Vitrogen 100 (3 mg/ml; Celtrix, Palo Alto, CA), 1× MEM, 2.35 mg/ml NaHCO<sub>3</sub>, 0.02 M Hepes, pH 7.6, and 12% dH<sub>2</sub>O. Cells in suspension were then plated onto Nunc filters (Cat. No. 162243, 10 mm, 0.02- to 0.2-µm pore size; Applied Scientific, San Francisco, CA). The type I collagen solution was allowed to gel by incubation at 37°C, 95% air/5% CO<sub>2</sub> prior to addition of medium. Cultures were fed every 3–4 days and grown for 10–12 days, until MDCK cell cysts with lumen were formed.

### Antibodies/Reagents

Hybridoma cells secreting mouse anti-E-cadherin mAb (rr1; Gumbiner and Simons, 1986) were a kind gift from B. Gumbiner

(Sloan-Kettering, New York, NY). Rat mAb R40.76 against ZO-1, a tight junction peripheral membrane protein (Anderson *et al.*, 1988; Stevenson *et al.*, 1986), was obtained from B. Stevenson or Chemicon (Chemicon International, Temecula, CA). Rabbit polyclonal Ab against bovine desmosomal proteins desmoplakins I and II (dpl1/II; Pasdar and Nelson, 1988a) was generously provided by M. Pasdar (University of Alberta, Edmonton, Canada) and W. J. Nelson (Stanford University, Stanford, CA). Mouse mAb 3F2 supernatant against gp135, a MDCK apical membrane glycoprotein (Ojakian and Schwimmer, 1988), was kindly provided by W. J. Nelson (Stanford University) and G. Ojakian (SUNY Health Science Center, Brooklyn, NY). The marker proteins identified by the above antibodies are described in Table 1. All secondary antibodies used for immunofluorescence (goat anti-mouse-FITC, goat anti-rat-FITC, and goat anti-rabbit-FITC) were purchased from Jackson ImmunoResearch Laboratories (West Grove, PA). Propidium iodide (ppl) was purchased from Sigma Chemical Co. (St. Louis, MO). Recombinant human HGF was generously provided by R. Schwall (Genentech, South San Francisco, CA).

### Production of Fibroblast-Conditioned Media Containing SF/HGF

To obtain conditioned medium containing SF/HGF, MRC5 human lung fibroblasts (ATCC CCL171) were grown to confluence in DME (DMEH21, obtained from the UCSF cell culture facility) containing 10% FBS (Hyclone, Logan, UT), 100 U/ml penicillin, and 100 µg/ml streptomycin in T75 tissue culture flasks (Corning, Corning, NY) or, for 2× conditioned medium, in T150 ridged tissue culture flasks (Corning). The medium was replaced with 30 ml of fresh medium and cell culture was continued for 3 days. Conditioned medium was collected, centrifuged to remove cell debris, and frozen at –20°C until use. Control conditioned medium was obtained by growing D550 human foreskin fibroblasts (kindly provided by Ward D. Peterson, Detroit Medical Center, Detroit, MI) under the same culture conditions as for MRC5 cells, but in MEM-EBSS supplemented with 0.1 mM nonessential amino acids (100× stock, UCSF cell culture facility), 0.1% lactalbumin hydrolysate (Sigma), 0.1 mg/ml sodium pyruvate (100× stock, UCSF cell culture facility), and 10% FBS.

### **Treatment of MDCK Cysts with SF/HGF-Containing Media**

Three-dimensional cultures of MDCK cells grown to form cysts were treated for various numbers of days with D550 or MRC5 fibroblast-conditioned media diluted 1:1 with MEM-EBSS, 5% FBS. Cultures were refed daily with freshly diluted conditioned medium.

### **Immunofluorescence and Confocal Microscopy**

Cells in collagen gel cultures were processed for immunofluorescence at room temperature as follows: cultures were rinsed with PBS, pH 7.4, containing 1 mM  $\text{CaCl}_2$  and 0.5 mM  $\text{MgCl}_2$  ( $\text{PBS}^+$ ), fixed for 30 min with 4% paraformaldehyde in  $\text{PBS}^+$ , permeabilized for 30 min with 0.025% saponin in  $\text{PBS}^+$ , rinsed with  $\text{PBS}^+$ , and quenched for 10 min with 75 mM  $\text{NH}_4\text{Cl}$ , 20 mM glycine in  $\text{PBS}^+$ , pH 8.0. Nonspecific binding sites were blocked by rocking for 30 min in  $\text{PBS}^+$ , 0.025% saponin, 0.7% fish skin gelatin (block buffer) followed by 10 min in block buffer + 0.1 mg/ml boiled RNase A. Samples were then rocked 1–3 days at 4°C in primary antibodies diluted into blocking buffer containing 0.02% azide. Primary antibody concentrations were as follows: rr1 mAb supernatant, 3:1; R40.76 anti ZO-1 ascites, 1:150; R40.76 anti ZO-1 mAb supernatant, 3:1; rabbit anti-dp/II, 1:100; and gp135 mAb supernatant, 3:1. After extensive washing with  $\text{PBS}^+$ /saponin and blocking buffer, samples were incubated overnight at 4°C in blocking buffer containing 0.02% azide with FITC-conjugated secondary antibodies diluted 1:100 and pPI diluted 1:1000 from a 3–4 mg/ml stock. Samples were then washed extensively, postfixed with 4% paraformaldehyde in 0.1 M cacodylate buffer, pH 7.4, and mounted in Vectashield (Vector Labs, Burlingame, CA). Specific staining was clearly detected in confocal images of collagen gel samples. However trapping of secondary antibody aggregates within the collagen gel sometimes resulted in bright spots of staining in the collagen gel surrounding the cell cultures.

Confocal images were collected using a krypton-argon laser with K1 and K2 filter sets coupled to a Bio-Rad MRC600 confocal head and an Optiphot II Nikon microscope with a Plan Apo 60 $\times$  1.4 NA objective. Collagen gel cultures were imaged in the x-y plane of the sample with a motor step size of 0.5 or 1  $\mu\text{m}$ , Kalman filtering with five frames/image, and the diaphragm set at 1/3 open. To ensure a complete view of the complex three-dimensional aspects of the structures that were studied, we always obtained sets of serial sections collected in the x-y plane that completely spanned through control cysts or tubule-containing structures. Generally the figures shown present either selected individual x-y sections or projections of several consecutive sections that were selected from these complete serial sections. The data were analyzed using Comos and NIH Image software. Images were converted to TIFF format. Contrast levels of the images were adjusted and composites were prepared using Adobe Photoshop (Adobe Co., Mountain View, CA) on a PowerMacintosh 7200/75 (Apple, Cupertino, CA).

## **RESULTS**

Spatial and temporal changes in epithelial cell surface domains were analyzed during tubulogenesis by examining the distribution of marker proteins for apical, basolateral, and junctional membrane specializations during the devel-

opment of tubules from SF/HGF-stimulated MDCK cell cysts grown in collagen.

### **Development of Lumen-Containing Tubules from MDCK Cell Cysts Occurs in Four Distinct Stages**

To investigate how cell-cell interactions and polarity are altered during morphogenetic transitions in the development of lumen-containing tubules from polarized cysts, we studied MDCK cell cysts stimulated for various amounts of time with medium containing SF/HGF, a factor known to induce epithelial tubulogenesis.

MDCK cell cysts were treated between 0 and 7 days with either a control conditioned medium that does not contain SF/HGF or a SF/HGF-containing conditioned medium. Since other growth factors that act as upstream inducers of tubulogenesis may be present in the conditioned medium, we also examined cultures stimulated with purified recombinant human SF/HGF. Similar results were obtained with purified recombinant human SF/HGF (data not shown), suggesting that the downstream events examined in this study were induced by either conditioned medium or purified SF/HGF. Cell morphology and polarity were analyzed in individual confocal sections and projections of serial confocal sections by immunofluorescence detection of nuclei (pPI staining) and cell membrane proteins E-cadherin and GP135. Morphological transitions that were observed during tubule development are first shown diagrammatically in Fig. 1 and are supported in data presented below. Although morphogenesis of lumen-containing tubules occurs as a continuous process, we observe four distinct stages of tubule development which we define as follows: (1) extensions, (2) chains, (3) cords, and (4) tubules. Cysts (Fig. 1A) are composed of a spherical monolayer of MDCK cells that seals off a fluid-filled central lumen. Extensions, formed after 1 day of stimulation, consist of membrane protrusions from individual cells of the cyst that extend into the extracellular matrix (Fig. 1B). Chains of cells that are connected to the cyst develop within 1–3 days of stimulation (Fig. 1C). After 3–5 days of SF/HGF treatment, cords form that are two to three cells thick and develop discontinuous lumens (Fig. 1D). Finally, tubules develop in which discontinuous lumens have enlarged, coalesced, and become continuous with the lumen of the cyst (Fig. 1E). The development of tubules in this system is sequential, although not completely synchronous, and tubules in several stages of development may be found emanating from a single cyst. Therefore, we present our data in terms of morphological stages rather than absolute time after addition of SF/HGF-containing medium.

### **Extension and Chain Stages of Tubulogenesis: Polarity of MDCK Membrane Domains Is Lost in Cells That Extend from a Cyst to Form a Branching Chain**

To analyze epithelial membrane polarity during SF/HGF-induced tubulogenesis we collected stacks of 1- $\mu\text{m}$  serial

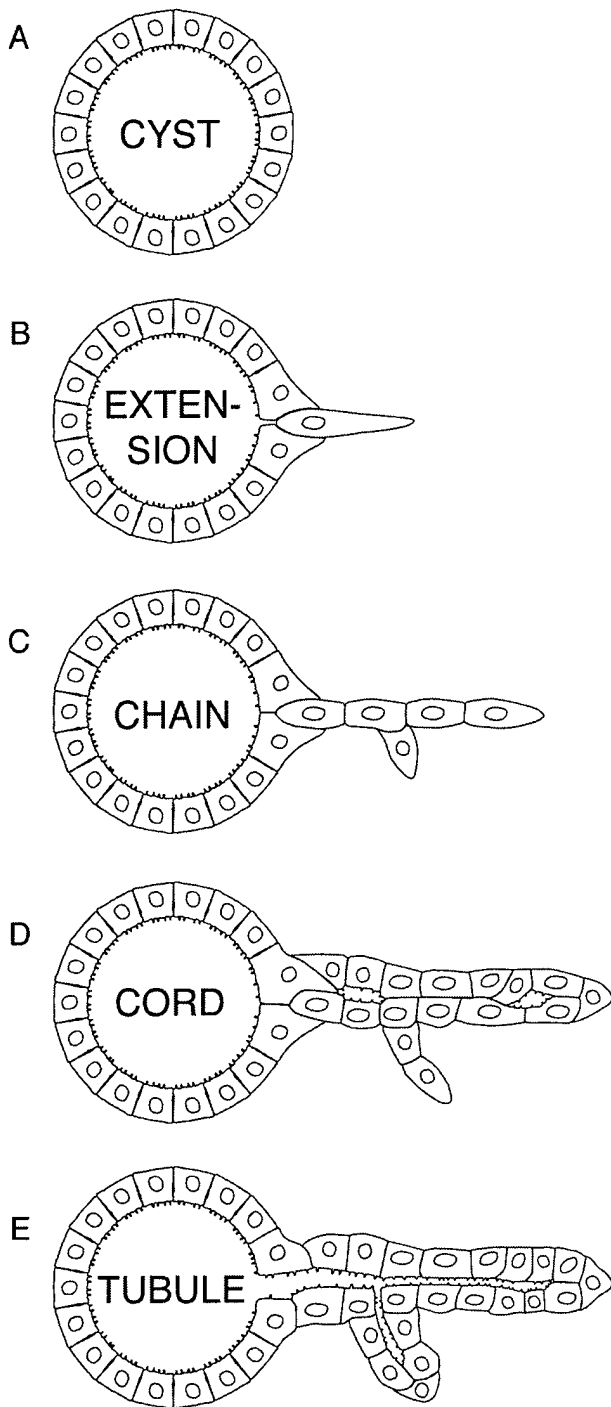


**FIG. 1.** Model of tubule morphogenesis. Development of tubules from polarized cysts is a continuous process that passes through four morphologically distinguishable stages which we have defined as follows: (A, stage 0) polarized cysts, (B, stage 1) extensions, (C, stage 2) chains, (D, stage 3) cords, and (E, stage 4) lumen-containing tubules. Microvilli are indicated as small membrane projections into the lumens. See text for detailed explanation.

confocal sections of immunofluorescently labeled samples from various stages of tubule development. We analyzed many single images and projections of image stacks for the localization of E-cadherin and GP135, well-known markers for basolateral and apical membranes, respectively (Behrens *et al.*, 1985; Gumbiner and Simons, 1986; Gumbiner *et al.*, 1988; Le Bivic *et al.*, 1990; Ojakian and Schwimmer, 1988; Shore and Nelson, 1991; Vestweber and Kemler, 1985). E-cadherin is a cell-cell adhesion protein that concentrates in the region of the apical junctional complex of MDCK cells (Nathke *et al.*, 1994), but is expressed throughout the basolateral membrane and maintains cell-cell contacts through calcium-dependent homotypic interactions with adjacent cells (Takeichi, 1991). Intracellular targeting assays have shown that in this strain of MDCK II cells 98% of newly synthesized E-cadherin is targeted directly to the basolateral surface after synthesis (Crepaldi *et al.*, 1994). The function of gp135 has not been identified. Samples were double-labeled with ppI to denote the localization of nuclei relative to these membrane markers. Representative individual confocal sections, with images split to distinguish membrane markers from nuclear staining, are shown in Fig. 2.

MDCK cell cysts grown in the absence of SF/HGF stimulation are shown in Figs. 2A and 2B. In cysts, E-cadherin is localized predominantly at lateral membranes in regions of cell-cell contact but is also found at membranes that are in contact with the extracellular matrix (Fig. 2A, arrows). E-cadherin is absent at membranes facing the lumen of the cyst (Fig. 2A, filled arrowheads). Gp135 is localized toward the interior of the cyst relative to ppI-stained nuclei and delineates the luminal membrane of MDCK cell cysts (Figs. 2B and 2B', arrows). Some gp135 appears to be within the cyst lumen, but most likely represents staining of apical microvilli. Gp135 is clearly absent from lateral cell-cell borders and cell-substrate contacts in MDCK cell cysts. These results confirm that MDCK cell cysts grown in three-dimensional collagen gel cultures are polarized with markers of the basolateral surface at cell-cell and cell-ECM borders and markers of the apical surface at luminal membranes of the cyst.

The first stage of SF/HGF-induced tubule formation, development of extensions, is shown in Figs. 2C and 2D. During extension formation, individual cells of a cyst are stimulated to protrude into the surrounding collagen matrix. E-cadherin staining surrounds the cellular extensions, localizing at both cell-substrate and cell-cell borders (Fig. 2C, arrows). The open arrowhead in Fig. 2C points out the mouth of a narrow luminal space between two cells that adjoin opposite sides and project under the extending cell where it has receded from the cyst. The filled arrowhead in Fig. 2C points to the remaining luminal surface of the extending cell. Note that this surface is devoid of E-cadherin. E-cadherin remains at lateral membrane borders of cells in the cyst wall that are not extending. Note, however, that often cysts are not perfect hollow spheres (e.g., in Fig. 2C) and E-cadherin is also found at lateral

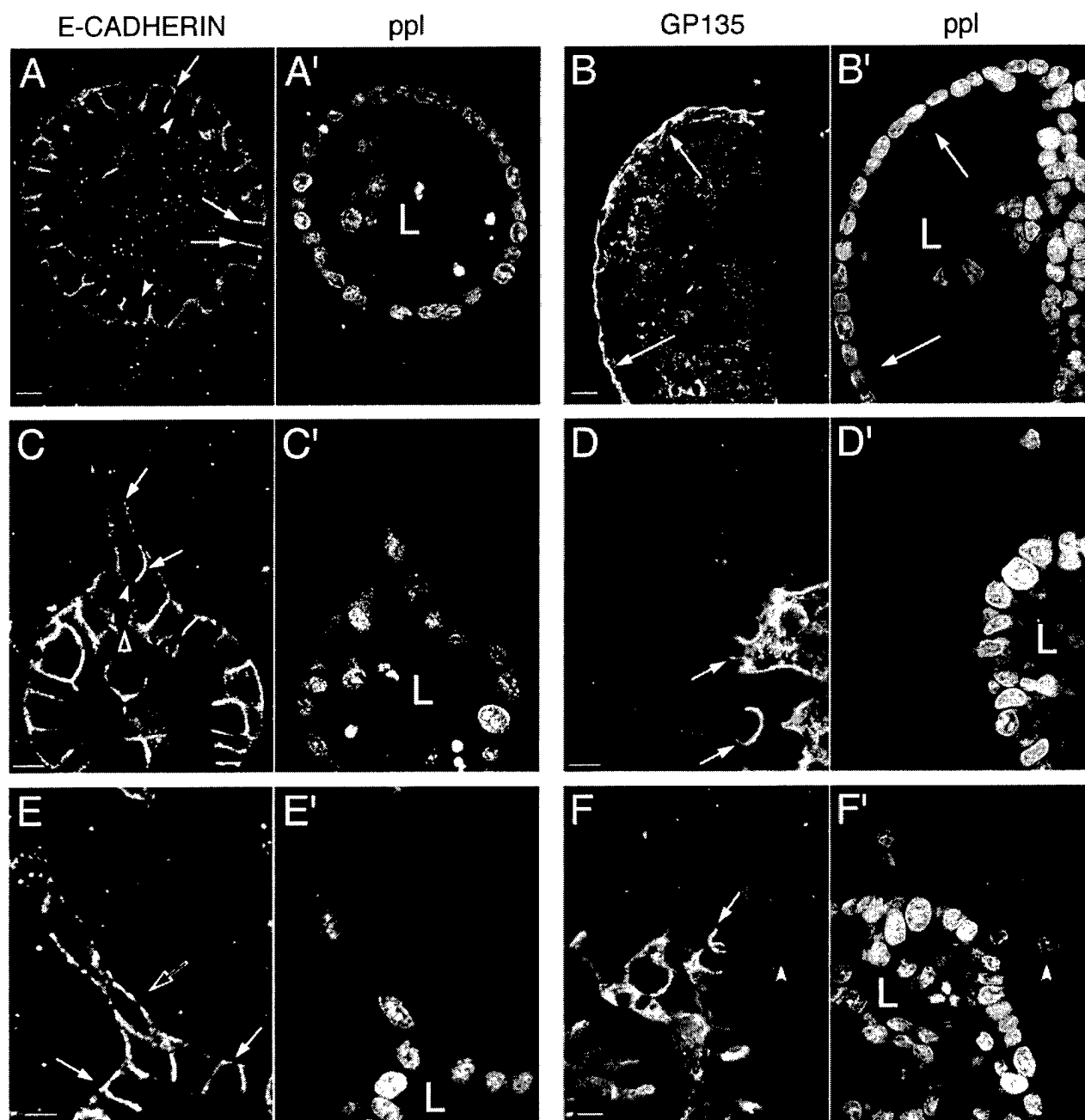


**FIG. 2.** Distinct apical/basolateral polarity is lost during early stages of tubulogenesis. In A-F' each image pair represents a single confocal section taken from serially sectioned samples that were scanned simultaneously for FITC and ppl. Images are split so that staining for E-cadherin (A, C, and E) or gp135 (B, D, and F) is in the left half and nuclear staining (ppl; A'-F') is in the right half. E-cadherin is strictly basolateral in polarized cysts (A, closed arrows), as E-cadherin staining is not detected at apical luminal membranes (A, closed arrowheads). Closed arrows in B and B' are aligned to demonstrate that gp135 is strictly localized to the apical membrane facing the lumen of polarized cysts. During the formation of cellular extensions (C, C') E-cadherin staining is observed on membranes surrounding the extension in regions of cell-cell and cell-substrate contact (closed arrows). E-cadherin is excluded from the luminal membrane (closed arrowhead), indicating that apical/basolateral polarity is retained. Cells neighboring the site of tubule initiation project apically under the extending cell (open arrowhead). Gp135 staining in D (closed arrows) indicates that polarity of apical membranes is retained in extensions. Cells in chains are completely surrounded by E-cadherin (E, open arrow) but basolateral polarity of E-cadherin is maintained in the cyst (E, closed arrows). Gp135 staining has largely disappeared from cells in chains and only background staining remains (F and F', closed arrowheads). At the luminal surfaces of cells within the cyst and at the base of the chain gp135 staining is retained (F, closed arrow). L, lumen. Bar, 10  $\mu$ m.

cell-cell borders between cells of the cyst wall and cells within the cyst. Gp135 is localized at the remaining luminal membrane of the extending cells, establishing that at this stage of tubule development distinct apical membranes are maintained (Fig. 2D, arrows). Note that cells remain attached to the cyst during migration into the ECM to form extensions (Figs. 2C and 2D). These results demonstrate that during initial stages of tubulogenesis, membrane morphology is altered but apical and basolateral subdomains remain distinct.

The second stage of tubulogenesis, chain formation, is shown in Figs. 2E and 2F. In this stage, single-file chains of cells that are either linear (Figs. 2E, 2E') or branching (data not shown) develop. E-cadherin is localized at both cell-cell and cell-ECM contacts, circumscribing each cell of the chain (Fig. 2E, open arrow). Thus, E-cadherin is randomly distributed at membrane surfaces of cells in the chain. In contrast, basolateral polarity of E-cadherin is maintained in cells of the cyst wall that are not undergoing morphogenesis (Fig. 2E, closed arrows). Gp135 staining disappears from cells in a short chain (Fig. 2F, arrowheads), indicating that apical membrane polarity is lost. In contrast, gp135 staining is retained at the luminal surfaces in cells within the cyst, including cells at the base of the chain (Fig. 2F, arrow). Occasionally, intensely stained intracellular patches of GP135 are also observed (data not shown), suggesting that some of the gp135 may also be associated with intracellular vesicles (Vega-Salas *et al.*, 1988). These results show that MDCK cells lose apical/basolateral polarity but retain cell-cell contacts during reorganization into chains.

### ***Cord and Tubule Stages of Tubulogenesis: MDCK Cell Polarity Is Regained as a Tubule Lumen Is Formed***

Subsequent stages of tubulogenesis were analyzed in serial confocal sections and three-dimensional image projections. Representative single confocal sections of cords and tubules, double-stained for ppI and either E-cadherin or gp135, are shown in Fig. 3. Figure 3A shows a cord two to three cells in diameter that is devoid of a lumen. E-cadherin surrounds each cell in the cord, localizing to regions of cell-cell and cell-substrate contact. These results were confirmed by careful analysis of serial sections and projections (data not shown). Gp135 staining is detected at or near cell-cell borders formed during the development of cords (Fig. 3B, arrows) and is not found on membranes in regions of cell-substrate contact (Fig. 3B, arrowhead). Sites of cell-cell contact at which gp135 is localized may be described as "protolumens," since they may indicate the location of future lumen formation. It is also possible that minute lumens that are below the resolution of the confocal microscope exist in these regions. These results show that the localization of the apical membrane marker, gp135, is highly polarized in regions of cell-cell contact upon formation of cords. In contrast, the basolateral membrane marker,

E-cadherin, is found over the entire cell surface and overlaps regions of gp135 localization at cell-cell contacts in cords.

The maturation of cords into tubules is shown in Figs. 3C and 3D. Discontinuous lumens (Fig. 3C', L) develop at sites of cell-cell contact. E-cadherin completely surrounds each cell in regions that retain cord-like structure (Fig. 3C, open arrow). In contrast, the basolateral polarity of E-cadherin is restored in lumen-containing regions of developing tubules (Fig. 3C, closed arrows). As tubule maturation proceeds lumens enlarge and become continuous with the lumen of the cyst (Fig. 3D', L). Gp135 is localized at "free" cell surfaces facing morphologically distinguishable tubule lumens (Fig. 3D, arrows). We conclude from these results that tubules develop via *de novo* formation of lumens within cords at discrete sites of cell-cell contact. In addition, these results suggest that apical/basolateral membrane polarity is restored during *de novo* lumen formation.

### ***SF/HGF-Induced Tubulogenesis Causes Differential Rearrangement of Desmosomal, Tight Junction, and Adherens Cell-Cell Junction Proteins***

We have shown above that cells remain in contact as they rearrange to form tubules. However, E-cadherin localization is dramatically altered during sequential stages of tubulogenesis. Randomization of E-cadherin distribution during the chain and cord stages implies that cell-cell adhesion is modified during SF/HGF-induced tubulogenesis. To further understand the mechanisms through which cell-cell contacts are maintained as cells rearrange during tubulogenesis, we analyzed the localization of tight junction and desmosomal proteins at various stages of tubulogenesis.

In polarized epithelia, multiple DS are located along lateral membranes and function to maintain lateral cell-cell contacts (Garrod, 1993). To establish the localization of DS during tubulogenesis samples were labeled with an antibody that recognizes both desmoplakins I and II (dpI/II), cytoplasmic plaque components of the desmosomal complex (Pasdar *et al.*, 1991; Pasdar and Nelson, 1988b). Nuclei were counterstained with ppI. Serial confocal sections of many cyst cultures treated for various amounts of time with either control or SF/HGF-containing medium were collected and analyzed. Representative individual confocal sections are shown in Fig. 4. The distribution of dpI/II in polarized MDCK cell cysts is shown in Fig. 4A. Note that this confocal image captures cells of the cyst both in cross section (Figs. 4A and 4A', lower left) and as a grazing section across the curvature of the cyst (Figs. 4A and 4A', upper right). DpI/II appeared in punctate spots along basolateral plasma membranes of cells in polarized MDCK cell cysts (Fig. 4A, arrowheads). After stimulation by SF/HGF, dpI/II accumulated in large intracellular pools within extensions of cells that responded to SF/HGF by protruding into the extracellular matrix (Figs. 4B and 4B', aligned arrows). However, dpI/II were also localized in punctate clusters that are likely to be desmosomal plaques at cell-cell borders between the extending cell and cells of the cyst wall

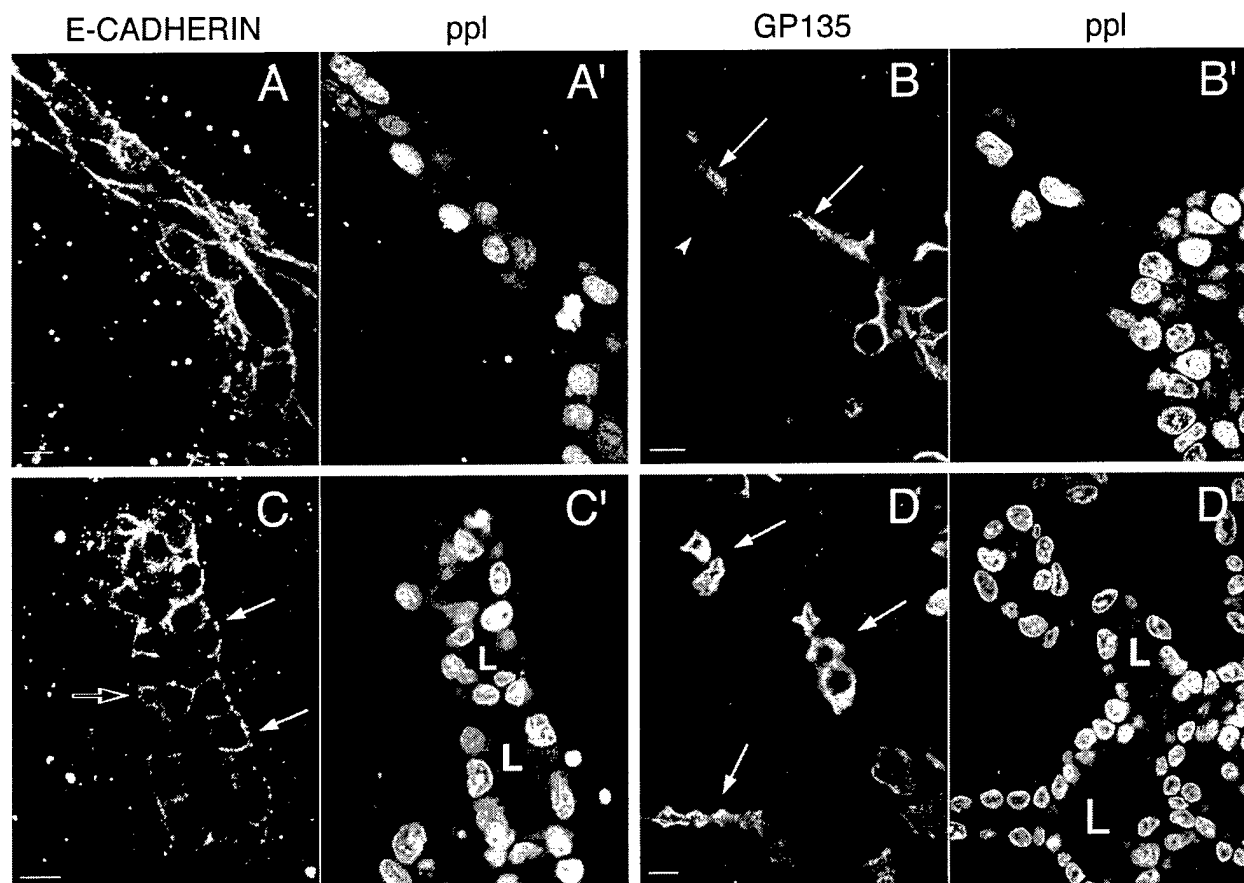


**FIG. 3.** Apical/basolateral polarity is restored in maturing tubules during *de novo* lumen formation. Single confocal images taken from serial sections through cords and developing tubules are shown. In A–D' images are split so that staining for E-cadherin (FITC; A and C) or gp135 (FITC; B and D) is in the left half and nuclear staining (ppl; A'–D') is in the right half. (A and A') Cells in cords are completely surrounded by E-cadherin. (B and B') During the development of cords gp135 staining reappears and is strictly localized to regions of cell–cell contact that represent newly forming luminal membrane (closed arrows). Gp135 staining is absent on membranes in contact with extracellular matrix (B, arrowhead). (C and C') Tubules develop from cords by *de novo* lumen formation. Cells in regions of developing tubules without lumens (C, open arrow) are completely surrounded by E-cadherin. In lumen-containing regions of tubules E-cadherin staining is basolaterally polarized (C, closed arrows). (D and D') Gp135 staining in lumen-containing tubules shows that apical membrane polarity is fully restored (closed arrows). L, lumen. Bar, 10  $\mu$ m.

(Fig. 4B, arrowhead). This suggests that desmosomal adhesion contributed to the maintenance of the cell–cell contacts between the extending cell and the cyst. DpI/II were absent from the luminal membrane of the extending cell (data not shown), indicating that, similar to E-cadherin, basolateral polarization of cell surface dpI/II is maintained at this stage of tubulogenesis. During the formation of chains dpI/II were localized in large intracellular pools in cells of the chain (Fig. 4C, arrows). Punctate spots of dpI/II were also found between cells of chains (Fig. 4C, arrowhead) but were often difficult to detect (not shown). This suggests that dpI/II is localized to desmosomal plaques at membrane borders between cells of chains. However, the increase in intracellular dpI/II does not result in a corresponding increase in the number or size of desmosomal plaques. The

apparent increase in the total immunofluorescence signal may be due to increased accessibility of antibody to non-plasma-membrane dpI/II. However, it may also reflect an upregulation of protein synthesis in cells in which motility is stimulated by SF/HGF. Finally, once polarized lumen-containing tubules are formed dpI/II are localized in punctate spots at lateral membrane cell–cell borders and are not detected in intracellular pools (data not shown).

The TJ is located at the apical-most aspect of the lateral membrane of polarized epithelial cells where it separates the apical and basolateral membrane domains and forms a selective permeability barrier to paracellular transport (Gumbiner, 1987; Rodriguez-Boulant and Nelson, 1989). ZO-1, a cytoplasmic plaque component of the TJ, is found exclusively at the tight junction of polarized epithelial cells

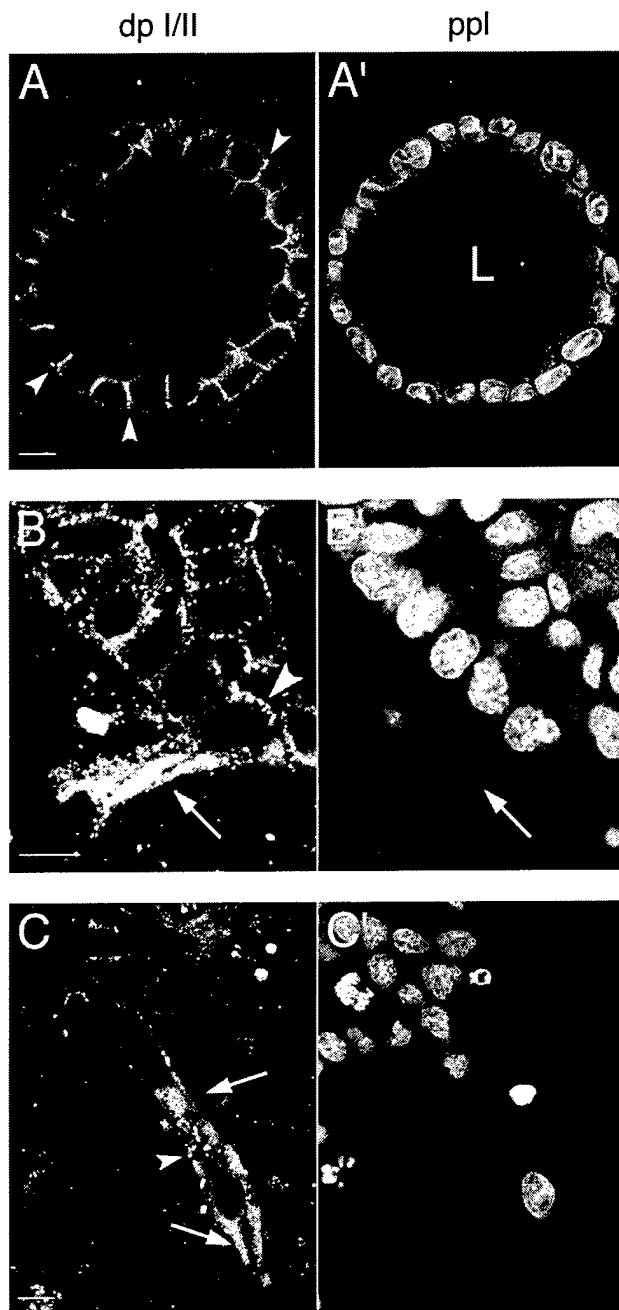


**FIG. 4.** Desmosomal plaque proteins appear in large intracellular pools during early stages of tubule development. Each image pair is a representative single confocal section taken from serially sectioned samples that were scanned simultaneously for FITC and ppl. The images are split, with dpI/II shown on the left side and nuclei on the right side. (A, A') In polarized cysts dpI/II are localized to discrete spots along lateral cell membranes (arrowheads). (B, B') Arrows in B and B' are aligned to show that during formation of extensions dpI/II appears in large intracellular pools in the region of the cell extending into the extracellular matrix. DpI/II are retained in punctate complexes along membranes at cell-cell borders (arrowhead). (C, C') Cells in chains contain intracellular pools of

(Siliciano and Goodenough, 1988; Stevenson *et al.*, 1988, 1986). In polarized MDCK cell cysts, ZO-1 is localized at the apical-most aspect of lateral cell-cell borders (Fig. 5A, arrows). By summing multiple confocal sections through a cyst and creating a projection of the images starting above the level of the bottom nuclei (Fig. 5B') we found that ZO-1 forms an apical "net" (Fig. 5B') that faces the lumen and rings the apical aspect of each cell of the cyst (Fig. 5B). During the extension stage of SF/HGF-induced morphogenesis, ZO-1 remains at the luminal aspect of lateral membranes of cells extending from the cyst (Fig. 5C, arrow). Note that the gain of the image in Fig. 5C was increased after collection in Adobe Photoshop to make it possible to detect background staining and visualize the connection of the unlabeled cell extension to the cyst. As tubule formation continues, ZO-1 localizes to regions of membrane that link cells into single-file chains (Fig. 5D, arrows), indicating that ZO-1 remains at sites of cell-cell contact throughout the formation of chains. During *de novo* lumen formation, ZO-1 localizes to the apical-most aspect of lateral membrane borders between cells surrounding the newly formed lumen (Fig. 5E, arrowhead), suggesting that at this stage of tubule development the apical polarization of the TJ is reestablished. In regions of the developing tubule where lumen formation is more advanced, ZO-1 staining outlines the apical membrane, reminiscent of ZO-1 localization at the apical-most aspect of lateral membranes in polarized cysts (Fig. 5E, arrow). The localization of ZO-1 throughout tubulogenesis at membranes involved in cell-cell contact suggests that ZO-1-containing junctions contribute to the maintenance of cell-cell adhesion during all stages of tubule morphogenesis. Concomitant with repolarization of the tubule epithelium, ZO-1 demarcates lumenally polarized tight junctions that separate the apical and basolateral plasma membrane domains. Taken together, our results show that the treatment of MDCK cell cysts with SF/HGF causes disparate changes in the distribution of E-cadherin, desmoplakins, and ZO-1 and suggest that adhesion through each of these cell-cell junctions is differentially regulated during SF/HGF-induced tubulogenesis.

## DISCUSSION

Numerous studies have increased our understanding of molecules that induce tubulogenesis and regulate branching activity (Montesano *et al.*, 1991a; Sakurai *et al.*, 1997a,b; Sariola and Sainio, 1997; Sutherland *et al.*, 1996; Vainio and Muller, 1997). However, the morphogenetic mechanisms by which cells reorganize membrane subdo-

dpI/II (arrows). Punctate spots of dpI/II also appear at cell-cell borders between cells of the chain (arrowhead). L, lumen. Bar, 10  $\mu$ m.

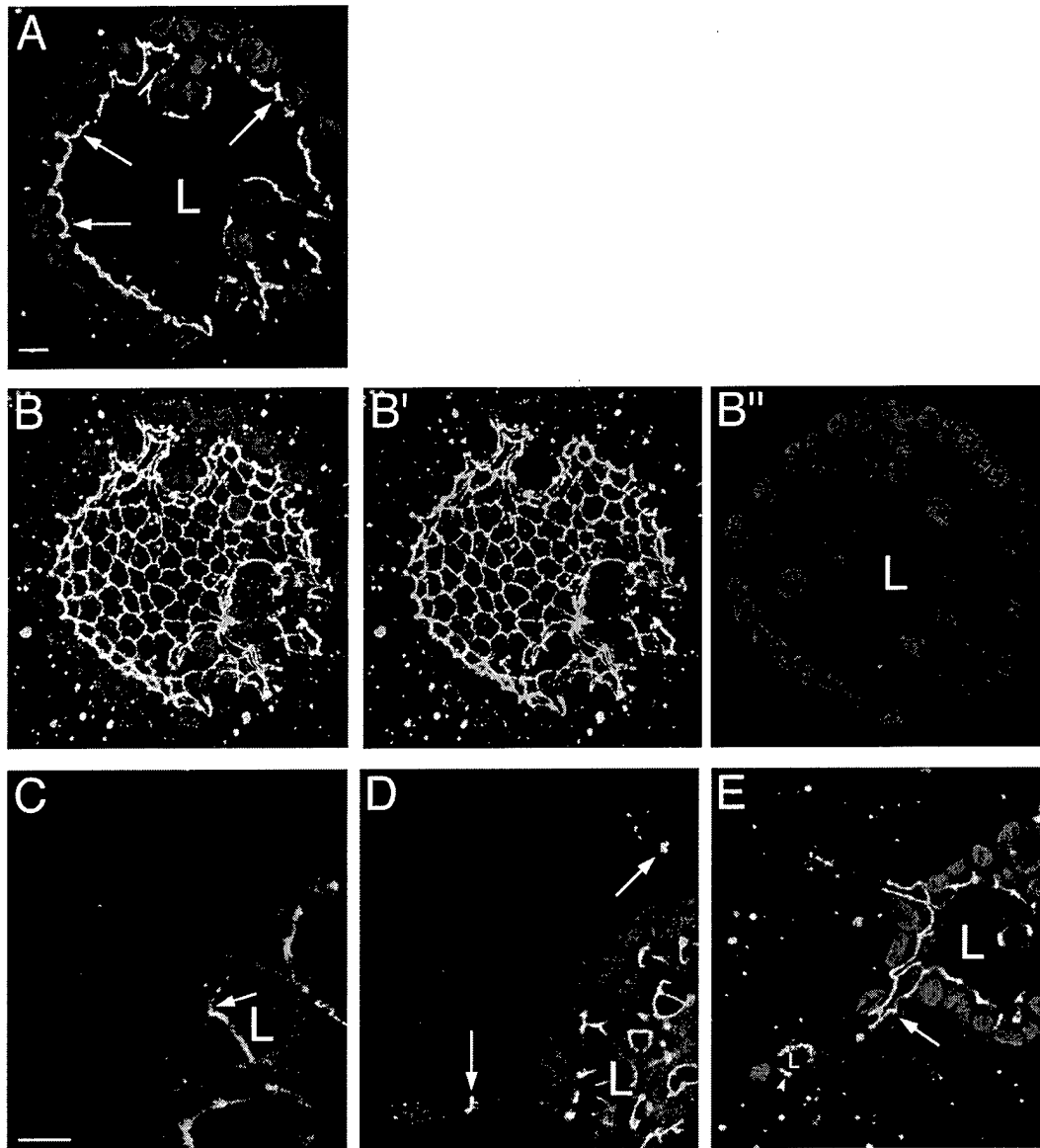


**FIG. 5.** The tight junction marker, ZO-1, localizes at sites of cell-cell contact at all stages of tubule formation. In A-E serial confocal sections were collected from samples at different stages of tubule morphogenesis. FITC (ZO-1, green) and ppl (red) for all images were scanned simultaneously. A, C, D, and E are representative single confocal sections. B, B', and B'' each show a projected sum of 13 2- $\mu$ m serial sections from the same sample as in A. (A) In a cross section through a polarized cyst arrows show that ZO-1 is apically polarized. (B, B', and B'') The image in B shows the overlay of projections in B' and B'' that were split to show ZO-1 on the left and nuclei on the right. A net of ZO-1 staining is detected in B'. B'' shows that sections for these projections start above the level of the nuclei of cells that are in the center of the image. The double image in B shows that ZO-1 staining is above the level of the nuclei, demonstrating that ZO-1 is localized to the apical-most aspect of lateral cell-cell borders and forms a ring around each cell of the cyst. (C) In extensions, ZO-1 is detected at the remaining apical membrane facing the lumen of the cyst (arrow). (D) During the formation of chains, ZO-1 is concentrated at cell-cell borders between cells of the chains (arrows). (E) During the development of a lumen-containing tubule ZO-1 remains at cell-cell borders and localizes to the apical-most aspect of lateral membranes of both a newly formed lumen (arrowhead) and a more mature lumen (arrow). L, lumen. Bar, 10  $\mu$ m. Bar in A applies to B, D, and E.

mains and cell-cell contacts during tubulogenesis have not previously been well characterized.

### ***Distinct Stages in Tubulogenesis***

Based on a detailed three-dimensional analysis we have defined four stages in the development of tubules from MDCK cell cysts (see Fig. 1) in which we have identified unique arrangements of marker proteins for apical/basolateral polarity and cell junctional complexes. These stages define the morphogenetic mechanisms for tubule formation in this system. In the first phase of SF/HGF-induced tubule formation, the extension stage, individual cells protrude into the surrounding collagen matrix while remaining attached to the cyst. Apical and basolateral membranes are morphologically altered but cell polarity and cell junctions are maintained. Some individual scattered cells are detected in these cultures but do not appear to contribute to tubule development. The second stage, chain formation, is characterized by the appearance of single-file linear or branched chains of cells in which an apical membrane marker (gp135) is absent or intracellular, a basolateral membrane marker (E-cadherin) has a nonpolar distribution around the entire cell surface, desmosomes (dpl/II) are predominantly localized in intracellular pools, and a TJ marker (ZO-1) is highly localized to the small regions of cell-cell contact between cells in the chain. During the third stage, cord formation, chains of cells thicken into cords in which apical polarity is again observed while the basolateral marker protein, E-cadherin, remains randomly distributed. *De novo* lumen formation occurs at sites of cell-cell contact where apical membrane markers are located. Small lumens begin to appear in segregated regions along the length of the developing tubule. ZO-1 localizes to apical cell-cell contact points and basolateral repolarization is initiated in cells surrounding the nascent lumens. In the final stage of tubulogenesis, tubule maturation, individual lumens coalesce, enlarge, and become continuous with the lumen of the cyst. Apical and basolateral membranes of cells of the tubule become clearly polarized and the arrangement of cell junctions that normally is found in polarized epithelial cells is completely restored.

Our analysis has yielded at least two new and surprising insights into the mechanisms of tubulogenesis, which are: (i) a novel model of cell and membrane subdomain rearrangement during tubulogenesis and (ii) differential regulation of junctional proteins.

### ***A Novel Model of Tubulogenesis***

The pattern of cell rearrangements and intercellular migration that we observe is clearly different from that previously proposed in both the outpouching and the two-step dissociation/reassociation models of tubulogenesis. A key prediction of the outpouching model is that tubule lumens would remain continuous with the cyst lumen at all stages of tubule development (Gilbert, 1994). In fact, our results

demonstrate that tubule lumens are initially discontinuous, forming *de novo* at discrete regions along the length of developing tubules. In addition, we observed that newly formed tubule lumens do not necessarily connect to the lumen of the cyst. A second prediction of the outpouching model is that cells would retain their polarity, as they would continue to line a lumen at all stages of tubule formation. This is contrary to our observation that the cells undergo a transient loss of polarity. Therefore, an outpouching model does not explain our observed stages of tubulogenesis. The two-step dissociation/reassociation model predicts that we would have seen aggregates of two or more cells that were detached from cysts forming structures such as chains, cords, or tubules. We did not observe such structures. Rather, the chains, cords, and tubules that we observed were always in contact with cysts. Therefore, tubules did not arise by a complete loss of cell-cell contact followed by reassociation, as proposed by Thiery and Boyer (1992). This was consistent for over 250 cysts that we stimulated with SF/HGF and analyzed by complete serial sections.

We propose, therefore, a novel model of tubulogenesis that includes the following morphogenetic mechanisms: (1) stimulation of cell migration is the first step in tubulogenesis, (2) apical/basolateral polarity is transiently lost and is restored concomitant with lumen formation, (3) discontinuous tubule lumens form *de novo* in regions of developing tubules, and (4) cell-cell contacts are retained at all stages of tubulogenesis.

A key observation from our results is that tubule formation is initiated by the extension and migration of cells without loss of cell-cell contact. Migration of cells without loss of cell-cell contact has previously been found to be important for organ formation during development *in vivo*. For example, chain migration of neuronal precursors contributes to the formation of the olfactory bulb (Lois *et al.*, 1996). The fundamental role of SF/HGF in this tubulogenesis model system may be to induce cells to migrate out from a polarized epithelium to develop extensions and form a chain. Previous studies have shown that altering cell-substrate contacts by collagen overlay is sufficient to initiate the direct conversion of MDCK cell monolayers into tubulocysts (Schwimmer and Ojakian, 1995; Zuk and Matlin, 1996). In the collagen overlay technique, the conversion of a monolayer of cells into a tubule-like structure may recapitulate the last two stages that we have identified in SF/HGF-induced tubulogenesis, namely the conversion of a chain into a cord and subsequently a cord into a lumen-containing tubule. In contrast to our studies, this direct conversion of a monolayer into a tubule-like structure essentially bypasses the requirement for an inducing molecule such as SF/HGF. Therefore, during tubulogenesis, once SF/HGF induces formation of a chain in contact with collagen, the further formation of a cord and a tubule may be the result of a mechanism intrinsic to the MDCK cells, without requiring further SF/HGF signaling.

We have observed that cells branching from chains and

tips of tubules also undergo changes in morphology, polarity, and cell-cell contacts that are similar to the changes in the initial cell extensions from cysts (A. Pollack and K. Mostov, unpublished results). In addition, our recent studies of interactions of  $\beta$ -catenin and APC protein during tubulogenesis have shown that mechanisms regulating cell migration are important for both formation of extensions and the later development of mature tubules rather than polyp-like structures (Pollack *et al.*, 1997). Our results suggest that cell migration is an important mechanism at multiple stages of tubule development. Therefore, we propose that a triggering function of SF/HGF may be important, not only for inducing formation of extensions and chains, but also for stimulating elongation of the tips of tubules and initiating cell movements in the development of branches.

Our analysis of cell polarity during tubule development has also contributed to the formulation of a model of tubulogenesis. A key mechanism derived from this analysis is the dynamic regulation of cell polarity during tubulogenesis: cells transiently lose their polarity during the formation of chains, but subsequently regain polarity as they form mature tubules. During tubulogenesis, after initial loss of polarity, apical polarity is reestablished first in regions of cell-cell contact in cords, followed by basolateral repolarization during lumen formation. Previous studies have shown that changes in cell-cell and cell-substrate interactions alter epithelial cell polarity (Rodriguez-Boulant and Nelson, 1989; Vega-Sales *et al.*, 1987; Wang *et al.*, 1990a). For example, when MDCK cysts are first grown in a liquid suspension culture the apical surface of the cells is localized at the outside membrane of the cyst, facing the medium. When recultured in collagen gels, these cells undergo a reversal of polarity without loss of cell-cell contacts. During this process the apical marker gp135 disappears by internalization and degradation and then is resynthesized (Wang *et al.*, 1990b). The loss of gp135 from the transiently nonpolarized cells during SF/HGF-induced tubulogenesis, and the subsequent accumulation of gp135 at the nascent apical surface, may be regulated analogously. Therefore, mechanisms driving changes in epithelial polarity during tubulogenesis may be similar to other systems in which epithelial cell subdomains rearrange. This requires further study. Importantly, our results show that dynamic rearrangement of proteins that are normally polarized to specific membrane subdomains, without a loss of cell-cell contacts, is an important feature of epithelial tubule development. In addition, we provide a perspective of how sequential changes in apical/basolateral polarity fit into the larger context of the morphogenetic process of tubulogenesis.

### **Differential Regulation of Junctional Proteins during Tubulogenesis**

A second new insight demonstrated by our studies is that components of the three types of cell-cell junctions, adhe-

rens junctions, desmosomes, and tight junctions, underwent very different patterns of regulation during tubulogenesis: E-cadherin redistributed throughout the cell surface, *dpl/II* accumulated intracellularly, and ZO-1 was found at regions of cell-cell contact. Although junctional proteins were modified, cell-cell contacts were retained throughout the intricate cell rearrangements during morphogenesis of a tubule from a cyst. The selective regulation of distinct cell-cell junctional components during tubulogenesis contrasts strikingly with results from previous studies in which calcium "switch" or antibody disruption of E-cadherin-based adhesion caused coordinate regulation of adhesion through desmosomes, adherens junctions, and tight junctions (Behrens *et al.*, 1985; Gumbiner and Simons, 1986; Gumbiner *et al.*, 1988; Siliciano and Goodenough, 1988). We suggest that differential regulation of cell-cell junctional proteins, both spatially and temporally, is likely to be crucial to maintain cell-cell contacts during the development of tubules.

We have previously shown that E-cadherin surrounding the cell perimeter in extensions, chains, and cords colocalizes with  $\beta$ -catenin, a protein that is normally associated with the cytoplasmic domain of E-cadherin and is required for E-cadherin-based cell-cell adhesion (Pollack *et al.*, 1997). In addition, we have reported that monolayer cultures of MDCK cells treated with SF/HGF show an increase in E-cadherin synthesis, which correlates with SF/HGF-induced morphogenetic cell rearrangements (Balkovetz *et al.*, 1997). It appears, therefore, that as cells extend and form chains, they produce additional E-cadherin, which is expressed on surfaces not yet in contact with other cells. This E-cadherin is not initially utilized for cell-cell contact, either because it is differentially regulated so that it is not yet competent for cell-cell adhesion, or perhaps simply because no other cell surface is present with which the E-cadherin can interact. As chains are transformed into cords, this E-cadherin is utilized for the establishment of new cell-cell contacts.

During the initial extension formation, ZO-1 remains at the cell surface at the boundary between the apical and the basolateral domains, showing that the fence function of tight junctions remains intact. Next, during the chain stage ZO-1 is localized only to the regions of cell-cell contact. We speculate that this ZO-1, which is much more highly localized to the regions of cell-cell contact than E-cadherin, may play a role in maintaining cell-cell contact during this stage of tubulogenesis. The ZO-1 subsequently relocates to the apex of cells, surrounding newly formed lumens. It is interesting to compare our results with observations made in the calcium switch system. There, ZO-1 is initially colocalized with E-cadherin along the length of the region of cell-cell contact. Subsequently, the ZO-1 is segregated to the region of the tight junctions near the apex of the cell (Rajasekaran *et al.*, 1996).

Finally, the desmosome components, *dpl/II*, are found in large intracellular pools, initially appearing in cells that are stimulated to migrate by SF/HGF. SF/HGF has been found

to cause loss of desmosomal plaques in MDCK cells during scattering (Stoker and Perryman, 1985) and to disrupt desmosomal contacts in keratinocytes (Watabe *et al.*, 1993). SF/HGF treatment of MDCK cell monolayers also causes accumulation of dpI/II in large intracellular pools during morphogenetic cell rearrangements (A. Pollack and K. Mostov, unpublished observations). These studies have provided evidence that SF/HGF induces either internalization or new synthesis and cytoplasmic retention of dpI/II. Taken together with the results of our studies, we suggest that modulating desmosomal adhesion by removal of dpI/II from the cell surface is important for morphogenetic cell rearrangements during tubulogenesis.

Our studies suggest that SF/HGF selectively modulates, rather than disrupts, cell-cell adhesion during tubulogenesis. The segregation of SF/HGF's effects on components of adherens junctions, desmosomes, and tight junctions may be critical for regulating the formation of lumen-containing tubules. During metanephric kidney development *in vivo*, cells do not appear to dissociate as new structures are formed (Vestweber *et al.*, 1985; Garrod and Fleming, 1990). Formation of ureter and tubular structures in the developing kidney coincides with the expression of E-cadherin (Vestweber *et al.*, 1985) and desmoplakin-containing desmosomes (Garrod and Fleming, 1990) at epithelial cell-cell borders. Patterns of desmoplakin expression and the structure of the desmosomes change during kidney development, indicating that lability of desmosomes is important for kidney morphogenesis (Burdett, 1993; Garrod and Fleming, 1990). These *in vivo* studies suggest that regulation of cell-cell adhesion molecules is important early in kidney development. Differential regulation of cell-cell junctional proteins in both space and time may allow the adhesive properties of specific areas of individual cells to be modulated so that cells "let go" and reconnect as they rearrange. Previously, components of cell-cell junctions have been shown to be regulated by phosphorylation (Behrens *et al.*, 1993; Matsuyoshi *et al.*, 1992; Nigam *et al.*, 1991; Shibamoto *et al.*, 1994; Volberg *et al.*, 1992). Investigation into a role of SF/HGF-induced phosphorylation as a mechanism of differential regulation of cell-cell adhesion during tubulogenesis requires future study.

During tubulogenesis, specific modulation of adhesion and polarity may enable a developing system to restructure without having to completely redifferentiate. Regulating the extent to which adhesion and polarity are altered during morphogenesis may prime a developing system to rapidly restore or acquire epithelial function. In morphogenetic processes such as wound repair (Bement *et al.*, 1993; Madara, 1990) it is critical that epithelial cell rearrangements occur with a minimal disruption of polarity and adhesion in order to maintain the functional intactness and permeability characteristics of the epithelial tissue. Further insight into the interplay between the actions of SF/HGF and components of systems that regulate cell-cell and cell-substrate adhesion and polarity may provide a key to understanding the seemingly disparate abilities of SF/HGF

to induce epithelial cells to develop into cohesive structures rather than to scatter or invade.

In conclusion, in this study we have carefully analyzed the temporal and spatial regulation of cell polarity and cell-cell adhesion proteins subsequent to induction of tubulogenesis from a polarized epithelium to understand the mechanisms of cell rearrangements in the development of lumen-containing tubules. We suggest a novel multistage model of tubulogenesis in which SF/HGF stimulates initial cell migration and remodeling of cell polarity but differentially regulates cell-cell junctional proteins, such that cell-cell adhesion is maintained throughout cell rearrangements. In addition, we propose that an intrinsic program of epithelial repolarization may be critical to the formation of mature tubules. Our study is the first report of a detailed examination of cell rearrangements combined with analysis of the accompanying changes in cell adhesion, junctions, and polarity that occur during epithelial tubulogenesis in any model system. These results provide a framework for future investigations of cell movements, polarity, and junctions during morphogenetic cell rearrangements of tubulogenesis *in vivo* and in other *in vitro* systems that reflect this developmental process in a variety of organs.

## ACKNOWLEDGMENTS

We thank Lucy O'Brian, Carol Gregorio, Josh Lipschutz, Angelique Boyer, and W. James Nelson for their advice and careful reading of the manuscript. We thank Herman Gordon for assistance with computer illustration. We thank Ralph Schwall at Genentech for generous gifts of recombinant HGF. Supported by NIH Grants AI36953 and HL55980 and by DOD Grant DAMD17-97-1-7249 to Keith Mostov, who is an Established Investigator of the American Heart Association. Also supported by NIH Grant HL58696 to Ray Runyan and NIH Training Grant Fellowship HL07249 to Anne Pollack.

## REFERENCES

- Anderson, J. M., Stevenson, B. R., Jesaitis, L. A., Goodenough, D. A., and Mooseker, M. S. (1988). Characterization of ZO-1, a protein component of the tight junction from mouse liver and Madin-Darby canine kidney cells. *J. Cell Biol.* **106**, 1141-1149.
- Balkovetz, D. F., Pollack, A. L., and Mostov, K. E. (1997). Hepatocyte growth factor alters the polarity of Madin-Darby canine kidney cell monolayers. *J. Biol. Chem.* **272**, 3471-3477.
- Barros, E. J., Santos, O. F., Matsumoto, K., Nakamura, T., and Nigam, S. K. (1995). Differential tubulogenic and branching morphogenetic activities of growth factors: Implications for epithelial tissue development. *Proc. Natl. Acad. Sci. USA* **92**, 4412-4416.
- Behrens, J., Birchmeier, W., Goodman, S. L., and Imhof, B. A. (1985). Dissociation of Madin-Darby canine kidney epithelial cells by the monoclonal antibody anti-arc-1: Mechanistic aspects and identification of the antigen as a component related to uvomorulin. *J. Cell Biol.* **101**, 1307-1315.
- Behrens, J., Vakaet, L., Friis, R., Winterhager, E., Van Roy, F., Mareel, M. M., and Birchmeier, W. (1993). Loss of epithelial

- differentiation and gain of invasiveness correlates with tyrosine phosphorylation of the E-cadherin/beta-catenin complex in cells transformed with a temperature-sensitive v-SRC gene. *J. Cell Biol.* **120**, 757-766.
- Bement, W. M., Forscher, P., and Mooseker, M. S. (1993). A novel cytoskeletal structure involved in purse string wound closure and cell polarity maintenance. *J. Cell Biol.* **121**, 565-578.
- Berdichevsky, F., Alford, D., D'Souza, B., and Taylor-Papadimitriou, J. (1994). Branching morphogenesis of human mammary epithelial cells in collagen gels. *J. Cell Sci.* **107**, 3557-3568.
- Birchmeier, C., and Birchmeier, W. (1993). Molecular aspects of mesenchymal-epithelial interactions. *Annu. Rev. Cell Biol.* **9**, 511-540.
- Boccaccio, C., Ando, M., Tamagnone, L., Bardelli, A., Michieli, P., Battistini, C., and Comoglio, P. M. (1998). Induction of epithelial tubules by growth factor HGF depends on the STAT pathway. *Nature* **391**, 285-288.
- Brinkmann, V., Foroutan, H., Sachs, M., Weidner, K. M., and Birchmeier, W. (1995). Hepatocyte growth factor/scatter factor induces a variety of tissue-specific morphogenic programs in epithelial cells. *J. Cell Biol.* **131**, 1573-1586.
- Burdett, I. D. (1993). Internalisation of desmosomes and their entry into the endocytic pathway via late endosomes in MDCK cells. Possible mechanisms for the modulation of cell adhesion by desmosomes during development. *J. Cell Sci.* **106**, 1115-1130.
- Cantley, L. G., Barros, E. J., Gandhi, M., Rauchman, M., and Nigam, S. K. (1994). Regulation of mitogenesis, motogenesis, and tubulogenesis by hepatocyte growth factor in renal collecting duct cells. *Am. J. Physiol.* **267**, F271-F280.
- Comoglio, P. M. (1993). Structure, biosynthesis and biochemical properties of the HGF receptor in normal and malignant cells. *Exs* **65**, 131-165.
- Crepaldi, T., Gautreau, A., Comoglio, P. M., Louvard, D., and Arpin, M. (1997). Ezrin is an effector of hepatocyte growth factor-mediated migration and morphogenesis in epithelial cells. *J. Cell Biol.* **138**, 423-434.
- Crepaldi, T., Pollack, A. L., Prat, M., Zborek, A., Mostov, K., and Comoglio, P. M. (1994). Targeting of the SF/HGF receptor to the basolateral domain of polarized epithelial cells. *J. Cell Biol.* **125**, 313-320.
- Derman, M. P., Cunha, M. J., Barros, E. J., Nigam, S. K., and Cantley, L. G. (1995). HGF-mediated chemotaxis and tubulogenesis require activation of the phosphatidylinositol 3-kinase. *Am. J. Physiol.* **268**, F1211-F1217.
- Drubin, D. G., and Nelson, W. J. (1996). Origins of cell polarity. *Cell* **84**, 335-344.
- Dugina, V. B., Alexandrova, A. Y., Lane, K., Bulanov, E., and Vasiliev, J. M. (1995). The role of the microtubular system in the cell response to HGF/SF. *J. Cell Sci.* **108**, 1659-1667.
- Furlong, R. A. (1992). The biology of hepatocyte growth factor/scatter factor. *Bioessays* **14**, 613-617.
- Garrod, D. R. (1993). Desmosomes and hemidesmosomes. *Curr. Opin. Cell Biol.* **5**, 30-40.
- Garrod, D. R., and Fleming, S. (1990). Early expression of desmosomal components during kidney tubule morphogenesis in human and murine embryos. *Development* **108**, 313-321.
- Gilbert, S. F. (1994). "Developmental Biology." Sinauer, Sunderland, MA.
- Gumbiner, B. (1987). Structure, biochemistry, and assembly of epithelial tight junctions. *Am. J. Physiol.* **253**, C749-C758.
- Gumbiner, B., and Simons, K. (1986). A functional assay for proteins involved in establishing an epithelial occluding barrier: Identification of a uvomorulin-like polypeptide. *J. Cell Biol.* **102**, 457-468.
- Gumbiner, B., Stevenson, B., and Grimaldi, A. (1988). The role of the cell adhesion molecule uvomorulin in the formation and maintenance of the epithelial junctional complex. *J. Cell Biol.* **107**, 1575-1587.
- Gumbiner, B. M. (1992). Epithelial morphogenesis [comment]. *Cell* **69**, 385-387.
- Kjelsberg, C., Sakurai, H., Spokes, K., Birchmeier, C., Drummond, I., Nigam, S., and Cantley, L. G. (1997). Met <sup>-/-</sup> kidneys express epithelial cells that chemotax and form tubules in response to EGF receptor ligands. *Am. J. Physiol.* **272**, F222-F228.
- Klambt, C., Glazer, L., and Shilo, B. Z. (1992). breathless, a *Drosophila* FGFR receptor homolog, is essential for migration of tracheal and specific midline glial cells. *Genes Dev.* **6**, 1668-1678.
- Le Bivic, A., Sambuy, Y., Mostov, K., and Rodriguez-Boulant, E. (1990). Vectorial targeting of an endogenous apical membrane sialoglycoprotein and uvomorulin in MDCK cells. *J. Cell Biol.* **110**, 1533-1539.
- Lois, C., Garcia-Verdugo, J.-M., and Alvarez-Buylla, A. (1996). Chain migration of neuronal precursors. *Science* **271**, 978-981.
- Louvard, D. (1980). Apical membrane aminopeptidase appears at site of cell-cell contact in cultured kidney epithelial cells. *Proc. Natl. Acad. Sci. USA* **77**, 4132-4136.
- Madara, J. L. (1990). Maintenance of the macromolecular barrier at cell extrusion sites in intestinal epithelium: Physiological rearrangement of tight junctions. *J. Membr. Biol.* **116**, 177-184.
- Matsuyoshi, N., Hamaguchi, M., Taniguchi, S., Nagafuchi, A., Tsukita, S., and Takeichi, M. (1992). Cadherin-mediated cell-cell adhesion is perturbed by v-src tyrosine phosphorylation in metastatic fibroblasts. *J. Cell Biol.* **118**, 703-714.
- Montesano, R., Matsumoto, K., Nakamura, T., and Orci, L. (1991a). Identification of a fibroblast-derived epithelial morphogen as hepatocyte growth factor. *Cell* **67**, 901-908.
- Montesano, R., Schaller, G., and Orci, L. (1991b). Induction of epithelial tubular morphogenesis in vitro by fibroblast-derived soluble factors. *Cell* **66**, 697-711.
- Moore, M. W., Klein, R. D., Farinas, I., Sauer, H., Armanini, M., Phillips, H., Reichardt, L. F., Ryan, A. M., Carver-Moore, K., and Rosenthal, A. (1996). Renal and neuronal abnormalities in mice lacking GDNF. *Nature* **382**, 76-79.
- Nathke, I. S., Hinck, L., Swedlow, J. R., Papkoff, J., and Nelson, W. J. (1994). Defining interactions and distributions of cadherin and catenin complexes in polarized epithelial cells. *J. Cell Biol.* **125**, 1341-1352.
- Nigam, S. K., Denisenko, N., Rodriguez-Boulant, E., and Citi, S. (1991). The role of phosphorylation in development of tight junctions in cultured renal epithelial (MDCK) cells. *Biochem. Biophys. Res. Commun.* **181**, 548-553.
- Ojakian, G. K., and Schwimmer, R. (1988). The polarized distribution of an apical cell surface glycoprotein is maintained by interactions with the cytoskeleton of Madin-Darby canine kidney cells. *J. Cell Biol.* **107**, 2377-2387.
- Pasdar, M., Krzeminski, K. A., and Nelson, W. J. (1991). Regulation of desmosome assembly in MDCK epithelial cells: Coordination of membrane core and cytoplasmic plaque domain assembly at the plasma membrane. *J. Cell Biol.* **113**, 645-655.
- Pasdar, M., and Nelson, W. J. (1988a). Kinetics of desmosome assembly in Madin-Darby canine kidney epithelial cells: Tem-

- pore and spatial regulation of desmoplakin organization and stabilization upon cell-cell contact. I. Biochemical analysis. *J. Cell Biol.* **106**, 677-685.
- Pasdar, M., and Nelson, W. J. (1988b). Kinetics of desmosome assembly in Madin-Darby canine kidney epithelial cells: Temporal and spatial regulation of desmoplakin organization and stabilization upon cell-cell contact. II. Morphological analysis. *J. Cell Biol.* **106**, 687-695.
- Pichel, J. G., Shen, L., Sheng, H. Z., Granholm, A. C., Drago, J., Grinell, A., Lee, E. J., Huang, S. P., Saarma, M., Hoffer, B. J., Sariola, H., and Westphal, H. (1996). Defects in enteric innervation and kidney development in mice lacking GDNF. *Nature* **382**, 73-76.
- Pollack, A. L., Barth, A. I. M., Altschuler, Y., Nelson, W. J., and Mostov, K. E. (1997). Dynamics of beta-catenin interactions with APC protein regulate epithelial tubulogenesis. *J. Cell Biol.* **137**, 1651-1662.
- Ponzetto, C., Bardelli, A., Zhen, Z., Maina, F., dalla Zonca, P., Giordano, S., Graziani, A., Panayotou, G., and Comoglio, P. M. (1994). A multifunctional docking site mediates signaling and transformation by the hepatocyte growth factor/scatter factor receptor family. *Cell* **77**, 261-271.
- Rajasekaran, A. K., Hojo, M., Huima, T., and Rodriguez-Boulan, E. (1996). Catenins and zonula occludens-1 form a complex during early stages in the assembly of tight junctions. *J. Cell Biol.* **132**, 451-463.
- Rodriguez-Boulan, E., and Nelson, W. J. (1989). Morphogenesis of the polarized epithelial cell phenotype. *Science* **245**, 718-725.
- Rosen, E. M., Nigam, S. K., and Goldberg, I. D. (1994). Scatter factor and the c-met receptor: A paradigm for mesenchymal/epithelial interaction. *J. Cell Biol.* **127**, 1783-1787.
- Royal, I., Fournier, T. M., and Park, M. (1997). Differential requirement of Grb2 and PI3-kinase in HGF/SF-induced cell motility and tubulogenesis. *J. Cell. Physiol.* **173**, 196-201.
- Sachs, M., Weidner, K. M., Brinkmann, V., Walther, I., Obermeier, A., Ullrich, A., and Birchmeier, W. (1996). Motogenic and morphogenic activity of epithelial receptor tyrosine kinases. *J. Cell Biol.* **133**, 1095-1107.
- Saelman, E. U., Keely, P. J., and Santoro, S. A. (1995). Loss of MDCK cell alpha 2 beta 1 integrin expression results in reduced cyst formation, failure of hepatocyte growth factor/scatter factor-induced branching morphogenesis, and increased apoptosis. *J. Cell Sci.* **108**, 3531-3540.
- Sakurai, H., Barros, E. J., Tsukamoto, T., Barasch, J., and Nigam, S. K. (1997a). An in vitro tubulogenesis system using cell lines derived from the embryonic kidney shows dependence on multiple soluble growth factors. *Proc. Natl. Acad. Sci. USA* **94**, 6279-6284.
- Sakurai, H., and Nigam, S. K. (1997). Transforming growth factor-beta selectively inhibits branching morphogenesis but not tubulogenesis. *Am. J. Physiol.* **272**, F139-F146.
- Sakurai, H., Tsukamoto, T., Kjelsberg, C. A., Cantley, L. G., and Nigam, S. K. (1997b). EGF receptor ligands are a large fraction of in vitro branching morphogens secreted by embryonic kidney. *Am. J. Physiol.* **273**, F463-F472.
- Sanchez, M. P., Silos-Santiago, I., Frisen, J., He, B., Lira, S. A., and Barbacid, M. (1996). Renal agenesis and the absence of enteric neurons in mice lacking GDNF. *Nature* **382**, 70-73.
- Santos, O. F., Moura, L. A., Rosen, E. M., and Nigam, S. K. (1993). Modulation of HGF-induced tubulogenesis and branching by multiple phosphorylation mechanisms. *Dev. Biol.* **159**, 535-548.
- Santos, O. F., and Nigam, S. K. (1993). HGF-induced tubulogenesis and branching of epithelial cells is modulated by extracellular matrix and TGF-beta. *Dev. Biol.* **160**, 293-302.
- Sariola, H., and Sainio, K. (1997). The tip-top branching ureter. *Curr. Opin. Cell Biol.* **9**, 877-884.
- Schuchardt, A., D'Agati, V., Larsson-Blomberg, L., Costantini, F., and Pachnis, V. (1994). Defects in the kidney and enteric nervous system of mice lacking the tyrosine kinase receptor Ret [see comments]. *Nature* **367**, 380-383.
- Schwimmer, R., and Ojakian, G. K. (1995). The alpha 2 beta 1 integrin regulates collagen-mediated MDCK epithelial membrane remodeling and tubule formation. *J. Cell Sci.* **108**, 2487-2498.
- Shibamoto, S., Hayakawa, M., Takeuchi, K., Hori, T., Oku, N., Miyazawa, K., Kitamura, N., Takeichi, M., and Ito, F. (1994). Tyrosine phosphorylation of beta-catenin and plakoglobin enhanced by hepatocyte growth factor and epidermal growth factor in human carcinoma cells. *Cell Adhes. Commun.* **1**, 295-305.
- Shore, E. M., and Nelson, W. J. (1991). Biosynthesis of the cell adhesion molecule uvomorulin (E-cadherin) in Madin-Darby canine kidney epithelial cells. *J. Biol. Chem.* **266**, 19672-19680.
- Siliciano, J. D., and Goodenough, D. A. (1988). Localization of the tight junction protein, ZO-1, is modulated by extracellular calcium and cell-cell contact in Madin-Darby canine kidney epithelial cells. *J. Cell Biol.* **107**, 2389-2399.
- Stevenson, B. R., Anderson, J. M., and Bullivant, S. (1988). The epithelial tight junction: Structure, function and preliminary biochemical characterization. *Mol. Cell. Biochem.* **83**, 129-145.
- Stevenson, B. R., Siliciano, J. D., Mooseker, M. S., and Goodenough, D. A. (1986). Identification of ZO-1: A high molecular weight polypeptide associated with the tight junction (zonula occludens) in a variety of epithelia. *J. Cell Biol.* **103**, 755-766.
- Stoker, M., and Perryman, M. (1985). An epithelial scatter factor released by embryo fibroblasts. *J. Cell Sci.* **77**, 209-223.
- Sutherland, D., Samakoullis, C., and Krasnow, M. A. (1996). branchless encodes a *Drosophila* FGF homolog that controls tracheal cell migration and the pattern of branching. *Cell* **87**, 1091-1101.
- Takeichi, M. (1991). Cadherin cell adhesion receptors as a morphogenetic regulator. *Science* **251**, 1451-1455.
- Thiery, J. P., and Boyer, B. (1992). The junction between cytokines and cell adhesion. *Curr. Opin. Cell Biol.* **4**, 782-792.
- Vainio, S., and Muller, U. (1997). Inductive tissue interactions, cell signaling, and the control of kidney organogenesis. *Cell* **90**, 975-978.
- Vega-Salas, D. E., Salas, P. J., and Rodriguez-Boulan, E. (1988). Exocytosis of vacuolar apical compartment (VAC): A cell-cell contact controlled mechanism for the establishment of the apical plasma membrane domain in epithelial cells. *J. Cell Biol.* **107**, 1717-1728.
- Vega-Salas, D. E., Salas, P. J. I., D., G., and Rodriguez-Boulan, E. (1987). Formation of the apical pole of epithelial MDCK cells: Polarity of an apical protein is independent of tight junctions while segregation of a basolateral marker requires cell-cell interactions. *J. Cell Biol.* **104**, 905-916.
- Vestweber, D., and Kemler, R. (1985). Identification of a putative cell adhesion domain of uvomorulin. *EMBO J.* **4**, 3393-3398.
- Vestweber, D., Kemler, R., and Ekblom, P. (1985). Cell-adhesion molecule uvomorulin during kidney development. *Dev. Biol.* **112**, 213-221.
- Volberg, T., Zick, Y., Dror, R., Sabanay, I., Gilon, C., Levitzki, A., and Geiger, B. (1992). The effect of tyrosine-specific protein

- phosphorylation on the assembly of adherens-type junctions. *EMBO J.* **11**, 1733-1742.
- Wang, A. Z., Ojakian, G. K., and Nelson, W. J. (1990a). Steps in the morphogenesis of a polarized epithelium. I. Uncoupling the roles of cell-cell and cell-substratum contact in establishing plasma membrane polarity in multicellular epithelial (MDCK) cysts. *J. Cell Sci.* **95**, 137-151.
- Wang, A. Z., Ojakian, G. K., and Nelson, W. J. (1990b). Steps in the morphogenesis of a polarized epithelium. II. Disassembly and assembly of plasma membrane domains during reversal of epithelial cell polarity in multicellular epithelial (MDCK) cysts. *J. Cell Sci.* **95**, 153-165.
- Watabe, M., Matsumoto, K., Nakamura, T., and Takeichi, M. (1993). Effect of hepatocyte growth factor on cadherin-mediated cell-cell adhesion. *Cell. Struct. Funct.* **18**, 117-124.
- Weidner, K. M., Di Cesare, S., Sachs, M., Brinkmann, V., Behrens, J., and Birchmeier, W. (1996). Interaction between Gab1 and the c-Met receptor tyrosine kinase is responsible for epithelial morphogenesis. *Nature* **384**, 173-176.
- Weidner, K. M., Sachs, M., Riethmacher, D., and Birchmeier, W. (1995). Mutation of juxtamembrane tyrosine residue 1001 suppresses loss-of-function mutations of the met receptor in epithelial cells. *Proc. Natl. Acad. Sci. USA* **92**, 2597-2601.
- Weimbs, T., Low, W.-H., Chapin, S. J., and Mostov, K. E. (1997). Apical targeting in polarized epithelial cells: There's more afloat than rafts. *Trends Cell Biol.* **7**, 393-399.
- Woolf, A. S., Kolatsi-Joannou, M., Hardman, P., Andermarcher, E., Moorby, C., Fine, L. G., Jat, P. S., Noble, M. D., and Gherardi, E. (1995). Roles of hepatocyte growth factor/scatter factor and the met receptor in the early development of the metanephros. *J. Cell Biol.* **128**, 171-184.
- Zuk, A., and Matlin, K. S. (1996). Apical beta 1 integrin in polarized MDCK cells mediates tubulocyst formation in response to type I collagen overlay. *J. Cell Sci.* **109**, 1875-1889.

Received for publication April 13, 1998

Revised September 16, 1998

Accepted September 18, 1998

# Intracellular Redirection of Plasma Membrane Trafficking after Loss of Epithelial Cell Polarity

Seng Hui Low,<sup>\*†</sup> Masumi Miura,<sup>\*</sup> Paul A. Roche,<sup>‡</sup> Anita C. Valdez,<sup>‡</sup> Keith E. Mostov,<sup>†</sup> and Thomas Weimbs<sup>\*†§||</sup>

<sup>\*</sup>Department of Cell Biology, Lerner Research Institute, and <sup>§</sup>Urological Institute, The Cleveland Clinic Foundation, Cleveland, Ohio 44195; <sup>†</sup>Department of Anatomy, Department of Biochemistry and Biophysics, Cardiovascular Research Institute, University of California, San Francisco, California 94143; and <sup>‡</sup>Experimental Immunology Branch, National Cancer Institute, National Institutes of Health, Bethesda, Maryland 20892

Submitted May 16, 2000; Accepted June 26, 2000  
Monitoring Editor: Suzanne R. Pfeffer

In polarized Madin-Darby canine kidney epithelial cells, components of the plasma membrane fusion machinery, the t-SNAREs syntaxin 2, 3, and 4 and SNAP-23, are differentially localized at the apical and/or basolateral plasma membrane domains. Here we identify syntaxin 11 as a novel apical and basolateral plasma membrane t-SNARE. Surprisingly, all of these t-SNAREs redistribute to intracellular locations when Madin-Darby canine kidney cells lose their cellular polarity. Apical SNAREs relocate to the previously characterized vacuolar apical compartment, whereas basolateral SNAREs redistribute to a novel organelle that appears to be the basolateral equivalent of the vacuolar apical compartment. Both intracellular plasma membrane compartments have an associated prominent actin cytoskeleton and receive membrane traffic from cognate apical or basolateral pathways, respectively. These findings demonstrate a fundamental shift in plasma membrane traffic toward intracellular compartments while protein sorting is preserved when epithelial cells lose their cell polarity.

## INTRODUCTION

Traffic between membranous compartments is mediated by the soluble N-ethylmaleimide-sensitive factor attachment protein (SNARE) machinery in virtually all membrane traffic pathways investigated so far (Rothman and Warren, 1994; Hanson *et al.*, 1997; Hay and Scheller, 1997; Nichols and Pelham, 1998). During vesicle docking, membrane proteins on the vesicle membrane (v-SNAREs) and the target membrane (t-SNAREs) bind to each other to form a complex that ultimately leads to fusion of the lipid bilayers. One aspect of the SNARE hypothesis is that successful membrane fusion requires the binding of matching combinations of v- and t-SNAREs, thereby ensuring the necessary specificity of vesicle fusion. Accordingly, each membrane organelle and each class of transport vesicles should be defined by a certain set of t- and v-SNARE isoforms. Many SNAREs have been identified to date, and protein sequence analysis has shown that v- and t-SNAREs of the currently known SNARE subfamilies are evolutionarily related to each other and belong to a common superfamily (Weimbs *et al.*, 1997b, 1998). It is conceivable that the specificity of vesicle fusion is not directly determined by t-SNARE/v-SNARE interactions per se

but rather by interactions involving larger complexes, including SNAREs and their regulatory proteins, such as those of the rab and sec1 protein families (Christoforidis *et al.*, 1999; Gonzalez and Scheller, 1999; Pfeffer, 1999).

Epithelial cells display an additional layer of complexity in that they are typically polarized and possess two distinct plasma membrane domains (Louvard *et al.*, 1992; Simons *et al.*, 1992; Le Gall *et al.*, 1995; Drubin and Nelson, 1996; Yeaman *et al.*, 1999). The apical and basolateral plasma membrane domains have different protein and lipid compositions that reflect the different functions of these domains. This plasma membrane polarity is established and maintained by protein sorting and specific vesicle trafficking routes in the biosynthetic and endocytic pathways. In agreement with the SNARE hypothesis, the apical and basolateral plasma membrane domains of epithelial cells contain distinct t-SNAREs (Weimbs *et al.*, 1997a). Two protein families have been identified as t-SNAREs, the syntaxin and SNAP-25 families. In the polarized renal epithelial Madin-Darby canine kidney (MDCK) cell line, syntaxins 3 and 4 are localized at the apical or basolateral plasma membrane, respectively (Low *et al.*, 1996). Syntaxin 3 functions in transport from the *trans*-Golgi network (TGN) as well as the endosomal recycling pathway, both leading to the apical plasma membrane (Low *et al.*, 1998a). Syntaxin 2 is localized

|| Corresponding author. E-mail address: weimbst@ccf.org.

to both domains of MDCK cells (Low *et al.*, 1996), as is SNAP-23 (Low *et al.*, 1998b), a ubiquitously expressed member of the SNAP-25 family (Ravichandran *et al.*, 1996). SNAP-23 binds to syntaxins 3 and 4 *in vivo* (Galli *et al.*, 1998; St-Denis *et al.*, 1999) and is involved in biosynthetic and endocytic recycling and transcytotic pathways to both plasma membrane domains in MDCK cells (Leung *et al.*, 1998; Low *et al.*, 1998a). The subcellular localization of these SNAREs is generally very similar in other epithelial cell lines and tissues, although variations have been reported (Gaisano *et al.*, 1996; Delgrossi *et al.*, 1997; Weimbs *et al.*, 1997a; Fujita *et al.*, 1998; Galli *et al.*, 1998; Riento *et al.*, 1998).

Temporary or permanent loss of cell polarity is a common phenomenon during the development of epithelial tissues (Sorokin and Ekblom, 1992; Birchmeier *et al.*, 1996) as well as in a number of pathological conditions (Louvard *et al.*, 1992; Fish and Molitoris, 1994; Birchmeier *et al.*, 1996). It is largely unknown how apical and basolateral membrane traffic pathways behave in epithelial cells that have lost or not yet acquired their cellular polarity under any of these circumstances. This is a fundamental question in cell biology. For example, changes in these pathways may play an important role in the acquisition of the invasive phenotype of tumor cells, e.g., by mistargeting of cell adhesion molecules or erroneous secretion of proteases that attack basement membrane and extracellular matrix proteins. It is well established that the malignancy of epithelium-derived tumors (carcinomas) correlates directly with the degree of dedifferentiation. A hallmark of dedifferentiation or anaplasia is the loss of cellular polarity. A better knowledge of the changes in membrane traffic pathways that occur when epithelial cells lose or gain cell polarity will help us understand normal epithelial function as well as pathological conditions.

In this work, we have investigated the subcellular localization of plasma membrane t-SNAREs as part of the machinery that controls membrane traffic in polarized versus nonpolarized MDCK cells. We identified syntaxin 11 as a novel plasma membrane t-SNARE in addition to syntaxins 2, 3, and 4 and SNAP-23. All plasma membrane t-SNAREs undergo dramatic changes in subcellular localization in MDCK cells depending on their state of cell polarity. Apical t-SNAREs relocate to an intracellular vacuolar apical compartment (VAC), whereas basolateral t-SNAREs relocate to a novel compartment. The presence of t-SNAREs in these intracellular compartments suggests that they function in the fusion of incoming transport vesicles and that these compartments are actively connected to cellular membrane traffic. Indeed, we find that the apical and basolateral intracellular compartments are functionally equivalent to the apical or basolateral plasma membranes of fully polarized cells, respectively, in that they receive membrane traffic from cognate apical or basolateral transport pathways.

These results suggest that fundamental rearrangements occur with respect to membrane traffic in epithelial cells that have lost their cellular polarity. Nevertheless, the localization of plasma membrane t-SNAREs does not become randomized; instead, the cells redirect plasma membrane transport pathways into intracellular compartments and preserve protein sorting.

## MATERIALS AND METHODS

### Materials

Cell culture media were from Cell Gro, Mediatech (Washington, DC). FBS was from Hyclone (Logan, UT). G418 was obtained from GIBCO-BRL (Gaithersburg, MD). Transwell polycarbonate cell culture filters were purchased from Corning Costar (Cambridge, MA). Canine apo-transferrin was purchased from Sigma Chemical (St. Louis, MO), loaded with iron, and dialyzed against PBS. The cDNA of human syntaxin 11 in the expression vector pcDNA3 has been described (Valdez *et al.*, 1999). cDNAs for the expression of syntaxin-GST fusion proteins were gifts from Dr. Mark Bennett (University of California at Berkeley).

### Antibodies

Polyclonal antibodies against rat syntaxins 2, 3, and 4 were raised in rabbits against GST fusion proteins of the cytoplasmic domains. The antibodies were affinity-purified with the use of the respective syntaxin cytoplasmic domains that were separated from GST by thrombin cleavage and coupled to Affigel (Bio-Rad, Richmond, CA). The rabbit polyclonal antibody against an N-terminal peptide of human SNAP-23 was affinity-purified as described previously (Low *et al.*, 1998b). The affinity-purified rabbit polyclonal antibody against a peptide of the N-terminal 15 amino acids of human syntaxin 11 has been described (Valdez *et al.*, 1999). The rat mAb against ZO-1 and the mouse mAbs against ubiquitin and  $\alpha$ -fodrin (nonerythroid spectrin) were obtained from Chemicon International (Temecula, CA). The mouse mAbs against  $\gamma$ -tubulin and pan-cytokeratin were obtained from Sigma. AC17, a mouse mAb against the lysosomal/late endosomal membrane glycoprotein LAMP-2 (Nabi and Rodriguez-Boulton, 1993), was a gift from E. Rodriguez-Boulton (Cornell University Medical College, New York, NY). The mouse mAb against gp135, an endogenous apical plasma membrane protein in MDCK cells (Ojakian and Schwimmer, 1988), was a gift from G. Ojakian (State University of New York Health Science Center, Brooklyn, NY). The mouse mAb against E-cadherin, rr1 (Gumbiner and Simons, 1986), was donated by B. Gumbiner (Sloan-Kettering, New York, NY). The mouse mAb 6.23.3 against an endogenous MDCK basolateral plasma membrane protein of 58 kDa (Balcarova-Stander *et al.*, 1984) was a gift from K. Matlin (Harvard Medical School, Boston, MA). The rabbit polyclonal antibody against canine gp80/clusterin (Urban *et al.*, 1987) was a gift from C. Koch-Brandt (Universität Mainz, Mainz, Germany). Purified human polymeric immunoglobulin A (IgA) was kindly provided by J.-P. Vaerman (Catholic University of Louvain, Brussels, Belgium). Anti-Na<sup>+</sup>/K<sup>+</sup>-ATPase ( $\alpha$  subunit, MA3-928) was from Affinity Bioreagents (Golden, CO). Fluorescein dichlorotriazine-labeled anti-human IgA antibody was from Organon Teknika (Durham, NC). The antibody against canine apo-transferrin has been described (Apodaca *et al.*, 1994). The mouse mAb against Golgin-97 was from Molecular Probes (Eugene, OR). Secondary antibodies cross-absorbed against multiple species and conjugated to FITC, Texas Red, or Cy5 were from Jackson ImmunoResearch (West Grove, PA).

### SDS-PAGE and Immunoblotting

Total membrane fractions of MDCK, HepG2, HeLa, and HT29 cells were prepared by scraping the cells from confluent dishes in PBS containing protease inhibitors and homogenization by repeated passage through a 22-gauge needle. Nuclei and unbroken cells were removed by centrifugation at  $500 \times g$  for 2 min. The membranes were recovered by centrifugation at  $16,000 \times g$  for 10 min and dissolved in SDS-PAGE sample buffer. Equal amounts of protein were separated on a 12% SDS-polyacrylamide gel followed by transfer to nitrocellulose and incubation with the affinity-purified syntaxin 11 antibody. Bands were visualized by ECL.

## Cell Culture

MDCK strain II cells were maintained in MEM supplemented with 10% FBS, 100 U/ml penicillin, and 100  $\mu$ g/ml streptomycin in 5% CO<sub>2</sub>/95% air. For experiments with polarized MDCK cells, the cells were cultured on 12-mm, 0.4- $\mu$ m pore size Transwell polycarbonate filters for the indicated periods. For experiments with nonpolarized MDCK cells, the cells were sparsely seeded onto glass coverslips in MEM without FBS and allowed to attach for 2 h. Afterward, the medium was changed to s-MEM (GIBCO-BRL) with three washes of 10 min each, and the cells were incubated overnight (i.e., 16–18 h). In some experiments, the cells were allowed to endocytose IgA or transferrin during this overnight incubation by adding 50  $\mu$ g/ml polymeric IgA or 1  $\mu$ g/ml iron-loaded canine transferrin, respectively.

## Transfection

For expression of human syntaxin 11, MDCK cells were transfected with the syntaxin 11 cDNA in the expression vector pCDNA3 by the calcium phosphate method, followed by selection in medium containing 350  $\mu$ g/ml G418 (as described by Breitfeld *et al.*, 1989). For all experiments, a mixture of the G418-resistant cells, displaying a wide range of expression levels, was used. MDCK cells stably expressing rat syntaxins 2, 3, and 4 have been described (Low *et al.*, 1996). MDCK cells expressing human SNAP-23 were described by Low *et al.* (1998b). MDCK cells expressing the wild-type rabbit polymeric immunoglobulin receptor (pIgR) (Mostov and Deitcher, 1986), signalless pIgR (Casanova *et al.*, 1991), or glycosylphosphatidylinositol (GPI)-pIgR (Mostov *et al.*, 1986) have been described previously.

## Confocal Immunofluorescence Microscopy

Cells were fixed either in methanol at  $-20^{\circ}\text{C}$  or with 4% paraformaldehyde, permeabilized with 0.025% (wt/vol) saponin (Sigma) in PBS, and then blocked with 10% FBS or 5% BSA followed by sequential incubations with primary antibodies and FITC- and/or Texas red-conjugated secondary antibodies. In some cases, nuclei were stained with 5  $\mu$ g/ml propidium iodide (Vector Laboratories, Burlingame, CA) after treatment with 100  $\mu$ g/ml RNase A. The samples were analyzed with the use of a Leica (Bensheim, Germany) TCS-NT confocal microscope.

## RESULTS

### Syntaxin 11 Is Expressed at the Plasma Membrane in Polarized but Not in Nonpolarized MDCK Cells

The following t-SNAREs are localized to the plasma membrane in mammalian cells. The neuron-specific syntaxins 1A, 1B, and SNAP-25 function in the fusion of synaptic vesicles with the presynaptic plasma membrane. The more widely expressed syntaxins 2, 3, and 4 and SNAP-23 have been studied in various cell types, in which they are generally localized at the plasma membrane (Bennett *et al.*, 1993; Low *et al.*, 1996; Wang *et al.*, 1997; Galli *et al.*, 1998; Low *et al.*, 1998b). All other syntaxin homologues studied so far are localized to various intracellular organelles where they are believed to be functionally involved in membrane trafficking pathways directed to these organelles.

The recently discovered syntaxin 11 has an unusual primary structure in that it lacks a C-terminal transmembrane domain (Advani *et al.*, 1998; Tang *et al.*, 1998; Valdez *et al.*, 1999). Nevertheless, syntaxin 11 is membrane-bound. In transiently transfected, nonpolarized NRK or HeLa cells, syntaxin 11 was found in intracellular vesicles that partially colocalized with endosomal and TGN markers (Advani *et al.*, 1998; Valdez *et al.*, 1999). Syntaxin 11 is widely expressed in several tissues, including tissues rich in epithelia such as lung, placenta, liver, and kidney, whereas it is absent in brain (Advani *et al.*, 1998; Tang *et al.*, 1998; Valdez *et al.*, 1999). This tissue distribution prompted us to investigate whether syntaxin 11 is expressed in several pure epithelial cell lines. By Western blotting, syntaxin 11 can be detected in total membrane fractions of MDCK cells and Caco-2 colon carcinoma cells as well as in HeLa cells, but it is undetectable in the intestinal epithelial cell line HT-29 and in hepatocyte-derived HepG2 cells (Figure 1). The gel mobility of endogenous syntaxin 11 in HeLa cells is slightly higher than that in MDCK and Caco-2 cells. The reason for this difference is unknown, but it may result from differences in posttranslational modification.

Next, we studied the subcellular localization of syntaxin 11 in MDCK cells because this epithelial cell line has been most extensively studied with respect to the localization and function of t-SNAREs. Because our syntaxin 11 antibody did not react well for immunocytochemistry with the endogenous canine protein, MDCK cells were stably transfected with the cDNA of the human protein. Confocal immunoflu-

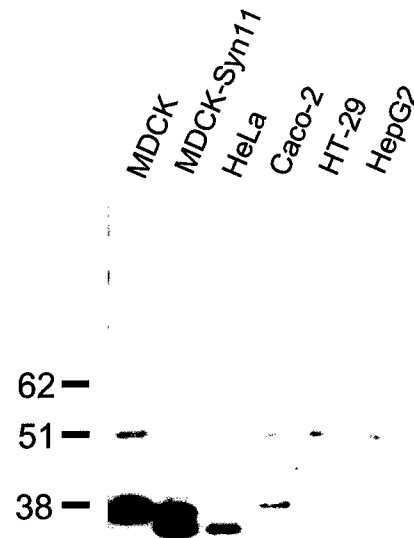


**Figure 1.** Syntaxin 11 is endogenously expressed in epithelial cell lines. Total membrane lysates were prepared from the following cultured cell lines: canine kidney epithelium-derived MDCK cells, MDCK cells stably transfected with human syntaxin 11, human colon carcinoma-derived Caco-2 and HT-29 cells, human liver epithelial HepG2 cells, and human HeLa cells. Equal amounts of protein were separated on a 12% SDS-polyacrylamide gel, transferred to nitrocellulose, and probed with an affinity-purified polyclonal antibody against an N-terminal peptide of the human syntaxin 11 sequence. Endogenous syntaxin 11 could be detected in MDCK, Caco-2, and HeLa cells. Identical signals were obtained with Western blots probed with antisera from two additional rabbits. All bands disappeared after competition with the syntaxin 11 peptide (our unpublished results). The electrophoretic mobility of syntaxin 11 in HeLa cells and exogenously expressed syntaxin 11 in MDCK cells is higher than that of endogenous syntaxin 11 in MDCK and Caco-2 cells.

orescence microscopy revealed that syntaxin 11 is localized predominantly at the plasma membrane in polarized MDCK cells rather than in intracellular compartments, as reported previously for nonpolarized cells. The majority of syntaxin 11 localizes to both the apical and basolateral plasma membranes, with some additional intracellular punctate staining mostly in the apical cytoplasm (Figure 2). This localization was independent of the level of syntaxin 11 expression found by comparing individual cells with a wide range of expression levels in a mixed population of stably transfected cells. Also, as shown in Figure 1, the level of exogenous human syntaxin 11 expression was similar to the endogenous level in MDCK cells.

Surprisingly, in nonpolarized MDCK cells, e.g., soon after plating and not allowing the cells enough time to form cell–cell interactions, syntaxin 11 was found to be intracellular, with very little if any plasma membrane staining (Figure 2E). Under these conditions, syntaxin 11 localizes to bright punctate vesicles, as reported previously in nonpolarized fibroblastic cells (Advani *et al.*, 1998; Valdez *et al.*, 1999). Costaining of syntaxin 11 with an antibody against the lysosomal/late endosomal protein LAMP-2 shows no significant overlap, indicating that syntaxin 11 is not simply being degraded in nonpolarized MDCK cells (Figure 2E). The observed dramatic change in the localization of syntaxin 11 depending on the state of cellular polarity of MDCK cells suggests that it normally functions at the plasma membrane in polarized epithelial cells, while it may have a different function in nonpolarized cells.

#### **The Subcellular Localization of All Plasma Membrane t-SNAREs Changes during the Development of Epithelial Polarity**

As with syntaxin 11, we observed that the previously characterized plasma membrane t-SNAREs in MDCK cells also undergo similar dramatic changes in subcellular localization depending on the degree of cellular polarity. Figure 3 shows a time course of MDCK cells at various stages during the establishment of a fully polarized monolayer. The cells were plated at high density onto polycarbonate filters, and the localizations of syntaxins 2, 3, 4, and 11 and SNAP-23, as well as the tight junction protein ZO-1, were monitored at different times after plating. After 2 h, the cells are irregularly shaped and start to form cell–cell contacts. At this stage, all plasma membrane t-SNAREs are found predominantly in intracellular vesicles in addition to a variable amount of plasma membrane staining. In ~10% of the cells, large intracellular vacuolar structures can be observed (arrows). After 1 d, the monolayer is confluent and uninterrupted circumferential tight junctions are established. A substantial portion of all SNAREs has relocated to the plasma membrane in a polarized manner. Syntaxins 2 and 11 as well as SNAP-23 are found at both the basolateral and the apical plasma membrane in addition to some remaining intracellular labeling. Syntaxin 3 is absent from the basolateral domain but localizes to the apical domain in addition to intracellular lysosomes, as established previously (Low *et al.*, 1996; Delgrossi *et al.*, 1997). Syntaxin 4, in turn, is absent from the apical domain but has partially relocated to the basolateral domain. During the course of the experiment, until d 7, the cells grow somewhat in height and form a

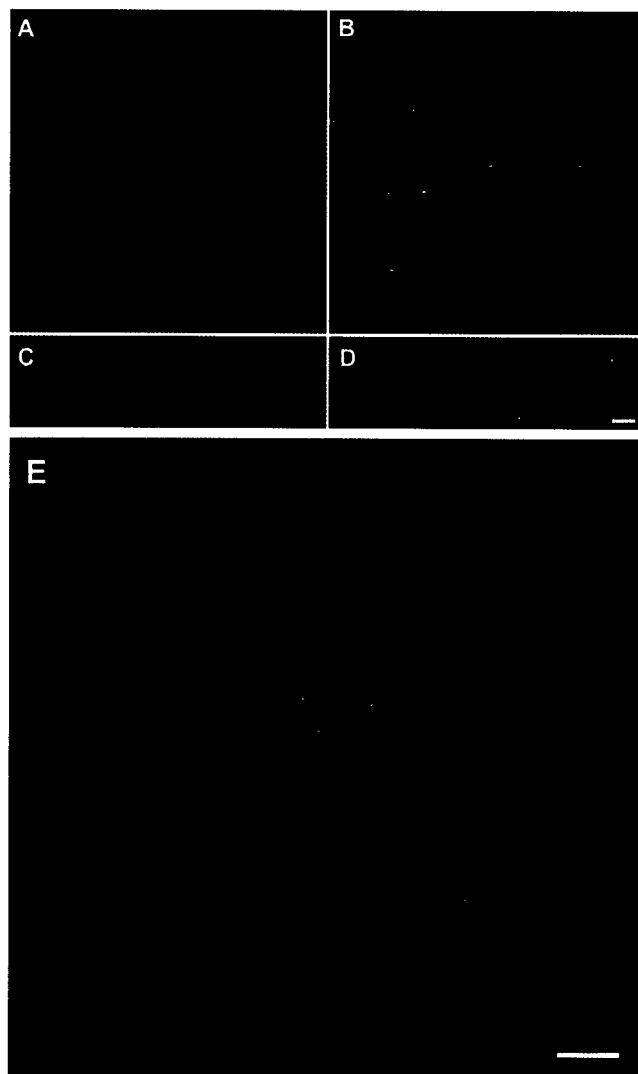


**Figure 2.** Syntaxin 11 is localized at the plasma membrane in polarized but not in nonpolarized MDCK cells. A mixed population of MDCK cells stably expressing human syntaxin 11 was grown either for 3 d on polycarbonate filters (A–D) or for 2 h on glass coverslips (E). The cells were stained with antibodies against syntaxin 11 (A, C, and E, green), the lateral plasma membrane protein E-cadherin (B and D), or the late endosomal/lysosomal protein LAMP-2 (E, red). B and D also show nuclear DNA staining with propidium iodide. A and B show horizontal confocal optical sections just above the nuclei. C and D show vertical optical sections with the apical plasma membrane at the top. Syntaxin 11 colocalizes with E-cadherin at the lateral plasma membrane. E shows a representative horizontal optical section through the middle of the cells. Syntaxin 11 does not significantly colocalize with LAMP-2. The absence of a syntaxin 11 signal in neighboring nonexpressing cells (A and E) demonstrates the specificity of the antibody. Bars, 5  $\mu$ m.

straight apical surface. All of the SNAREs continue to move to their final destination at their specific plasma membrane domains; however, even after 7 d some intracellular staining remains in each case, as observed previously (Low *et al.*, 1996, 1998b).

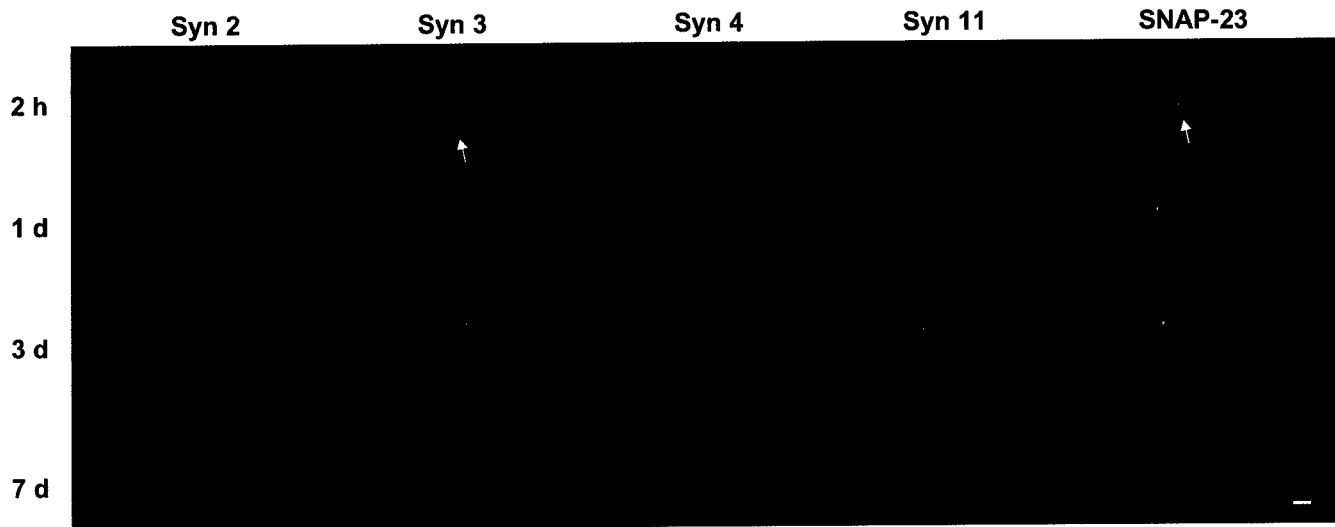


**Figure 3.** All plasma membrane t-SNAREs relocate from intracellular compartments to their final plasma membrane domains during development of MDCK cells into a polarized monolayer. MDCK cells stably expressing syntaxins 2, 3, 4, and 11 and SNAP-23 were seeded at high density onto polycarbonate filters. At the indicated times, the cells were fixed and stained with affinity-purified antibodies against the respective SNAREs (green) as well as an antibody against the tight junction protein ZO-1 (red). Nuclei were stained with propidium iodide (red). Confocal optical sections through the monolayers are shown with the apical side on top. Once the cells have established contacts, the tight junctions can be seen as red dots at the junction between the apical and basolateral plasma membranes. At the earliest time, large intracellular vacuoles are occasionally detected (arrows), most frequently with syntaxin 3 and SNAP-23. While the distribution of all studied SNAREs is predominantly intracellular at 2 h, it shifts to a predominantly plasma membrane localization during the course of 7 d. Note that starting at d 1, syntaxin 3 is always excluded from the basolateral plasma membrane, whereas syntaxin 4 is always excluded from the apical plasma membrane. Bar, 5  $\mu$ m.

This change in subcellular localization of the machinery that normally mediates vesicle fusion at the plasma membrane suggests that these membrane traffic pathways are fundamentally altered in epithelial cells during the course of the establishment of cellular polarity.

#### ***Sustained Inhibition of Epithelial Polarity Causes Intracellular Accumulation of Apical and Basolateral t-SNAREs into Distinct Compartments***

To study the nature of the intracellular location of plasma membrane t-SNAREs in detail, we sought to arrest MDCK cells in a nonpolarized state. The formation of a polarized epithelial layer can be prevented experimentally by the inhibition of E-cadherin-mediated interactions between neighboring cells (Birchmeier *et al.*, 1996; Bracke *et al.*, 1996; Gumbiner, 1996). Inhibition of calcium-dependent homotypic E-cadherin binding by withdrawal of high calcium concentrations in the medium keeps MDCK cells in a nonpolarized state. It has been observed that, when grown in low-calcium medium (LCM), MDCK cells form large intracellular vacuoles that bear ultrastructural resemblance to the apical plasma membrane, including the presence of microvilli and an associated actin cytoskeleton. This compartment was termed "vacuolar apical compartment" or VAC (Vega-Salas *et al.*, 1987). Similar vacuoles are found in a variety of carcinomas (Remy, 1986; Kern *et al.*, 1987; Vega-Salas *et al.*, 1993).

We studied the subcellular localization of plasma membrane SNAREs in MDCK cells grown under these conditions. A high percentage (>50%) of the cells display one or

more large vacuolar compartments that are positive for the endogenous apical marker protein gp135 and are indistinguishable in appearance from previously described VACs (Figure 4). Plasma membrane t-SNAREs that normally localize to the apical domain (syntaxins 2, 3, and 11 and SNAP-23) colocalize with gp135 in these VACs. In contrast, the normally exclusively basolateral syntaxin 4 is excluded from gp135-positive VACs. Instead, in addition to small vesicles, in the majority of cells syntaxin 4 is found in larger structures that resemble VACs but exclude gp135. The SNAREs that are normally localized to both apical and basolateral plasma membrane domains (syntaxins 2 and 11 and SNAP-23) can be found in large gp135-negative structures (arrows) in addition to gp135-positive VACs. These results suggest that at least two distinct intracellular organelles exist in nonpolarized MDCK cells to which plasma membrane t-SNAREs are targeted.

To verify the results obtained with exogenously expressed syntaxin 3 in MDCK cells, we investigated whether endogenous syntaxin 3 would also localize to VACs in a different cell line. The human colon carcinoma cell line Caco-2 was grown in LCM as described above and stained for endogenously expressed syntaxin 3 and the microvillar protein villin. While syntaxin 3 and villin are localized at the apical plasma membrane in fully polarized Caco-2 cells (Delgrossi *et al.*, 1997; Galli *et al.*, 1998; Riento *et al.*, 1998; our unpublished results), they are strongly enriched in VACs in nonpolarized cells (Figure 5). This result indicates that the localization of syntaxin 3 in VACs is a general phenomenon of nonpolarized epithelial cells and not an artifact of syntaxin overexpression.

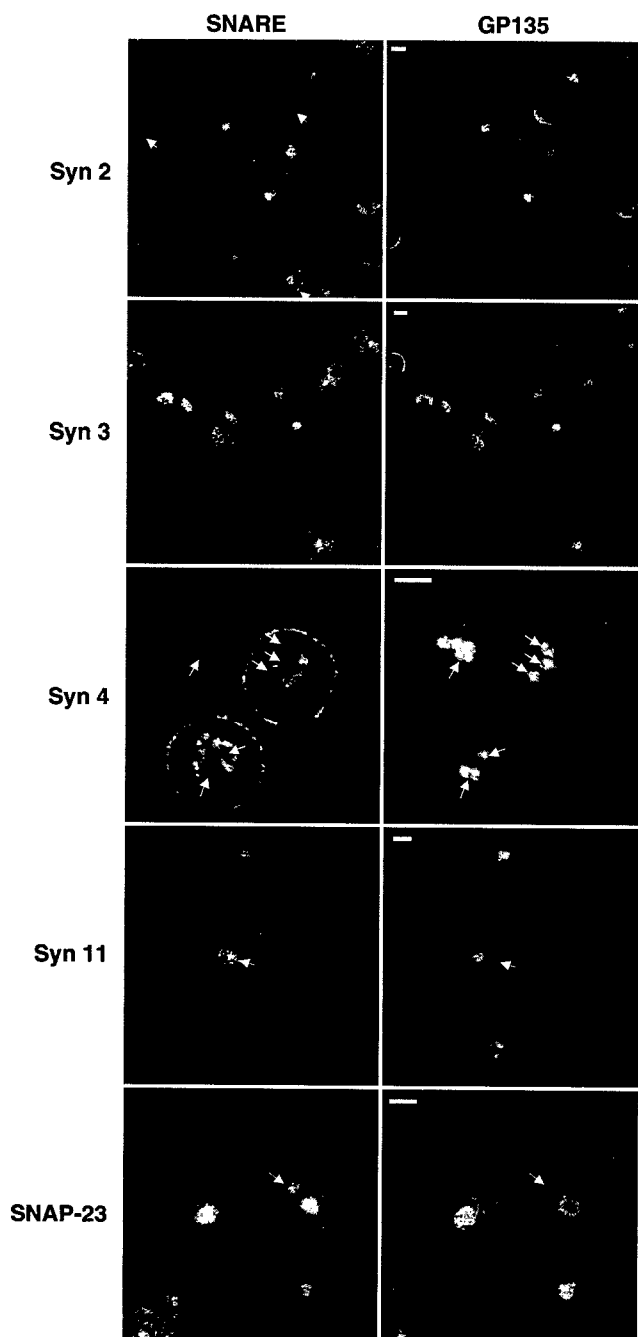


**Figure 4.** In nonpolarized MDCK cells, apical t-SNAREs localize to the VAC, whereas basolateral SNAREs are excluded from it. MDCK cells stably expressing syntaxins 2, 3, 4, and 11 and SNAP-23 were seeded onto glass coverslips in regular medium. After 2 h, the cells were switched to LCM and incubated for 16 h. Cells were fixed, permeabilized, and stained for the individual SNAREs (left column) and with an antibody against an endogenous apical plasma membrane protein, gp135 (right column). gp135 localizes to the VAC. Syntaxins 2, 3, and 11 and SNAP-23 colocalize with gp135 in VACs. In contrast, syntaxin 4 is excluded from VACs (arrows indicate VACs for better orientation). Syntaxins 2 and 11 and SNAP-23 are also found in large intracellular compartments that exclude gp135 (arrows) in addition to gp135-positive VACs. Bars, 5  $\mu$ m.

We and others found previously that syntaxin 3 partially localizes to lysosomes in addition to the apical plasma membrane in fully polarized MDCK and Caco-2 cells (Low *et al.*, 1996; Delgrossi *et al.*, 1997). To investigate whether VACs containing syntaxin 3 may represent an enlarged type of lysosomes in cells grown under low-calcium conditions, MDCK cells were colabeled for syntaxin 3 and the late endosomal/lysosomal protein LAMP-2. Figure 6 shows that VACs and lysosomes are clearly distinct. This result indicates that VACs are not connected to the late endosomal/lysosomal system and therefore are not degradative compartments. Moreover, none of the other plasma membrane SNAREs colocalized with LAMP-2 in MDCK cells grown in LCM (our unpublished results).

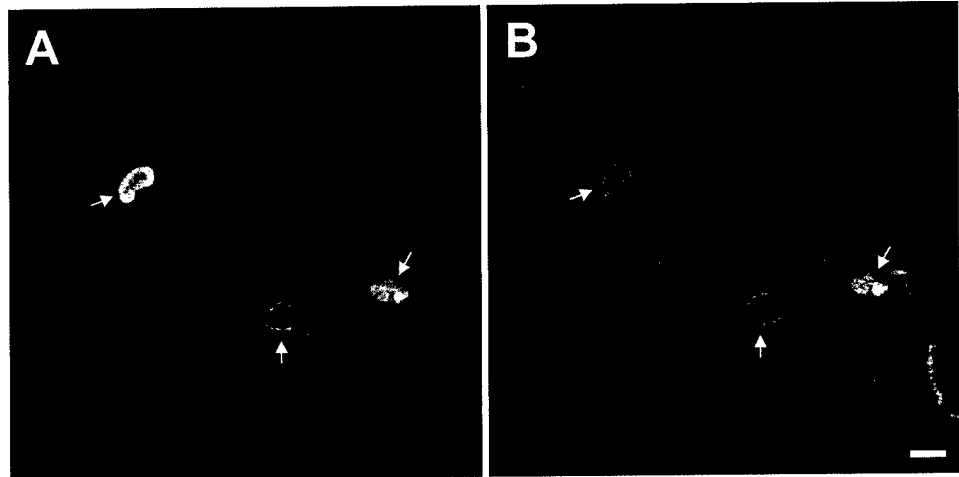
#### *Syntaxin 4 Is a Marker for a Novel Intracellular Organelle in Nonpolarized MDCK Cells*

VACs have been described previously in nonpolarized MDCK cells, and our finding that they contain apical-specific t-SNAREs suggest that they receive apical-specific membrane traffic. Our finding of syntaxin 4-positive intracellular organelles suggests that another class of intracellular plasma membrane-like organelles exists that may be the basolateral equivalent of the VAC. Because such an organelle has not been described before, we sought to investigate its composition and relationship to other organelles in more detail by the colabeling studies described below. Figure 7, A–D, shows that the basolateral syntaxin 4-positive compartment also contains two proteins that are normally specifically localized at the basolateral plasma membrane domain in polarized MDCK cells: an endogenous 58-kDa basolateral plasma membrane protein (6.23.3) and the Na/K-ATPase. Both proteins appear to be even more concentrated in the intracellular compartments than syntaxin 4, which is also present at the plasma membrane. These data indicate that the syntaxin 4-positive compartment has a protein composition similar to that of the basolateral plasma membrane of polarized cells.

It is important to note that the degree of intracellular localization of SNAREs or any of the plasma membrane marker proteins studied here in nonpolarized MDCK cells is relatively heterogeneous. We typically observed a range of individual cells displaying varying degrees of retention ranging from complete absence of plasma membrane markers from the plasma membrane to almost complete absence of these markers in intracellular organelles (see Figures 4–9). This heterogeneity was seen in all MDCK clones investigated, indicating that it is not due to clonal variation.

Next, we investigated whether E-cadherin might be accumulated in the syntaxin 4-positive compartment. In control cultures, E-cadherin colocalizes with syntaxin 4 at the cell-cell contacts (Figure 7, G and H). In contrast, E-cadherin expression is strongly down-regulated in cells grown in LCM (Figure 7, E and F). The remaining minor amounts of E-cadherin partially colocalize with syntaxin 4 in intracellular organelles in addition to spreading in a diffuse staining pattern, but they are not detectable at sites of cell-cell contact. Therefore, in contrast to the antigen 6.23.3 and the Na/K-ATPase, the normally lateral plasma membrane protein E-cadherin is not only redirected from the surface but its expression is also down-regulated.

**Figure 5.** Endogenous syntaxin 3 localizes to VACs in Caco-2 cells. The human colon carcinoma cell line Caco-2 was grown under low-calcium conditions as described in Figure 4. Endogenously expressed syntaxin 3 (A) and the microvillar protein villin (B) were labeled with the appropriate antibodies. Syntaxin 3 is strongly enriched in VACs that are also positive for villin, indicating that VACs are lined by microvilli (arrows). Bar, 5  $\mu$ m.



Both apical and basolateral plasma membrane domains of polarized epithelial cells are generally associated with an actin cytoskeleton. Phalloidin staining shows that in nonpolarized MDCK cells, in addition to the plasma membrane, both syntaxin 3-positive vacuoles (our unpublished results) and syntaxin 4-positive vacuoles (Figure 7, I and J) display an associated actin cytoskeleton. This result distinguishes VACs and the intracellular syntaxin 4-positive compartment from endosomes or other intracellular organelles that do not typically contain a prominent actin cytoskeleton.

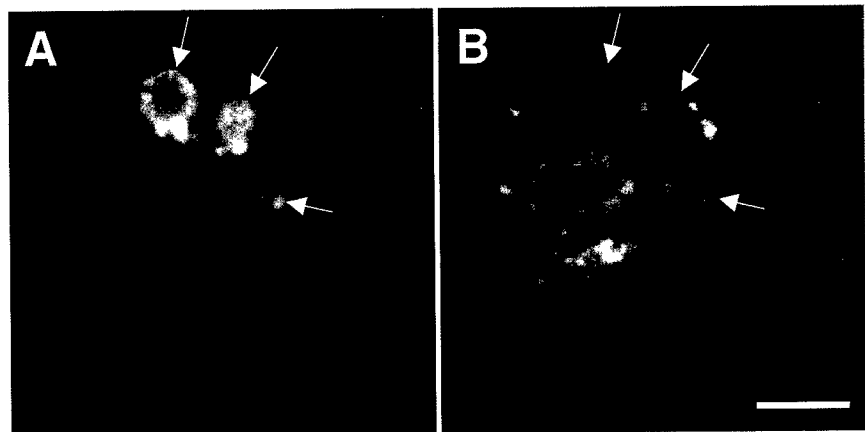
$\alpha$ -Fodrin (nonerythroid spectrin) is a component of the actin-associated cytoskeleton that normally underlies the lateral plasma membrane in polarized epithelial cells and has been implicated in the sorting of basolateral membrane proteins, such as the Na/K-ATPase, by selective retention at the basolateral surface (Nelson and Hammerton, 1989; Nelson *et al.*, 1990; Hammerton *et al.*, 1991). We found that in MDCK cells grown in LCM fodrin significantly colocalizes with syntaxin 4 in intracellular organelles in addition to plasma membrane staining and diffuse cytoplasmic staining (Figure 7, K and L). This suggests that intracellular syntaxin 4-positive organelles possess not only the machinery for fusion of incoming transport vesicles (syntaxin 4) but also

the cytoskeletal components required for selective retention of basolateral membrane proteins and explains the accumulation of Na/K-ATPase in these organelles (Figure 7, C and D).

Cytokeratin intermediate filaments are normally closely attached to the basolateral plasma membrane domain of polarized epithelial cells by anchoring to desmosomes and hemidesmosomes. Using a pan-keratin antibody, we found that intermediate filaments are largely retracted from the plasma membrane in MDCK cells grown in LCM. They are concentrated in the center of the cell, where they often appear to be closely associated with syntaxin 4-positive intracellular organelles (Figure 7, M and N).

The syntaxin 4-positive organelles often localize in a perinuclear position in MDCK cells grown in LCM. Because this is typically also the localization of the Golgi apparatus within nonpolarized cells, we double labeled cells for syntaxin 4 and the Golgi protein Golgin-97. Figure 7, O and P, shows that both proteins localize quite distinctly with no significant overlap, excluding the possibility that the syntaxin 4-positive organelles represent a distended Golgi apparatus in MDCK cells grown in LCM.

**Figure 6.** VACs are not related to lysosomes. MDCK cells expressing syntaxin 3 were grown in LCM for 16 h, fixed, permeabilized, and stained for syntaxin 3 (A) and the late endosomal/lysosomal protein LAMP-2 (B). Note that large vacuoles stain for syntaxin 3 but not LAMP-2 (arrows). Bar, 5  $\mu$ m.



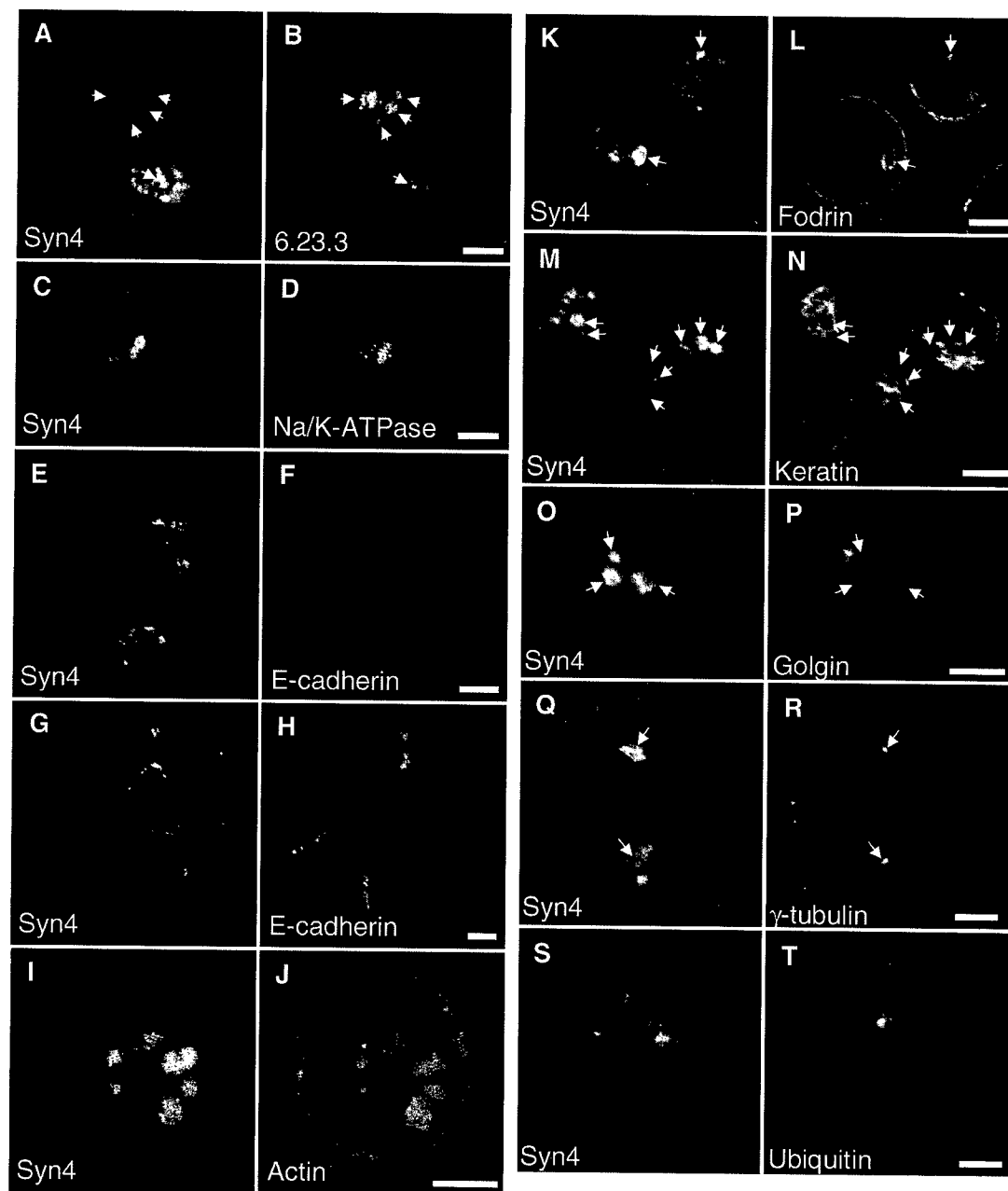


**Figure 7.** Syntaxin 4 is a marker for a novel intracellular organelle in nonpolarized MDCK cells. MDCK cells expressing syntaxin 4 were grown in LCM (A–F and I–T) or regular medium (G and H) for 16 h, fixed, permeabilized, and stained for syntaxin 4 (left columns). Cells were colabeled for the following antigens: (B) antigen 6.23.3, a 58-kDa basolateral plasma membrane protein; (D) Na/K-ATPase; (F and H) E-cadherin; (J) F-actin (staining with fluorescent phalloidin); (L) fodrin; (N) cytokeratin (antibody against pan-cytokeratin); (P) the Golgi protein Golgin-97; (R)  $\gamma$ -tubulin to stain the MTOCs; and (T) ubiquitin. Note that cells in E and F were grown in LCM and show very low E-cadherin signals, in contrast to cells in G and H, which were grown in regular medium. Micrographs for panels F and H were recorded at identical imaging settings for comparison of signal intensities. Note also that cells in S and T were grown in the presence of the proteasome inhibitor acetyl-leucyl-leucyl-norleucinal (ALLN) to allow the accumulation of aggresomes. Arrows at identical locations between panels are drawn for better orientation. Bars, 5  $\mu$ m.

Many cellular organelles tend to cluster around the microtubule organizing center (MTOC), which is typically found in a perinuclear position in nonpolarized cells and indicates that these organelles are clustered there by micro-

tubule-mediated transport. Costaining of MDCK cells grown in LCM for syntaxin 4 and  $\gamma$ -tubulin (Figure 7, Q and R) shows that although the syntaxin 4-positive organelles can be located very close to the MTOC, they show a more

dispersed distribution, suggesting that they are not necessarily being actively recruited toward the MTOC.

Recently, a novel organelle, termed an "aggresome," has been discovered in cells that either express excessive amounts of misfolded proteins or whose proteasome degradation machinery is inhibited (Johnston *et al.*, 1998; Wigley *et al.*, 1999). Aggresomes are pericentriolar cytoplasmic inclusions containing misfolded, ubiquitinated protein ensheathed in a cage of intermediate filament and closely associated with the centrosome. Because aggresomes share common features with our syntaxin 4 organelles morphologically, we investigated whether these two organelles could be related to or identical to each other. When MDCK cells grown in LCM were stained for syntaxin 4 and ubiquitin, only a diffuse cytoplasmic signal could be detected for ubiquitin, which was clearly different from the signal in large syntaxin 4-positive organelles (our unpublished results). Next, we treated the cells with the proteasome inhibitor acetyl-leucyl-leucyl-norleucinal to induce the formation of aggresomes. Under these conditions, ubiquitin-positive aggresomes can clearly be identified that do not significantly overlap with syntaxin 4-positive organelles (Figure 7, S and T), demonstrating that they are distinct.

Together, these data suggest that although "apical" and "basolateral" t-SNAREs are localized intracellularly in nonpolarized epithelial cells, they are nevertheless sorted to distinct compartments. These intracellular compartments resemble the respective plasma membrane domains due to the presence of apical or basolateral t-SNAREs as well as other plasma membrane marker proteins and an actin-based cytoskeleton.

#### **Intracellular Plasma Membrane Organelles Can Be Observed under Normal Calcium Conditions**

To exclude the possibility that the observed generation of apical and basolateral intracellular organelles in MDCK cells grown in LCM may be caused by a decrease in the intracellular calcium concentration or any other irrelevant effect, we seeded MDCK cells sparsely in medium containing serum and a normal concentration of calcium. After 16 h, the cells were stained for syntaxin 4 and gp135. Under these conditions, a mixture of patches of confluent cells and smaller aggregates down to single cells is observed. Consistently, cells that are located at the edge of a cell patch tend to display intracellular syntaxin 4-positive organelles, whereas syntaxin 4 is restricted to the basolateral plasma membrane in cells that are completely surrounded by other cells (Figure 8A). Single cells very frequently show intracellular syntaxin 4-positive organelles under these conditions, whereas gp135-positive VACs are relatively sparse (Figure 8, C and D). Omission of serum increases the frequency of VACs, in agreement with a previous report (Vega-Salas *et al.*, 1993), but it has no other apparent effect on syntaxin 4-positive organelles (Figure 8, E and F). Altogether, these results demonstrate that the occurrence of intracellular apical and basolateral organelles is not a function of the calcium concentration per se but rather depends on the degree of cell-cell interactions.

#### **Protein Sorting Is Preserved in Nonpolarized MDCK Cells**

The presence of normally apical and basolateral plasma membrane t-SNAREs in cognate intracellular compartments in nonpolarized cells suggests that these SNAREs function in the membrane fusion of vesicles from incoming transport pathways that are equivalent to the plasma membrane-directed transport pathways in polarized cells. We investigated how several proteins whose trafficking in polarized MDCK cells is well characterized are targeted in nonpolarized cells.

The soluble secretory protein gp80/clusterin is endogenously expressed in MDCK cells and is normally secreted apically and basolaterally (~2:1 ratio) in polarized MDCK cells (Urban *et al.*, 1987). Figure 9, G and H, shows that at steady state, 16 h after plating in LCM, large amounts of gp80 are retained inside individual cells and localize to both gp135-positive VACs and syntaxin 4-positive basolateral organelles. The protein must have reached these organelles on a direct route after biosynthesis, because otherwise it would be secreted and lost from the cells. To estimate what proportion of gp80 is secreted versus accumulated, we performed pulse-chase experiments and compared polarized cells grown on polycarbonate filters with nonpolarized cells grown in LCM. After 3 h, the secretion of newly synthesized gp80 from polarized cells was complete, with 62% secreted apically and 36% secreted basolaterally (Figure 10A). In contrast, 13% of gp80 remained intracellular after 3 h on a whole-population basis in nonpolarized cells. Considering that only approximately half of the cells display clearly identifiable apical and basolateral intracellular compartments under the culture conditions, we estimate that in individual cells approximately one-fourth of the synthesized gp80 is diverted into apical and basolateral intracellular organelles, and the remainder is secreted.

Next, we investigated trafficking of the pIgR. In polarized MDCK cells, pIgR is first transported to the basolateral plasma membrane domain and is subsequently transcytosed to the apical plasma membrane and released into the apical medium after proteolytic cleavage (Mostov *et al.*, 1995). We asked whether pIgR would be "transcytosed" into the VAC in nonpolarized MDCK cells. Figure 9A shows that after 16 h of incubation in LCM, a large amount of pIgR accumulates in the VAC. To support the interpretation that this is equivalent to the situation in polarized cells and follows an indirect route via the plasma membrane, we incubated nonpolarized MDCK cells expressing pIgR in the presence of polymeric IgA, the ligand of pIgR. If at least a fraction of the pIgR is targeted first to the plasma membrane before it reaches the VAC, we would expect it to have the ability to transport IgA from the medium into the VAC. Figure 9D shows that this is the case. After incubation for 16 h, the majority of the internalized IgA is found in gp135-positive VACs, demonstrating the specificity of this cognate transcytotic pathway in nonpolarized MDCK cells.

Two mutant forms of the pIgR have been generated previously that are deficient in direct TGN-to-basolateral plasma membrane transport in polarized MDCK cells and are instead targeted directly to the apical domain. Signalless pIgR (SL-pIgR) is a transmembrane protein in which the basolateral targeting signal in the cytoplasmic domain of pIgR has been deleted (Casanova *et al.*, 1991). In GPI-an-

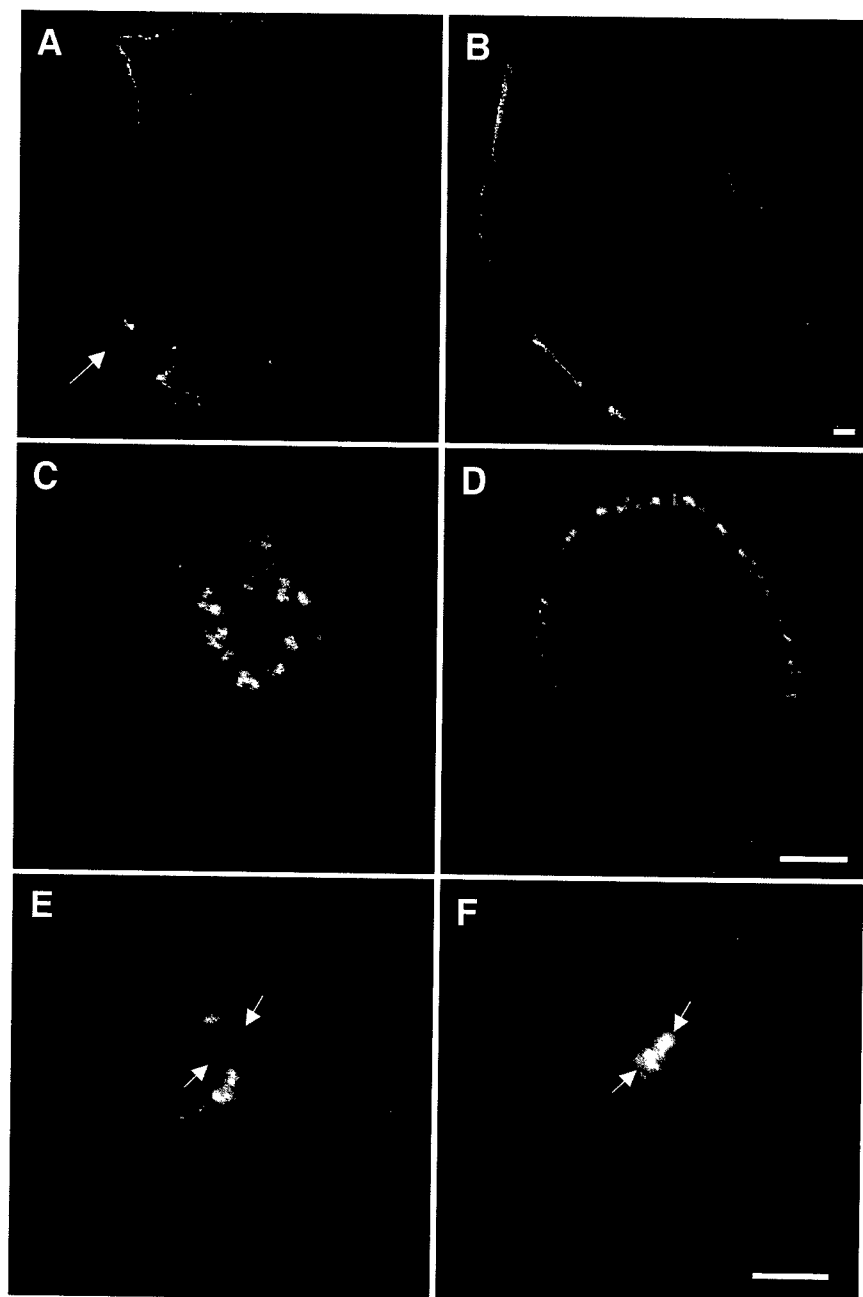


**Figure 8.** Intracellular syntaxin 4-positive organelles can be observed under normal extracellular calcium conditions in cells that are not within a monolayer. MDCK cells expressing syntaxin 4 were grown for 16 h in medium containing a normal calcium concentration. The medium for A–D contained 5% FCS, whereas the medium for E and F was serum-free. Cells were costained for syntaxin 4 (left column) and gp135 (right column). Syntaxin 4 frequently localizes to intracellular organelles in single cells (C) as well as in cells at the periphery of a colony (A, arrow) regardless of the presence of serum. In contrast, syntaxin 4 is mostly restricted to the plasma membrane in cells in the midst of a colony. Prominent intracellular gp135-positive VACs are frequent in cells grown in the absence of serum (E and F, arrows) but rare when serum is included. Bars, 5  $\mu$ m.

chored pIgR (GPI-pIgR), the entire cytoplasmic domain has been deleted (Mostov *et al.*, 1986), resulting in the attachment of a GPI anchor (S.H.L., K.E.M., and T.W., unpublished data). We have shown previously that trafficking to the apical plasma membrane of SL-pIgR and GPI-pIgR involves syntaxin 3 and SNAP-23 (Low *et al.*, 1998a). As shown in Figure 9, B and C, both proteins are transported to the gp135-positive VAC in nonpolarized MDCK cells. To assess whether the VAC is reached directly after biosynthesis or indirectly after initial delivery to the plasma membrane, we measured the surface delivery of SL-pIgR quantitatively by pulse-chase analysis. We made use of the previous finding

that the extracytoplasmic domain of pIgR contains a cleavage site that allows the rapid release of this domain into the medium in the presence of low amounts of *Staphylococcus aureus* V8 endoprotease. Figure 10B shows that the surface delivery of SL-pIgR in filter-grown polarized cells is complete after 3 h, with an apical:basolateral ratio of  $\sim 4:1$ . In contrast to the observed diminished secretion of gp80 (see above), the kinetics of SL-pIgR surface delivery was nearly identical between polarized and nonpolarized cells. This indicates that almost all of the SL-pIgR that is found in the VAC at steady state has reached this organelle indirectly via the plasma membrane. This is supported by the finding that

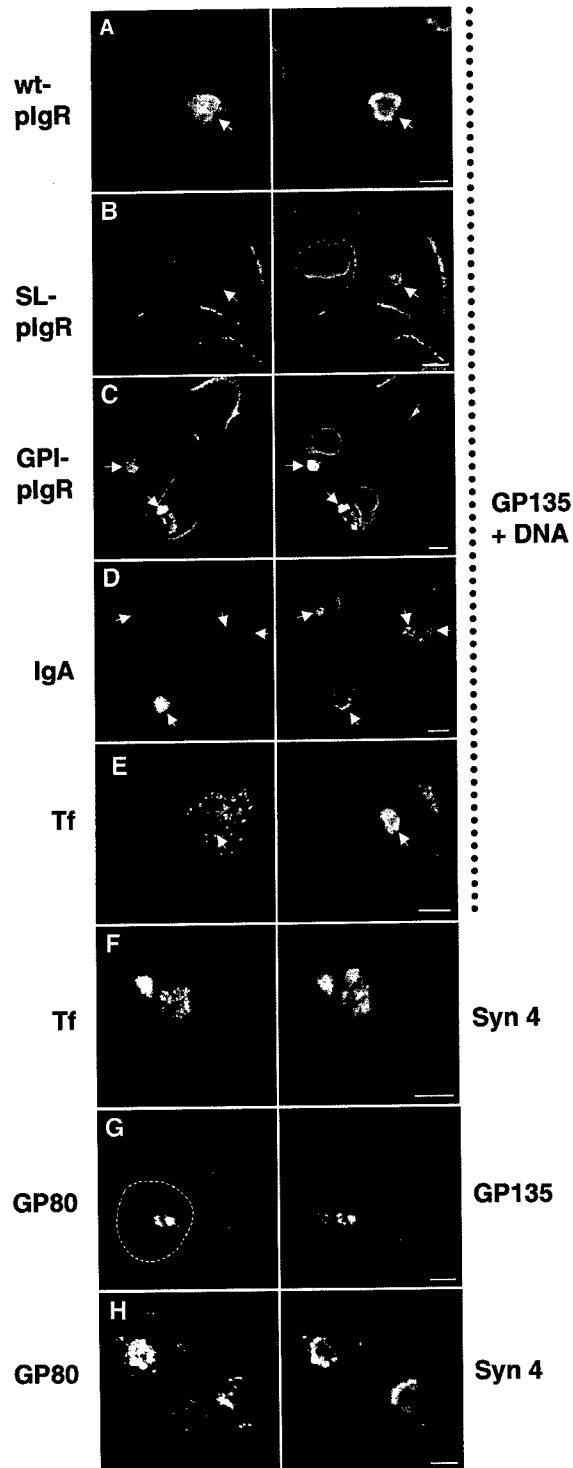


**Figure 9.** The "apical" and "basolateral" intracellular compartments receive membrane traffic from cognate polarized trafficking pathways. MDCK cells or MDCK cells stably expressing the wild-type pIgR (wt-pIgR), signalless pIgR (SL-pIgR), or a GPI-anchored mutant form of pIgR (GPI-pIgR) were grown in LCM for 16 h. IgA, 50  $\mu$ g/ml polymeric IgA was added during the 16-h incubation of cells expressing wild-type pIgR. Tf, 1  $\mu$ g/ml iron-loaded canine

both SL-pIgR and GPI-pIgR are able to transport IgA from the medium into the VACs (our unpublished results).

In contrast to IgA, transferrin is normally endocytosed from the basolateral plasma membrane and recycled back to the same domain in polarized MDCK cells. Only a very small percentage, if any, of internalized transferrin is transcytosed to the apical plasma membrane (Odorizzi and Trowbridge, 1997; Leung *et al.*, 1998). If the VAC is indeed a cognate compartment to the apical plasma membrane, we expect that transferrin added to the medium would have no access to this compartment. Figure 9E shows that this is the case. After 16 h of incubation, transferrin is internalized in nonpolarized MDCK cells but remains excluded from the gp135-positive VAC. Instead, internalized transferrin significantly colocalizes with syntaxin 4 in large intracellular organelles (Figure 9F). This result shows that transferrin is endocytosed and—instead of being recycled to the basolateral plasma membrane in polarized cells—at least a fraction of it is transported to the intracellular syntaxin 4 compartment. The majority of the additional small punctate transferrin staining does not coincide with syntaxin 4 but is typical for endosomes that transferrin normally travels through. These results indicate that the intracellular syntaxin 4 compartment is distinct from typical endosomes but receives endocytic traffic characteristic of the basolateral plasma membrane.

Together, these results strongly suggest that the intracellular apical and basolateral compartments in nonpolarized MDCK cells are cognate compartments to the apical and basolateral plasma membrane in polarized cells. They are equipped with a set of t-SNAREs that correspond to the respective domains of polarized cells and receive membrane traffic from equivalent biosynthetic and endocytic pathways. The overall conclusion from these findings is that protein sorting is still preserved after MDCK cells have lost their cell polarity and that apical and basolateral proteins are not simply randomly mixed together.

**Figure 9 (cont).** transferrin was added to MDCK cells during the incubation. The cells were fixed, permeabilized, and stained with an antibody against the endogenous apical plasma membrane protein gp135 to label VACs and propidium iodide as a nuclear stain (right column, as indicated). The pIgR was detected with the use of an antibody against the ectodomain (left column, top three panels). IgA, transferrin, syntaxin 4, and gp80/clusterin were detected with the use of specific antibodies. Note that wt-pIgR, SL-pIgR, and GPI-pIgR are transported to the VAC (arrows). Also, IgA added to the medium of wt-pIgR-expressing cells is transported to the VAC (arrows), indicating that wt-pIgR is first transported to the plasma membrane after biosynthesis, where it can bind IgA, internalize it, and transport it into the VAC. In contrast, internalized transferrin does not reach the VAC (arrow). Instead, it is deposited into a syntaxin 4-positive compartment (F). The endogenous soluble protein gp80/clusterin, which is normally secreted apically and basolaterally (~2:1 ratio) in polarized MDCK cells, is transported to both VACs (G) and syntaxin 4-positive organelles (H) in nonpolarized cells, suggesting that it reaches these compartments directly after biosynthesis. The panels in the left column show the same fields as those in the right column. Arrows are drawn for better orientation. The outline of one cell in G is drawn for clarity. Bars, 5  $\mu$ m.

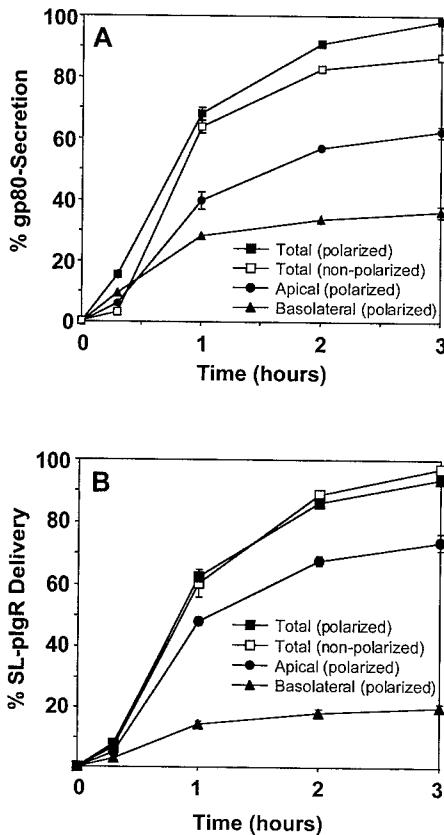


**Figure 10.** Quantitation of surface transport of the secreted protein gp80/clusterin in polarized and nonpolarized MDCK cells. MDCK cells (A) or MDCK cells stably expressing SL-pIgR (B) were grown as either a polarized monolayer on polycarbonate filters in regular medium or as nonpolarized cells on glass coverslips in LCM. Proteins were pulse-labeled with [ $^{35}$ S]cysteine. (A) The secretion of radiolabeled gp80 was monitored by collecting apical or basolateral medium (polarized) or total medium (nonpolarized) at different times and quantitation by SDS-PAGE and phosphorimaging and is represented as a percentage of total radiolabeled gp80 (intracellular plus secreted). Apically and basolaterally secreted gp80 was added to yield total secretion of gp80 from polarized cells. Note that after 3 h, gp80 secretion was nearly complete in polarized cells, whereas ~15% of gp80 remained intracellular in nonpolarized cells. (B) The surface delivery of newly synthesized SL-pIgR was monitored by the addition of a low concentration of V8 protease to the chase medium, which efficiently released the extracytoplasmic domain of pIgR into the medium. Quantitation was as described above. Note that the kinetics of SL-pIgR delivery in polarized and nonpolarized cells is nearly identical, indicating that the majority of SL-pIgR is delivered directly to the plasma membrane. Experiments were done in triplicate, and error bars represent SDs. Error bars were omitted when they were smaller than the symbol.

## DISCUSSION

In the present paper, we show that t-SNAREs that are normally localized at the plasma membrane in polarized epithelial cells distribute to intracellular compartments when cell polarity is lost or not yet established. Syntaxin 11 was identified as a new additional plasma membrane SNARE in polarized MDCK cells. This increases the number of epithe-

lial plasma membrane syntaxins to four and raises the question of whether they all serve separate membrane traffic pathways. Only syntaxins 3 and 4 show a polarized distribution at the apical and basolateral plasma membrane domain, respectively; syntaxins 2 and 11 and SNAP-23 localize to both domains. SNAP-23 may be a common binding partner of all plasma membrane syntaxins because it can bind to syntaxins 1, 2, 3, 4, and 11 (Ravichandran *et al.*, 1996; Valdez *et al.*, 1999). To date, the only functional information on the involvement of syntaxin homologues in plasma membrane traffic in polarized cells is available for syntaxin 3, which plays a role in transport from the TGN and from apical endosomes to the apical plasma membrane (Low *et al.*, 1998a; Lafont *et al.*, 1999), and syntaxin 4, which was found to be involved in the biosynthetic pathway leading to the basolateral plasma membrane (Lafont *et al.*, 1999). The role of the nonpolarized syntaxins 2 and 11 remains unclear, but they may serve nonpolarized pathways directed toward both domains. Syntaxin 11 has been reported to localize to endosomal and TGN-related compartments when it is exogenously expressed in nonpolarized NRK or HeLa cells (Advani *et al.*, 1998; Valdez *et al.*, 1999). We show that in nonpolarized MDCK cells, syntaxin 11 is also localized to punctate intracellular vesicles with very little, if any, detectable plasma membrane staining. However, as the cells form a polarized monolayer, the majority of syntaxin 11 relocates to both the apical and basolateral plasma membrane domains. This suggests that, at least in polarized epithelial cells, syntaxin 11 functions primarily as a plasma membrane t-SNARE. The tissue distribution of syntaxin 11 (Advani *et al.*, 1998; Tang *et al.*, 1998; Valdez *et al.*, 1999) suggests that it may be predominantly expressed in epithelial cells, which is supported by our finding that it is expressed in several epithelial cell lines. This emphasizes the importance of studying the localization and function of SNAREs in fully differentiated cells, such as polarized epithelial cells.

We found that all of the plasma membrane t-SNAREs relocate to varying degrees to intracellular compartments in MDCK cells when the formation of a polarized cell monolayer is prevented either temporarily during the course of the establishment of a monolayer or after a sustained inhibition of cell contacts in LCM. t-SNAREs are an integral part of the machinery accomplishing the final step of each membrane trafficking pathway. Therefore, this surprising result strongly suggests that membrane trafficking pathways that are normally directed to the plasma membrane in polarized epithelial cells undergo a fundamental shift toward intracellular compartments upon loss of cell polarity. This may have profound implications for our understanding of the pathogenesis of diseases involving a loss of epithelial polarity, e.g., the mistargeting of basement membrane proteins, proteases, integrins, etc., that play a role in the pathogenesis of invasive and metastatic carcinomas (Birchmeier *et al.*, 1996), or the mistargeting of ion transporters, growth hormone receptors, etc., in noncancerous epithelial diseases such as polycystic kidney disease (Murcia *et al.*, 1998; Sullivan *et al.*, 1998). Also, during tubule formation, e.g., in kidney development, epithelial cells temporarily lose their cellular polarity while cell rearrangements occur (Pollack *et al.*, 1998).

Is it possible that the observed intracellular localization of SNAREs in nonpolarized MDCK cells is an artifact caused by heterologous SNARE expression or calcium deficiency?

Most experiments presented here made use of canine MDCK cells that stably express rat (syntaxins 2, 3, and 4) or human (syntaxin 11 and SNAP-23) t-SNAREs. The following considerations argue against the idea that heterologously expressed SNAREs would be targeted differently from endogenous SNAREs. First, the expression levels are generally comparable to the endogenous levels (Figure 1) (Low *et al.*, 1996, 1998b). Second, the comparison of either different clones with varying SNARE expression levels or individual cells in a mixed clonal population fails to reveal a correlation between expression level and subcellular localization in both polarized and nonpolarized cells. Third, the localization of syntaxins (Low *et al.*, 1996) and SNAP-23 (Low *et al.*, 1998b) in transfected MDCK cells could be confirmed with endogenously expressed proteins in other cell lines or tissues (Gaisano *et al.*, 1996; Delgrossi *et al.*, 1997; Fujita *et al.*, 1998; Galli *et al.*, 1998; Riento *et al.*, 1998). Fourth, in this study, we have shown that endogenously expressed syntaxin 3 in Caco-2 cells localizes to VACs just as in transfected MDCK cells (Figure 5). Therefore, we consider it unlikely that SNARE expression levels as used in this study have adverse effects on SNARE targeting in MDCK cells. The possibility that cellular calcium depletion per se may cause the generation of intracellular plasma membrane organelles independent of epithelial cell polarity is unlikely for the following reasons. First, VACs have been observed by others in mammary carcinoma cells grown in medium containing a regular calcium concentration (Vega-Salas *et al.*, 1993). Second, VAC-like organelles are frequently found in a variety of carcinomas in situ (Remy, 1986; Vega-Salas *et al.*, 1993) and in intestinal epithelial cells in the genetic disorder microvillus inclusion disease (Ameen and Salas, 2000). Third, the intracellular calcium concentration has been measured previously in MDCK cells grown in high- or low-calcium medium and was found to be not significantly different (Vega-Salas *et al.*, 1987). Fourth, we observed VACs and syntaxin 4-positive basolateral organelles in MDCK cells that are grown either in regular-calcium medium for brief periods (Figure 3) or in single cells or cells at the edge of cell patches after sparse seeding and growth for 16 h (Figure 8).

The VAC has been described and characterized previously in nonpolarized MDCK cells and other epithelial cell lines as well as in carcinomas (Vega-Salas *et al.*, 1987, 1988, 1993; Gilbert and Rodriguez-Boulant, 1991; Brignoni *et al.*, 1993). In contrast, to our knowledge, the basolateral compartment that we identified here is a novel organelle that has not been described previously, perhaps because of the lack of availability of a marker protein such as syntaxin 4. Our data show that the syntaxin 4 compartment contains other, normally basolateral, plasma membrane proteins such as the Na/K-ATPase and the antigen 6.23.3. One basolateral marker protein, E-cadherin, was not strongly accumulated in the syntaxin 4-positive organelle but was instead down-regulated in nonpolarized cells, similar to a recent finding (Stewart *et al.*, 2000). The small amount of E-cadherin that was still present in the cells, however, did partially localize to the syntaxin 4-positive organelle. In addition, this organelle possesses a prominent membrane cytoskeleton containing actin and fodrin that is typical for the basolateral plasma membrane in polarized cells. This organelle excludes apical plasma membrane markers, including syntaxin 3. We showed that this novel organelle does not overlap with the

morphologically similar Golgi apparatus or the aggresome. The absence of the lysosomal protein LAMP-2 as well as ubiquitin makes it highly unlikely that the syntaxin 4-positive organelles, or VACs, are degradative compartments.

The presence of normally apical or basolateral plasma membrane t-SNAREs on intracellular organelles in nonpolarized cells suggests that plasma membrane proteins and secretory proteins are targeted to these vacuoles. Because apical and basolateral SNAREs are found in two separate organelles, this suggests that protein sorting is still preserved in nonpolarized MDCK cells. Our finding that internalized IgA reaches only the VAC but that transferrin reaches the syntaxin 4-positive organelle demonstrates that both compartments receive endocytic traffic and that trafficking into these organelles is specific. Both compartments also receive direct biosynthetic traffic because the soluble secretory protein gp80 accumulates in them. By pulse-chase analysis, however, we found that only a fraction of gp80 (estimated 25%) is deposited into VACs and syntaxin 4 organelles, whereas the majority is secreted. This fits with the finding that even in nonpolarized cells, variable amounts of plasma membrane SNAREs are typically located at the plasma membrane in addition to intracellular organelles. In contrast to the soluble marker gp80, the sorting of integral membrane proteins into apical and basolateral intracellular organelles appears to be more efficient. At steady state, gp135 is often very strongly enriched in VACs, whereas Na/K-ATPase and the 6.23.3 antigen are strongly enriched in basolateral organelles. Our data indicate that this high efficiency is mostly due to sorting after endocytosis of these proteins. Pulse-chase analysis of the SL-pIgR shows that nearly all of the newly synthesized protein is initially targeted to the surface. Because SL-pIgR is able to internalize IgA into VACs, and because we find SL-pIgR enriched in VACs at steady state, the majority of the protein must be internalized and transported to VACs after its initial plasma membrane delivery. This is the first direct evidence that trafficking into VACs follows mostly an indirect route via the plasma membrane. It had been suggested previously that trafficking of the influenza hemagglutinin into VACs occurs directly from the TGN (Brignoni *et al.*, 1995), but the possibility of an indirect pathway could not be experimentally excluded.

Together, our results suggests that apical/basolateral sorting is preserved in nonpolarized epithelial cells and leads to specific intracellular organelles. It has been found previously that nonpolarized, fibroblastic cells also have the capability to sort apical and basolateral plasma membrane proteins (presumably in the TGN) and transport them on separate routes to the identical plasma membrane (Musch *et al.*, 1996; Yoshimori *et al.*, 1996). A major difference between nonpolarized cells of epithelial and nonepithelial origin, therefore, may be that in the former plasma membrane proteins are eventually retained inside the cell rather than displayed at the surface.

What can be the possible function of intracellular apical and basolateral plasma membranes? These compartments are observed in epithelial cells that have lost their cellular polarity temporarily (e.g., sparsely seeded cells that have not yet established cell contacts) or permanently (e.g., when cell contacts are inhibited or in tumor cells). It is likely that many plasma membrane or secreted proteins are still synthesized

under these conditions. We speculate that there may be two reasons for the intracellular sequestration of plasma membrane proteins by nonpolarized epithelial cells. The phenomenon may be a cellular survival mechanism to relocate (normally apical and basolaterally separated) ion channels and transporters to intracellular compartments that would prevent potential ATP depletion caused by futile cycles of ion transport in and out of the cell. Also, excessive intracellular ion accumulation or depletion would be prevented. This view is supported by our finding that the majority of Na/K-ATPase relocates to syntaxin 4-positive organelles. The phenomenon may also be an organismal protection mechanism, because it would prevent the unwanted surface display of inappropriate proteins, e.g., proteases and cell-cell- or cell-matrix interacting proteins that may promote tumor invasion and metastasis. Interestingly, a variety of hydrolytic enzymes that are normally expressed at the apical plasma membrane of Caco-2 cells have been found in VACs after microtubule disruption (Gilbert and Rodriguez-Boulton, 1991). The finding that neither the apical nor the basolateral vacuole appears to be a degradative, lysosomal compartment indicates that proteins may be stored in them for later use once cell contacts have been reestablished. This is supported by the observation that VACs can be rapidly exocytosed as a whole from MDCK cells after reestablishment of cell-cell contacts (Vega-Salas *et al.*, 1988) or after increasing the intracellular cAMP concentration (Brignoni *et al.*, 1993).

In conclusion, we have shown that upon loss of cell polarity, epithelial cells relocate plasma membrane t-SNAREs and redirect membrane trafficking pathways to intracellular cognate apical and basolateral compartments. This is likely to be a general phenomenon in epithelia and may play a fundamental role in the pathogenesis of epithelial diseases that involve a breakdown of cell polarity.

## ACKNOWLEDGMENTS

We greatly appreciate the generous gifts of antibodies and/or cDNAs from Drs. E. Rodriguez-Boulton, G. Ojakian, B. Gumbiner, K. Matlin, C. Koch-Brandt, and M. Bennett. T.W. and S.H.L. are grateful to Drs. Gary Herman (Department of Pediatrics, University of California, San Francisco) and Robert Kim (Department of Ophthalmology, University of California, San Francisco) for their support. This work was supported by National Institutes of Health grants RO1AI25144 and DAMD17-97-7249 to K.E.M., by fellowships from the Alexander von Humboldt Foundation to T.W., and from the Irvington Institute for Immunology to T.W. and S.H.L.

## REFERENCES

- Advani, R.J., Bae, H.R., Bock, J.B., Chao, D.S., Doung, Y.C., Prekeris, R., Yoo, J.S., and Scheller, R.H. (1998). Seven novel mammalian SNARE proteins localize to distinct membrane compartments. *J. Biol. Chem.* 273, 10317–10324.
- Ameen, N.A., and Salas, P.J.I. (2000). Microvillus inclusion disease: a genetic defect affecting apical membrane protein traffic in intestinal epithelium. *Traffic* 1, 76–83.
- Apodaca, G., Katz, K.A., and Mostov, K.E. (1994). Receptor-mediated transcytosis of IgA in MDCK cells via apical endosome. *J. Cell. Biol.* 125, 67–86.
- Balcarova-Stander, J., Pfeiffer, S.E., Fuller, S.D., and Simons, K. (1984). Development of cell surface polarity in the epithelial Madin-Darby canine kidney (MDCK) cell line. *EMBO J.* 3, 2687–2694.
- Bennett, M.K., Garcia-Ararras, J.E., Elferink, L.A., Peterson, K., Fleming, A.M., Hazuka, C.D., and Scheller, R.H. (1993). The syntaxin family of vesicular transport receptors. *Cell* 74, 863–873.
- Birchmeier, W., Behrens, J., Weidner, K.M., Hulsken, J., and Birchmeier, C. (1996). Epithelial differentiation and the control of metastasis in carcinomas. *Curr. Top. Microbiol. Immunol.* 213/1, 117–135.
- Bracke, M.E., Van Roy, F.M., and Mareel, M.M. (1996). The E-cadherin/catenin complex in invasion and metastasis. *Curr. Top. Microbiol. Immunol.* 213/2, 123–161.
- Breitfeld, P., Casanova, J.E., Harris, J.M., Simister, N.E., and Mostov, K.E. (1989). Expression and analysis of the polymeric immunoglobulin receptor. *Methods Cell Biol.* 32, 329–337.
- Brignoni, M., Pignataro, O.P., Rodriguez, M.L., Alvarez, A., Vega-Salas, D.E., Rodriguez-Boulton, E., and Salas, P.J. (1995). Cyclic AMP modulates the rate of 'constitutive' exocytosis of apical membrane proteins in Madin-Darby canine kidney cells. *J. Cell Sci.* 108, 1931–1943.
- Brignoni, M., Podesta, E.J., Mele, P., Rodriguez, M.L., Vega-Salas, D.E., and Salas, P.J. (1993). Exocytosis of vacuolar apical compartment (VAC) in Madin-Darby canine kidney epithelial cells: cAMP is involved as second messenger. *Exp. Cell Res.* 205, 171–178.
- Casanova, J.E., Apodaca, G., and Mostov, K.E. (1991). An autonomous signal for basolateral sorting in the cytoplasmic domain of the polymeric immunoglobulin receptor. *Cell* 66, 65–75.
- Christoforidis, S., McBride, H.M., Burgoyne, R.D., and Zerial, M. (1999). The Rab5 effector EEA1 is a core component of endosome docking. *Nature* 397, 621–625.
- Delgrossi, M.H., Breuza, L., Mirre, C., Chavrier, P., and Le Bivic, A. (1997). Human syntaxin 3 is localized apically in human intestinal cells. *J. Cell Sci.* 110, 2207–2214.
- Drubin, D.G., and Nelson, W.J. (1996). Origins of cell polarity. *Cell* 84, 335–344.
- Fish, E.M., and Molitoris, B.A. (1994). Alterations in epithelial polarity and the pathogenesis of disease states. *N. Engl. J. Med.* 330, 1580–1588.
- Fujita, H., Tuma, P.L., Finnegan, C.M., Locco, L., and Hubbard, A.L. (1998). Endogenous syntaxins 2, 3 and 4 exhibit distinct but overlapping patterns of expression at the hepatocyte plasma membrane. *Biochem. J.* 329, 527–538.
- Gaisano, H.Y., Ghai, M., Malkus, P.N., Sheu, L., Bouquillon, A., Bennett, M.K., and Trimble, W.S. (1996). Distinct cellular locations and protein-protein interactions of the syntaxin family of proteins in rat pancreatic acinar cells. *Mol. Biol. Cell* 7, 2019–2027.
- Galli, T., Zahraoui, A., Vaidyanathan, V.V., Raposo, G., Tian, J.M., Karin, M., Niemann, H., and Louvard, D. (1998). A novel tetanus neurotoxin-insensitive vesicle-associated membrane protein in SNARE complexes of the apical plasma membrane of epithelial cells. *Mol. Biol. Cell* 9, 1437–1448.
- Gilbert, T., and Rodriguez-Boulton, E. (1991). Induction of vacuolar apical compartments in the Caco-2 intestinal epithelial cell line. *J. Cell Sci.* 100, 451–458.
- Gonzalez, L., Jr., and Scheller, R.H. (1999). Regulation of membrane trafficking: structural insights from a Rab/effector complex. *Cell* 96, 755–758.
- Gumbiner, B., and Simons, K. (1986). A functional assay for proteins involved in establishing an epithelial occluding barrier: identification of a uvomorulin-like polypeptide. *J. Cell Biol.* 102, 457–468.

- Gumbiner, B.M. (1996). Cell adhesion: the molecular basis of tissue architecture and morphogenesis. *Cell* 84, 345-357.
- Hammerton, R.W., Krzeminski, K.A., Mays, R.W., Ryan, T.A., Wollner, D.A., and Nelson, W.J. (1991). Mechanism for regulating cell surface distribution of Na<sup>+</sup>/K<sup>+</sup>-ATPase in polarized epithelial cells. *Science* 254, 847-850.
- Hanson, P.I., Heuser, J.E., and Jahn, R. (1997). Neurotransmitter release: four years of SNARE complexes. *Curr. Opin. Neurobiol.* 7, 310-315.
- Hay, J.C., and Scheller, R.H. (1997). SNAREs and NSF in targeted membrane fusion. *Curr. Opin. Cell Biol.* 9, 505-512.
- Johnston, J.A., Ward, C.L., and Kopito, R.R. (1998). Aggresomes: a cellular response to misfolded proteins. *J. Cell Biol.* 143, 1883-1898.
- Kern, H.F., Roher, H.D., von Bulow, M., and Kloppel, G. (1987). Fine structure of three major grades of malignancy of human pancreatic adenocarcinoma. *Pancreas* 2, 2-13.
- Lafont, F., Verkade, P., Galli, T., Wimmer, C., Louvard, D., and Simons, K. (1999). Raft association of SNAP receptors acting in apical trafficking in Madin-Darby canine kidney cells. *Proc. Natl. Acad. Sci. USA* 96, 3734-3738.
- Le Gall, A.H., Yeaman, C., Muesch, A., and Rodriguez-Boulán, E. (1995). Epithelial cell polarity: new perspectives. *Semin. Nephrol.* 15, 272-284.
- Leung, S.M., Chen, D., DasGupta, B.R., Whiteheart, S.W., and Apodaca, G. (1998). SNAP-23 requirement for transferrin recycling in streptolysin-O-permeabilized Madin-Darby canine kidney cells. *J. Biol. Chem.* 273, 17732-17741.
- Louvard, D., Keding, M., and Hauri, H.P. (1992). The differentiating intestinal epithelial cell: establishment and maintenance of functions through interactions between cellular structures. *Annu. Rev. Cell Biol.* 8, 157-195.
- Low, S.H., Chapin, S.J., Weimbs, T., Kömüves, L.G., Bennett, M.K., and Mostov, K.E. (1996). Differential localization of syntaxin isoforms in polarized MDCK cells. *Mol. Biol. Cell* 7, 2007-2018.
- Low, S.H., Chapin, S.J., Wimmer, C., Whiteheart, S.W., Kömüves, L.K., Mostov, K.E., and Weimbs, T. (1998a). The SNARE machinery is involved in apical plasma membrane trafficking in MDCK cells. *J. Cell Biol.* 141, 1503-1513.
- Low, S.H., Roche, P.A., Anderson, H.A., van IJzendoorn, S.C.D., Zhang, M., Mostov, K.E., and Weimbs, T. (1998b). Targeting of SNAP-23 and SNAP-25 in polarized epithelial cells. *J. Biol. Chem.* 273, 3422-3430.
- Mostov, K.E., Altschuler, Y., Chapin, S.J., Enrich, C., Low, S.H., Luton, F., Richman-Eisenstat, J., Singer, K.L., Tang, K., and Weimbs, T. (1995). Regulation of protein traffic in polarized epithelial cells: the polymeric immunoglobulin receptor model. *Cold Spring Harbor Symp. Quant. Biol.* 60, 775-781.
- Mostov, K.E., de Bruyn Kops, A., and Deitcher, D.L. (1986). Deletion of the cytoplasmic domain of the polymeric immunoglobulin receptor prevents basolateral localization and endocytosis. *Cell* 47, 359-364.
- Mostov, K.E., and Deitcher, D.L. (1986). Polymeric immunoglobulin receptor expressed in MDCK cells transcytoses IgA. *Cell* 46, 613-621.
- Murcia, N.S., Woychik, R.P., and Avner, E.D. (1998). The molecular biology of polycystic kidney disease. *Pediatr. Nephrol.* 12, 721-726.
- Müsch, A., Xu, H., Shields, D., and Rodriguez-Boulán, E. (1996). Transport of vesicular stomatitis virus G protein to the cell surface is signal mediated in polarized and nonpolarized cells. *J. Cell Biol.* 133, 543-558.
- Nabi, I.R., and Rodriguez-Boulán, E. (1993). Increased LAMP-2 polyglucosamine glycosylation is associated with its slower Golgi transit during establishment of a polarized MDCK epithelial monolayer. *Mol. Biol. Cell* 4, 627-635.
- Nelson, W.J., and Hammerton, R.W. (1989). A membrane-cytoskeletal complex containing Na<sup>+</sup>/K<sup>+</sup>-ATPase, ankyrin, and fodrin in Madin-Darby canine kidney (MDCK) cells: implications for the biogenesis of epithelial cell polarity. *J. Cell Biol.* 108, 893-902.
- Nelson, W.J., Hammerton, R.W., Wang, A.Z., and Shore, E.M. (1990). Involvement of the membrane-cytoskeleton in development of epithelial cell polarity. *Semin. Cell Biol.* 1, 359-371.
- Nichols, B.J., and Pelham, H.R. (1998). SNAREs and membrane fusion in the Golgi apparatus. *Biochim. Biophys. Acta* 1404, 9-31.
- Odorizzi, G., and Trowbridge, I.S. (1997). Structural requirements for basolateral sorting of the human transferrin receptor in the biosynthetic and endocytic pathways of Madin-Darby canine kidney cells. *J. Cell Biol.* 137, 1255-1264.
- Ojakian, G.K., and Schwimmer, R. (1988). The polarized distribution of an apical cell surface glycoprotein is maintained by interactions with the cytoskeleton of Madin-Darby canine kidney cells. *J. Cell Biol.* 107, 2377-2387.
- Pfeffer, S.R. (1999). Transport-vesicle targeting: tethers before SNAREs. *Nat. Cell Biology.* 1, E17-E22.
- Pollack, A.L., Runyan, R.B., and Mostov, K.E. (1998). Morphogenetic mechanisms of epithelial tubulogenesis: MDCK cell polarity is transiently rearranged without loss of cell-cell contact during scatter factor/hepatocyte growth factor-induced tubulogenesis. *Dev. Biol.* 204, 64-79.
- Ravichandran, V., Chawla, A., and Roche, P.A. (1996). Identification of a novel syntaxin- and synaptobrevin/VAMP-binding protein, SNAP-23, expressed in non-neuronal tissues. *J. Biol. Chem.* 271, 13300-13303.
- Remy, L. (1986). The intracellular lumen: origin, role and implications of a cytoplasmic neostructure. *Biol. Cell* 56, 97-105.
- Riento, K., Galli, T., Jansson, S., Ehnholm, C., Lehtonen, E., and Olkkonen, V.M. (1998). Interaction of munc-18-2 with syntaxin 3 controls the association of apical SNAREs in epithelial cells. *J. Cell Sci.* 111, 2681-2688.
- Rothman, J.E., and Warren, G. (1994). Implications of the SNARE hypothesis for intracellular membrane topology and dynamics. *Curr. Biol.* 4, 220-233.
- Simons, K., Dupree, P., Fiedler, K., Huber, L.A., Kobayashi, T., Kurzchalia, T., Olkkonen, V., Pimplikar, S., Parton, R., and Dotti, C. (1992). Biogenesis of cell-surface polarity in epithelial cells and neurons. *Cold Spring Harbor Symp. Quant. Biol.* 57, 611-619.
- Sorokin, L., and Ekblom, P. (1992). Development of tubular and glomerular cells of the kidney. *Kidney Int.* 41, 657-664.
- St-Denis, J.F., Cabaniols, J.P., Cushman, S.W., and Roche, P.A. (1999). SNAP-23 participates in SNARE complex assembly in rat adipose cells. *Biochem. J.* 338, 709-715.
- Stewart, D.B., Barth, A.I., and Nelson, W.J. (2000). Differential regulation of endogenous cadherin expression in Madin-Darby canine kidney cells by cell-cell adhesion and activation of beta-catenin signaling. *J. Biol. Chem.* 275, 20707-20716.
- Sullivan, L.P., Wallace, D.P., and Grantham, J.J. (1998). Epithelial transport in polycystic kidney disease. *Physiol. Rev.* 78, 1165-1191.
- Tang, B.L., Low, D.Y., and Hong, W. (1998). Syntaxin 11: a member of the syntaxin family without a carboxyl terminal transmembrane domain. *Biochem. Biophys. Res. Commun.* 245, 627-632.
- Urban, J., Parczyk, K., Leutz, A., Kayne, M., and Kondor-Koch, C. (1987). Constitutive apical secretion of an 80-kD sulfated glycoprotein.

- tein complex in the polarized epithelial Madin-Darby canine kidney cell line. *J. Cell Biol.* 105, 2735-2743.
- Valdez, A.C., Cabaniols, J.-P., Brown, M.J., and Roche, P.A. (1999). Syntaxin 11 is associated with SNAP-23 on late endosomes and the trans-Golgi network. *J. Cell Sci.* 112, 845-854.
- Vega-Salas, D.E., Salas, P.J., and Rodriguez-Boulan, E. (1987). Modulation of the expression of an apical plasma membrane protein of Madin-Darby canine kidney epithelial cells: cell-cell interactions control the appearance of a novel intracellular storage compartment. *J. Cell Biol.* 104, 1249-1259.
- Vega-Salas, D.E., Salas, P.J., and Rodriguez-Boulan, E. (1988). Exocytosis of vacuolar apical compartment (VAC): a cell-cell contact controlled mechanism for the establishment of the apical plasma membrane domain in epithelial cells. *J. Cell Biol.* 107, 1717-1728.
- Vega-Salas, D.E., San Martino, J.A., Salas, P.J., and Baldi, A. (1993). Vacuolar apical compartment (VAC) in breast carcinoma cell lines (MCF-7 and T47D): failure of the cell-cell regulated exocytosis mechanism of apical membrane. *Differentiation* 54, 131-141.
- Wang, G., Witkin, J.W., Hao, G., Bankaitis, V.A., Scherer, P.E., and Baldini, G. (1997). Syndet is a novel SNAP-25 related protein expressed in many tissues. *J. Cell Sci.* 110, 505-513.
- Weimbs, T., Low, S.H., Chapin, S.J., and Mostov, K.E. (1997a). Apical targeting in polarized epithelial cells: there's more afloat than rafts. *Trends Cell Biol.* 7, 393-399.
- Weimbs, T., Low, S.H., Chapin, S.J., Mostov, K.E., Bucher, P., and Hofmann, K. (1997b). A conserved domain is present in different families of vesicular fusion proteins: a new superfamily. *Proc. Natl. Acad. Sci. USA* 94, 3046-3051.
- Weimbs, T., Mostov, K.E., Low, S.H., and Hofmann, K. (1998). A model for structural similarity between different SNARE complexes based on sequence relationships. *Trends Cell Biol.* 8, 260-262.
- Wigley, W.C., Fabunmi, R.P., Lee, M.G., Marino, C.R., Muallem, S., DeMartino, G.N., and Thomas, P.J. (1999). Dynamic association of proteasomal machinery with the centrosome. *J. Cell Biol.* 145, 481-490.
- Yeaman, C., Grindstaff, K.K., and Nelson, W.J. (1999). New perspectives on mechanisms involved in generating epithelial cell polarity. *Physiol. Rev.* 79, 73-98.
- Yoshimori, T., Keller, P., Roth, M.G., and Simons, K. (1996). Different biosynthetic transport routes to the plasma membrane in BHK and CHO cells. *J. Cell Biol.* 133, 247-256.